2017-11-13

Characterization of Adipose Tissue Inflammation in Alcoholic Liver Disease

Melissa A. Fulham
University of Massachusetts Medical School

CHARACTERIZATION OF ADIPOSE TISSUE INFLAMMATION IN ALCOHOLIC LIVER DISEASE

A Dissertation Presented

By

MELISSA ANN FULHAM

Submitted to the Faculty of the
University of Massachusetts Graduate School of Biomedical Sciences, Worcester
in partial fulfillment of the requirements for the degree of

DOCTOR OF PHILOSOPHY

NOVEMBER 13, 2017

INTERDISCIPLINARY GRADUATE PROGRAM

CHARACTERIZATION OF ADIPOSE TISSUE INFLAMMATION IN ALCOHOLIC LIVER DISEASE

A Dissertation Presented

By

MELISSA ANN FULHAM

This work was undertaken in the Graduate School of Biomedical Sciences

Interdisciplinary Graduate Program

Under the mentorship of

Pranoti Mandrekar, Ph.D., Thesis Advisor

Brian Lewis, Ph.D., Member of Committee

Roger Davis, Ph.D., Member of Committee

Evelyn Kurt-Jones, Ph.D., Member of Committee

Cynthia Ju, Ph.D., External Member of Committee

Silvia Corvera, M.D., Chair of Committee

Anthony Carruthers, Ph.D.,

Dean of the Graduate School of Biomedical Sciences

November 13, 2017

Dedication

This work is dedicated to my late aunt, Maureen Boyden.

With pride

Acknowledgements

First and foremost, I have to thank my advisor, Dr. Pranoti Mandrekar. She welcomed me into her lab and encouraged me to pursue this project, which challenged me every day. I have learned so much during my time in her lab and am a better, more independent scientist because of it. I am truly grateful for her support.

I thank Arlene Lim, our lab manager. Her technical expertise is invaluable and I am immensely thankful for all of the assistance she has given me during my time in the lab, as well as the friendship and camaraderie we have shared. I also thank the current members of the lab, Dr. Asmita Choudhury and Dr. Anuradha Ratna for their help with experiments and moral support. I would also like to thank former members of the lab, Dr. Sujatha Muralidharan and Dr. Meghna Talekar for their help and wisdom as well. I am indebted to two former lab members, Dr. Aditya Ambade and Donna Catalano, who both helped to train me when I joined the lab and continue to give me advice.

I would like to thank the Department of Medicine, including the many colleagues I have gained during my time here. I thank our lab neighbors, the members of Dr. Gyongyi Szabo's lab for their experimental advice as well as use of their equipment, which was essential for my project. I thank the members of Dr. John Harris' lab, especially Dr. Jillian Richmond and James Strassner for their assistance with my flow cytometry experiments.

I thank the Department of Animal Medicine, including Melissa Little and Greg Cottle. I would not have been able to do my experiments without their vital help. I would also like to thank Dr. Carol Schrader from the Flow Cytometry Core for her assistance in designing my flow cytometry panels.

I thank the faculty who have served on my TRAC and have guided my journey here in graduate school: Dr. Roger Davis, Dr. Kate Fitzgerald, Dr. Brian Lewis, my TRAC chair, and Dr. Silvia Corvera, my defense chair. I thank Dr. Evelyn Kurt-Jones for joining the group for my defense. I would also like to thank Dr. Cynthia Ju for traveling to UMass to serve as the external examiner for my defense.

I want to thank all of the friends I have met here, especially the gang from lunch. The lunch table has seen many of us come and go over the years, but it has always been a spot for all of us to commiserate about the struggles of grad school and fantasy football.

I thank my friend and former roommate, Dr. Sally Trabucco. We share a passion for baking and science; the former played a big part in handling the ups and downs of the latter.

My parents, Mark and Martha, my sister Meghan and her husband Marc, and my sister Mollie deserve the biggest thank you. Their unconditional love and support have carried me through this whole journey. I also want to thank the rest of my family, especially my grandparents, Robert and Janice. I am grateful to my

friend Lauren Naujalis for her unending support and always helping me to find happiness and joy in all that I do.

Finally, I want to thank my fiancé, Dr. Brendan Hilbert. I don't know how I would have made it through all of this without your support. I can't wait for our next adventure.

Abstract

Adipose tissue inflammation has an impact on liver health and it has been demonstrated that chronic alcohol consumption leads to the expression of pro-inflammatory markers in the adipose tissue. A thorough characterization of alcohol-induced adipose inflammation is lacking, and is important to understand in order to identify immune-related mechanisms that drive this phenomenon. Current therapeutic regimens for alcoholic liver disease are ineffective. It is critical to understand how other organs influence liver injury in this disease when developing novel and effective therapies in the future.

Alcoholic liver disease exhibits a sexual dimorphism; women are more susceptible to liver injury than men and the same paradigm exists in rodent models. Here, I demonstrate that female mice have greater alcohol-induced adipose tissue inflammation than male mice, evidenced by greater expression of pro-inflammatory cytokines and cell markers. Further, female mice also exhibit higher expression of toll-like receptor genes in the adipose tissue, suggesting a potential role for the innate immune system in alcohol-induced adipose inflammation.

Toll-like receptor 4 (TLR4) has been demonstrated to drive inflammation in both the liver and adipose tissue. I used both germline and conditional knockouts of *Tlr4* to characterize alcohol-induced changes in the immune cell composition of adipose tissue. Alcohol increased the number of pro-inflammatory adipose tissue macrophages. This macrophage phenotype switching is partially

dependent on TLR4; germline, but not myeloid-specific, *Tlr4*-deletion prevents macrophage phenotype switching. Overall, my work demonstrates that alcohol-induced adipose tissue inflammation is related to liver injury and that TLR4 contributes to adipose macrophage phenotype switching.

Table of Contents

List of Tables

List of Figures

List of Copyrighted Materials

Chapter II and parts of Chapter IV have been published in the following manuscript (permission not required):

Fulham MA, Mandrekar P (2016) Sexual Dimorphism in Alcohol Induced Adipose Inflammation Relates to Liver Injury. PLOS ONE 11(10): e0164225.https://doi.org/10.1371/journal.pone.0164225

Parts of Chapter III and Chapter IV have been submitted as a manuscript to the American Journal of Physiology. Cell Physiology.:

Fulham MA, Kurt-Jones EA, and Mandrekar P. (2017). Alcohol-induced adipose tissue macrophage phenotype switching is independent of myeloid toll-like receptor 4 expression.

List of Abbreviations and Symbols

18s	18S ribosomal RNA
4-HNE	4-hydroxynonenal
α-SMA	Alpha smooth muscle actin
Acad	Acyl-CoA dehydrogenase
Acc	Acetyl-CoA carboxylase
Acs	Acyl-CoA synthetase
ADH	Alcohol dehydrogenase
Adipoq	Adiponectin, C1Q and collagen domain containing
AH	Alcoholic hepatitis
ALD	Alcoholic liver disease
ALDH	Aldehyde dehydrogenase
ALT	Alanine aminotransferase
APC	Antigen presenting cell
Arg1	Arginase 1
AST	Aspartate aminotransferase
ATGL	Adipose triglyceride lipase
BAC	Blood alcohol content
Bid	BH3 interacting domain death agonist
BMDM	Bone marrow-derived macrophage
Ccl2/MCP-1	Chemokine (C-C motif) ligand 2/monocyte chemoattractant protein 1

Ccr2	Chemokine (C-C motif) ligand receptor 2
Ccr7	Chemokine (C-C motif) ligand receptor 7
CD14	Cluster of differentiation 14
CD19	Cluster of differentiation 19
CD1d	Cluster of differentiation 1d
CD206/*Mrc1*	Cluster of differentiation 206/Mannose receptor, C type 1
CD3	Cluster of differentiation 3
CD4	Cluster of differentiation 4
CD45	Cluster of differentiation 45
Cd68	Cluster of differentiation 68
Cdh5	Cadherin 5
ChREBP/*Mlxipl*	Carbohydrate response element-binding protein/MLX interacting protein-like
Clec10a/MGL1	C-type lectin domain containing 10A/Macrophage galactose N-acetyl-galactosamine (GalNAc) specific lectin 1
CXCL1	Chemokine (C-X-C motif) ligand 1
CXCR1	Chemokine (C-X-C motif) receptor 1
CXCR2	Chemokine (C-X-C motif) receptor 2
CYP2E1	Cytochrome P450, family 2, subfamily e, polypeptide 1
DC	Dendritic cell
Emr1/F4/80	EGF-like module-containing mucin-like hormone receptor-like 1
EtOH	Ethanol

EtOH-fed	Ethanol-fed/Alcohol-fed
Fas	Fatty acid synthase
FGF21	Fibroblast growth factor 21
FPM	First pass metabolism
GROα	Growth-regulated protein alpha
HCC	Hepatocellular carcinoma
HSC	Hepatic stellate cell
HSL	Hormone sensitive lipase
IL-10	Interleukin 10
IL-13	Interleukin 13
IL-17	Interleukin 17
IL-1β	Interleukin 1 beta
IL-22	Interleukin 22
IL-4	Interleukin 4
IL-6	Interleukin 6
IL-8	Interleukin 8
iNKT	Invariant natural killer t cell
IRF3	Interferon regulatory factor 3
Itgam/CD11b	Integrin subunit alpha M/cluster of differentiation molecule 11B
Itgax/CD11c	Integrin subunit alpha X/cluster of differentiation molecule 11C
KC	Kupffer cell
LBP	LPS binding protein

LoxP	Locus of X-over P1
LPS	Lipopolysaccharide
LTA	Lipoteichoic acid
Ly6c	Lymphocyte antigen 6 complex, locus C1
Ly6g	Lymphocyte antigen 6 complex, locus G
LysMCre	Lysozyme M Cre recombinase
MD-2	Myeloid differentiation factor 2
MDA	Malondialdehyde
MHC II	Major histocompatibility complex, class II
MPO	Myeloperoxidase
Myd88	Myeloid differentiation primary response 88
NAFLD	Non-alcoholic fatty liver disease
NIAAA	National Institute on Alcoholic Abuse and Alcoholism
NK cells	Natural killer cells
NKT cells	Natural killer T cells
Pair-fed	Isocaloric control
PAMPs	Pathogen-associated molecular patterns
Poly I:C	Polyinosinic-polycytidylic acid
PPARα	Peroxisome proliferator-activated alpha
PPARγ	Peroxisome proliferator-activated gamma
PPRE	PPAR response element
PRRs	Pattern-recognition receptors

Rag1	Recombination activating gene 1
ROS	Reactive oxygen species
SREBP-1c/*Srebpf1*	Sterol regulatory element-binding protein 1c/sterol regulatory element binding transcription factor 1
STAT3	Signal transducer and activator of transcription 3
SVF	Stromal vascular fraction
TGFβ	Transforming growth factor beta
Th17	T helper 17
TLR	Toll-like receptor
TLR2	Toll-like receptor 2
TLR3	Toll-like receptor 3
TLR4	Toll-like receptor 4
TLR9	Toll-like receptor 9
TNF-R1	Tumor necrosis factor receptor 1
TNF-R2	Tumor necrosis factor receptor 2
TNFα	Tumor necrosis factor alpha
Tregs	Regulatory T cells
TRIF	TIR-domain-containing adaptor inducing interferon beta

Preface

The work presented in this dissertation represents my own work done in the lab of Dr. Pranoti Mandrekar at the University of Massachusetts Medical School, with the following exceptions:

Appendix B

Figure B1: Dr. Aditya Ambade performed the animal experiments and collected adipose tissue.

Appendix C

Figure C2: Arlene Lim imaged histology slides for cell size analysis. Raziel Rojas-Rodriguez generated the automated measuring technique.

CHAPTER I

Introduction

Alcoholic Liver Disease

Epidemiology

Prevalence of Alcoholic Liver Disease

The ubiquitous consumption of alcohol in our society has severe health consequences. According to the World Health Organization, in the United States approximately 25% of adult drinkers exhibit heavy, episodic drinking (at least 60 grams of ethanol consumed in one occasion) (1). 90% of alcoholics, who drink more than 60 grams of ethanol per day, will develop the first stage of alcoholic liver disease (ALD): steatosis (2, 3). In the previous decade, the number of hospitalizations due to alcoholic hepatitis (AH) rose from 249,884 cases in 2002 up to 326,403 cases in 2010. Over the same time period, the cost of hospitalization increased from $25,276 up to $40,870, despite the length of hospital stay remaining approximately the same (6.6 days in 2002 down to 5.9 days in 2010) (4). ALD is a large healthcare and financial burden for our population.

Alcohol-related deaths

Alcohol has been connected to a number of different types of mortality and was responsible for 30,722 deaths in 2014 in the United States (excluding accidents and homicides) (5). This work will focus on those relating to ALD. Approximately 40% of AH patients die within 6 months of disease onset (6). Cirrhosis, which is the end-stage of ALD, is the twelfth leading cause of death in the United States and among those 37,890 deaths in 2013, 48% were alcohol-

related (7). Liver transplant is the only treatment option for cirrhosis patients and ALD patients account for approximately 20% of all liver transplants in the United States (8-10). Globally, alcohol was attributed to 80,600 deaths due to liver cancers, out of a total 752,100 liver related cancer deaths in 2010 (11). Data from the Surveillance, Epidemiology, and End Results (SEER) Program reveals that alcohol was a contributing factor in 21.2% of hepatocellular carcinoma (HCC) cases in the United States during the 1990's (12).

Sexual dimorphism

There are a number of risk factors and co-morbidities associated with ALD. First and foremost, drinking patterns are heavily related to development of ALD. Drinking outside of meals and binge drinking are both associated with an increased risk of ALD (3). Genetics can also influence ALD risk, with polymorphisms in the enzymes that metabolize ethanol (ADH, ALDH, and CYP2E1) increasing the risk of developing ALD (3). Lifestyle factors (i.e. unhealthy diet, smoking) also contribute to disease pathogenesis, as does the development of obesity, and other liver pathologies like Hepatitis C infection (2, 13). In addition to the lifestyle and genetic factors, one of the clearest risk factors for ALD is biological sex. ALD demonstrates a sexual dimorphism; women are more susceptible to liver injury than men despite consuming less alcohol (2, 14, 15). The risk for developing ALD and alcoholic cirrhosis increases for women when 7-13 alcoholic drinks/week are consumed and for men when 14-27 alcoholic drinks/week are consumed. At high levels of alcohol consumption men

have a relative risk factor of 7 for developing cirrhosis while women have a relative risk factor of 17 (16). Additionally, being a female is identified as an independent risk factor for developing acute AH and cirrhosis (13).

Three factors are thought to contribute to this dimorphism: first pass metabolism of ethanol, body water content, and sex hormones. Men have a greater first pass metabolism than women. Blood alcohol content (BAC) after oral consumption of alcohol is much lower than BAC after intravenous (I.V.) administration of alcohol in both men and women, which demonstrates that a large amount of ethanol is metabolized before reaching circulation (first pass metabolism). The oral BAC in men was much lower than the oral BAC in women, which means that men metabolize greater amounts of ethanol than women (17, 18). This is attributed to men having greater gastric ADH activity, thereby metabolizing more ethanol in the stomach than women (18). Women also have a smaller calculated distribution volume of ethanol than men. (17, 19). This is due to having smaller body water content than men because of a greater body fat content (19). The translocation of endotoxin from the gut to the liver is considered to be a crucial step in disease pathogenesis (20). Estrogen supplementation causes endotoxin-induced mortality in rats that received a sub-lethal dose of LPS I.V. This is prevented when the liver resident macrophages, Kupffer cells (KCs), are depleted or when oral antibiotics are administered to deplete gut bacteria (21, 22). Together, this demonstrates that the sexual dimorphism in ALD can be attributed, in part, to factors outside of the liver itself.

This sexual dimorphism also occurs in rodent models. Female rats subjected to the intragastric feeding model develop greater alcohol-induced liver injury than male rats, based on higher serum AST values, greater hepatic steatosis, and a higher grade of liver inflammation (23, 24). Sex hormones have a clear impact on liver injury in this model. Alcohol-fed ovariectomized rats have reduced liver steatosis and liver inflammation when compared to normal, alcohol-fed rats. Treating alcohol-fed, ovariectomized rats with 17, β-estradiol restores alcohol-induced liver injury (25). Interestingly, both estrogen and progesterone regulate expression of *Cyp2e1* in the livers of female mice during the estrous cycle. *Cyp2e1* expression is positively correlated with expression of the lipogenic factor *Srebp1c* (26). It is unknown, however, how sex steroids affect CYP2E1 in response to chronic alcohol consumption. This dimorphism is also evident in mice using the NIAAA model; alcohol-fed female mice have higher serum ALT and AST values than male mice (27). However, a thorough comparison of liver injury in this model is lacking.

Altogether, these studies illustrate several possible reasons why women are more susceptible to ALD than men. However, they do not provide a complete picture and do not explore the potential role of other organs, like the adipose tissue, that are also impacted by chronic alcohol consumption. Therefore, other tissue and systems should be investigated to determine whether they also contribute to this dimorphism.

Pathogenesis

Stages of liver injury

ALD represents a spectrum of liver injury. Most people who drink heavily (more than 60 grams of ethanol per day) usually will develop the first stage of ALD, steatosis (fatty liver), which is the accumulation of lipid within hepatocytes. It is reversible with alcohol abstinence (2, 3). 30% of drinkers will develop more severe injury, which includes fibrosis and cirrhosis (2, 3).

Fibrosis is a wound healing response marked by the accumulation of extracellular matrix proteins and collagen in the liver. The presence of a chronic insult, such as alcohol consumption, leads to continuous collagen production which can eventually progress to cirrhosis (28). Hepatic stellate cells (HSCs), which produce and deposit collagen, are activated by mediators released by hepatocytes and KCs in response to ethanol metabolism and inflammatory stimuli. (2, 28). About 20%-40% of heavy drinkers will develop some degree of fibrosis (14).

Around 10%-20% of heavy drinkers will develop cirrhosis, (14). Even with alcohol abstinence, 5%-15% of patients with liver fibrosis eventually progress to cirrhosis (3). The risk increases greatly in AH patients, as approximately half will go on to develop cirrhosis (3, 6). AH is a severe inflammatory reaction in the liver. Histological analysis of AH patients reveals the presence of neutrophils, which surround damaged hepatocytes (6, 29). Independent of developing cirrhosis, AH has a high mortality rate (6).

Intestinal permeability

In addition to events in the liver, ALD pathogenesis also involves the gastrointestinal tract. Chronic alcohol consumption increases intestinal permeability, which allows for bacterial products, like lipopolysaccharide (LPS, endotoxin), to translocate to the liver (20). ALD patients with various stages of liver injury all had increased intestinal permeability when compared to healthy controls that consume low amounts of alcohol. This permeability is reversed after a week-long hospitalization, presumably due to the lack of alcohol consumption (30). Endotoxemia, the state of elevated circulating endotoxin, occurs in patients across the spectrum of ALD; however, there is no correlation between the level of endotoxin and the degree of liver injury (20). Not only does ethanol modulate intestinal permeability, it also sensitizes the liver to further insult. In mice, chronic alcohol consumption enhances TLR ligand-induced liver injury (31). Ethanol sensitizes KCs to LPS-mediated injury and hepatocytes to TNFα-mediated cell death (32, 33). Alcohol consumption enhances endotoxin translocation to the liver and endotoxin-mediated liver injury, both of which contribute to disease pathogenesis.

Treatments

Alcoholic hepatitis

The overall strategy for treatment of AH patients includes abstaining from drinking alcohol and treating the acute liver inflammation with corticosteroids (6). However, this regimen is not very effective. The mortality rate for AH is very high:

40% of patients with severe AH die within six months of disease onset (6, 14, 34).

For any patient with any stage of ALD, alcohol abstinence is crucial to care, symptom management, and reversal of liver injury (3). There are drugs that can be used to aid in alcohol abstinence, however some can be hepatotoxic, like disulfiram and acamprosate (2, 14). Baclofen has had some success in cirrhosis patients, but its impact on AH patients is unknown (2, 6, 14). Many patients are malnourished due to poor lifestyle choices and receive appropriate nutritional support (2, 6, 14). These strategies are pivotal in order for patients to recover, but they are not sufficient to resolve the inflammatory response in the liver.

The use of corticosteroids to treat AH was proposed in the 1970's; since then, there have been no new successful therapies developed (35). Prednisolone, a corticosteroid, is currently used to treat liver inflammation in severe AH patients. The impact of prednisolone on hepatitis patients is controversial; some studies indicate increased survival with the corticosteroid therapy while others have determined that it has no positive impact (2, 6). Re-examining some of these data supports the use of prednisolone and it is the recommended treatment for AH patients by the American Association for the Study of Liver Diseases (2, 6, 34).

Therapies targeting specific inflammatory mediators have also been tested for use in AH patients, with little success. Pentoxifylline, which inhibits the transcription of *TNF*, the gene that encodes the pro-inflammatory cytokine TNFα,

has mixed success in the clinic (2, 6, 34). Unfortunately, there is a subset of AH patients that do not respond to prednisolone or pentoxifylline therapy, therefore it is imperative that novel drugs are developed in order to treat these patients (36). Two anti-TNFα drugs, infliximab and etanercept, had promising results from small scale studies (2, 6). However, both drugs failed in larger, randomized trials because they led to increased infections and mortality in AH patients (37, 38).

Other unsuccessful treatment strategies for AH patients include antioxidants to counteract the ROS generated by both ethanol metabolism and inflammation, as well as anabolic steroids to help increase muscle mass lost during corticosteroid treatment (2, 6).

New potential therapies to control hepatic inflammation have emerged within the past two decades. The pro-inflammatory cytokine IL-1β is being considered as a potential therapeutic target. Anakinra and rilonacept, two different IL-1β inhibitors are currently in clinical trials for AH treatment (39). Other immune-centric therapies that are currently under consideration for AH treatment include the manipulation of the gut microbiome via probiotics and antibiotics, as well as the use of hematopoietic growth factors to aid in liver regeneration (39). These trials offer hope of developing novel therapies for AH, however, it is important to continue to deepen our understanding of disease pathogenesis to guide logical therapeutic development.

Advanced liver injury

There are limited options for treating patients with advanced liver disease. There are no approved drugs for the treatment of alcoholic fibrosis (2). Liver transplant is the only curative treatment option for patients with alcoholic cirrhosis (14). Without a transplant, many patients with decompensated liver injury will die in 5 years, even if they abstain from drinking alcohol (40). The use of liver transplants to treat patients with cirrhosis can be controversial due to perceived or actual recidivism rates and patient non-compliance (3). In fact, while many patients will consume alcohol after transplant, only a small number will re-develop heavy drinking habits. Surprisingly, ALD patients who receive a transplant have similar survival rates to non-ALD liver transplant patients (2, 3). Overall, there is a scarcity of therapies to treat those with ALD. Therefore, we are obligated to deepen our understanding of disease pathogenesis so that new therapeutic targets can be discovered.

Ethanol metabolism causes liver injury

Ethanol metabolism generates ROS

Ethanol metabolism in hepatocytes directly contributes to liver injury. Ethanol is metabolized in a two-step process (Figure 1.1). Under normal conditions, the enzyme ADH metabolizes ethanol to acetaldehyde, which is subsequently metabolized to acetate by ALDH. The final product, acetate, spontaneously breaks down into water and carbon dioxide (41). However, during chronic alcohol consumption, CYP2E1 is the major enzyme that breaks down ethanol to acetaldehyde. This process produces ROS, which can lead to tissue

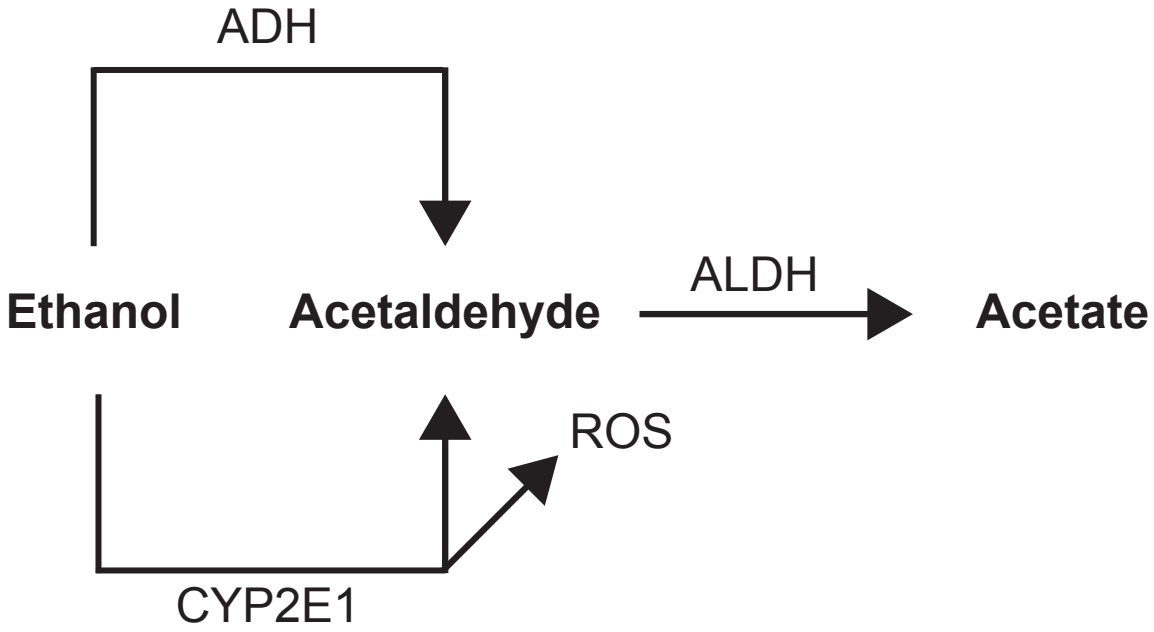

Figure 1.1: Ethanol metabolism. Ethanol molecules are broken down in a two-step process. Under normal conditions, ADH converts ethanol to acetaldehyde. Then, ALDH breaks down acetaldehyde into acetate. In chronic alcohol conditions, CYP2E1 catalyzes the first step, which also produces ROS as a byproduct.

damage (41, 42). CYP2E1-mediated ROS production leads to the formation of the lipid peroxidation products MDA and 4-HNE, which are immunogenic (39, 41, 43, 44). In hepatocytes, ROS generated by CYP2E1 activity causes ethanol-mediated apoptosis, which can be prevented by inhibiting either CYP2E1 or caspases (45). In KCs, the increased presence of ROS enhances the response to LPS and leads to increased production of TNFα (46). Additionally, acetaldehyde molecules can form protein and DNA adducts (41, 42). Adduct formation as a result of ethanol metabolism can activate immune cells in the liver, such as T cells (47).

Lipid metabolism

Steatosis is the first stage in ALD pathogenesis and occurs due to the simultaneous upregulation of lipogenesis and downregulation of fatty acid oxidation (2). The metabolism of ethanol in hepatocytes results in the activation of SRE-promoters, the increase in nuclear translocation SREBP-1c, and, ultimately, activation of SREBP-1c target genes (48). SREBP-1c activates lipogenesis by activating target genes that promote fatty acid synthesis, like *Fas* and *Acc* (49). Alcohol-fed *Srebf1*$^{-/-}$ (SREBP-1c knockout) mice exhibit reduced hepatic steatosis and liver injury compared to alcohol-fed WT mice (50). This supports the notion that SREBP-1c activation is an important step in alcohol-induced liver injury.

Recently, another lipogenic transcription has been identified in alcoholic steatosis. Carbohydrate response element-binding protein (ChREBP) binds to its

target promoter sequences, including lipogenic factors, in response to glucose (51). Alcohol administration via consecutive ethanol gavages increased the mRNA expression of the ChREBP gene (*Mlxipl*) as well as hepatic steatosis. The subsequent increase in ChREBP binding activity was dependent on the metabolism of ethanol via CYP2E1. Knockdown of ChREBP expression in hepatocytes was associated with decreased steatosis in the mice receiving alcohol, thereby alleviating liver injury. However, the knockdown of ChREBP also increased the mortality of these mice. This could be due to the dysregulation of ethanol metabolism due to greater circulating concentrations of ethanol and its metabolite, acetaldehyde (52).

Ethanol, more specifically the metabolite acetaldehyde, inhibits the DNA-binding activity of PPARα (53). PPARα binds to PPREs to activate β-oxidation of fatty acids via upregulation of its target genes, which include *Acs* and the *Acad* family (54). Alcohol-fed *Ppara*$^{-/-}$ mice have greater liver injury than WT mice (55). Importantly, treating alcohol-fed mice with a PPARα agonist reverses hepatic steatosis (56). Ethanol metabolism promotes the storage of lipids in hepatocytes by upregulating lipid synthesis via enhanced activation of SREBP-1c and ChREBP and downregulating lipid breakdown via inhibition of PPARα.

Inflammation contributes to disease pathogenesis

Macrophages

Along with the metabolic changes described above, the development of inflammation in the liver due to the interplay of immune cells and pro-

inflammatory cytokines and chemokines also contributes to liver injury, which is summarized briefly in Figure 1.2. Macrophages, more specifically the liver resident KCs, are considered to be the most important immune cell type to ALD. In non-pathological conditions, they function to maintain liver homeostasis by clearing away damaged cells in the liver and microorganisms from the blood (20, 39, 43, 57, 58). During ALD, gut permeability is increased which results in endotoxin migrating to the liver, which will then activate KCs (20). Chronic alcohol consumption increases the number of macrophages in the liver of humans (59). In mice, chronic alcohol consumption causes the infiltration of a heterogeneous macrophage population into the liver. One subset of these macrophages produces pro-inflammatory cytokines and chemokines that lead to further infiltration of immune cells. The other subset expresses genes that are involved in tissue remodeling and repair and also act to clear away apoptotic hepatocytes (60) Chronic alcohol exposure also increases the sensitivity of KCs to endotoxin injury, partially due to increased ROS (32, 46). KCs are a major source of many cytokines associated with ALD, including TNFα, IL-6, MCP-1, IL-8 (CXCL1 in mouse), and IL-1β (35, 61). They also produce the anti-inflammatory cytokine IL-10 (35). The pro-inflammatory cytokines directly impact other liver cell types (i.e. hepatocytes and HSCs) and drive the recruitment of other immune cells (33, 39). Depleting KCs in rats prevents liver injury in the intragastric feeding model and greatly improves liver steatosis, inflammation, and necrosis (62). Sterilizing the gut with antibiotics also reduces liver injury in rats (63). The

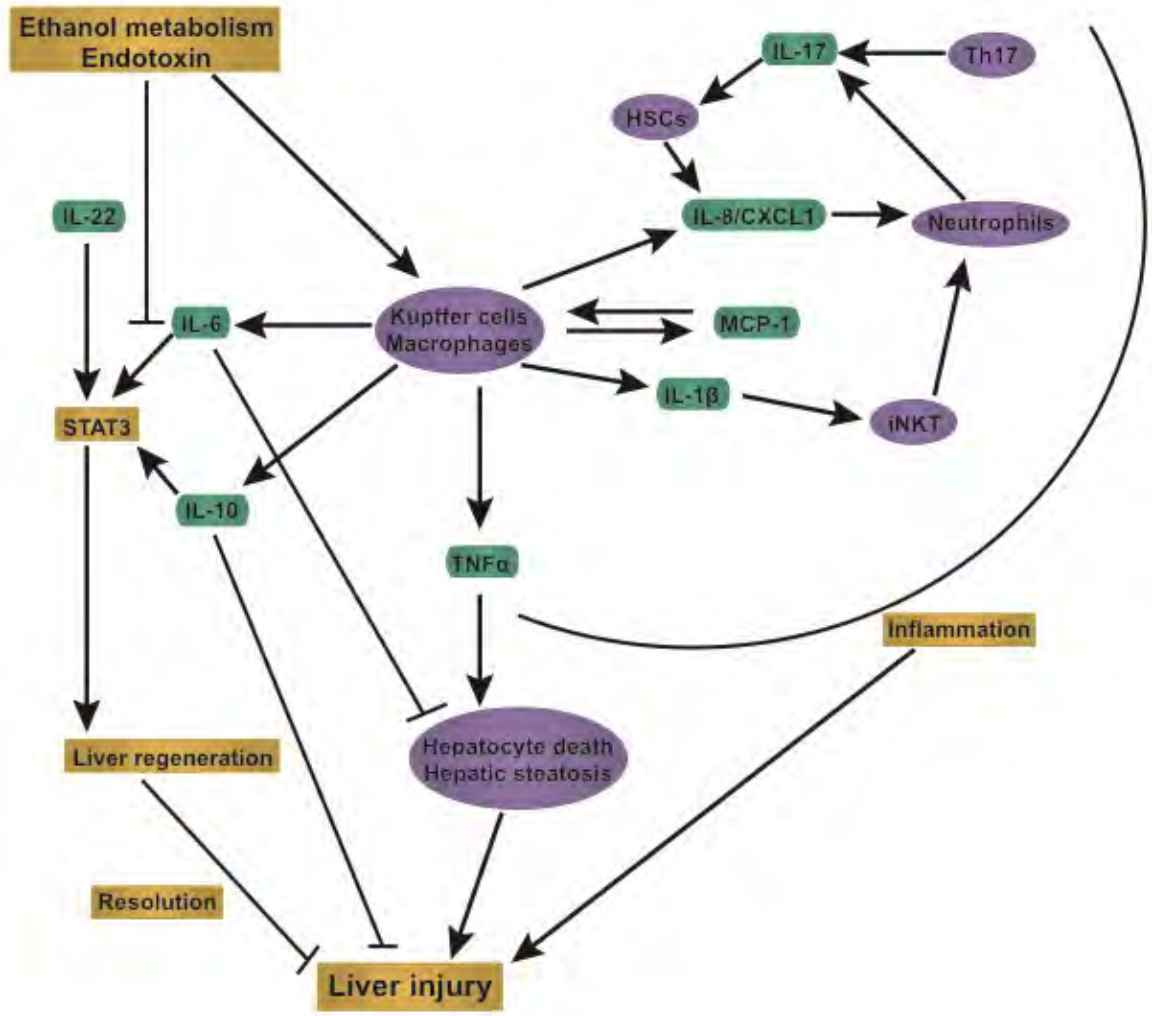

Figure 1.2: Hepatic inflammation in ALD. A combination of ethanol metabolism and the presence of endotoxin activates the resident KCs to produce cytokines and chemokines. TNFα impacts hepatocytes directly by inducing steatosis and apoptosis. MCP-1 production leads to further infiltration and accumulation of macrophages into the liver. Neutrophils are recruited through two mechanisms: directly through IL-8/CXCL1 and indirectly through the production of IL-1β and recruitment of iNKT cells. Both neutrophils and Th17 cells produce IL-17, which promotes IL-8/CXCL1 production in HSCs. IL-22, IL-6, and IL-10 signal through STAT3 to promote liver regeneration and inhibit liver injury through resolution of inflammation. Macrophages produce both IL-6 and IL-10, but alcohol inhibits IL-6 mediated STAT3 activation. The combination of inflammation and hepatic steatosis results in liver injury.

use of various genetic knockouts of genes important to macrophage function, specifically the TLR-signaling pathways or pro-inflammatory mediators, have further demonstrated that KCs contribute to ALD pathogenesis (64-67). However, these studies use models of early alcohol-induced liver injury, which do not fully recapitulate human disease. It remains to be determined how KCs impact liver injury in later stages of ALD (43, 68). Recently, the importance of the tissue regenerative functions of macrophages has been highlighted, and this process could be important for resolution of ALD (39, 60).

Neutrophils

Neutrophil infiltration into the liver in a key feature of AH in humans (29). Neutrophils, like macrophages, are important for clearing bacteria and dead cells in order to promote tissue repair, however in ALD they damage hepatocytes and contribute to the pro-inflammatory state in the liver (43, 69). Up until recently, it was nearly impossible to recapitulate this in animal models (29, 67, 68). The addition of ethanol binges on top of a long-term chronic alcohol diet leads to neutrophil accumulation in the livers of mice, which provides a platform to investigate how neutrophils contribute to disease pathogenesis, particularly in later stage models (67, 68, 70). In the NIAAA model, the use of clodronate to deplete KCs reduces, but does not entirely ameliorate, liver injury (67). Depleting neutrophils reduces liver injury, but not steatosis (70). Together, these studies indicate that neutrophils are contributing to disease pathogenesis in models that employ an ethanol binge, which represent later stages of liver injury than

previous models. The development of these new models that exhibit neutrophil infiltration could prove to be useful in the creation of novel AH therapeutics. Interestingly, AH patients with severe neutrophil infiltration had better short-term survival than patients with only mild infiltration. Whether this was due to the severe infiltration representing an earlier stage of hepatitis or whether neutrophils were promoting tissue regeneration is unclear (71).

Lymphocytes

The impact of alcohol on T cells is dichotomous. Chronic alcohol consumption reduces peripheral and splenic conventional T cells in humans and rodents, respectively (44, 72). Whereas neutrophils are the predominant infiltrating immune cell in AH, lymphocytes are the predominate infiltrate in alcoholic cirrhosis (73). Both $CD4^+$ and $CD8^+$ T cells are localized to necrotic and fibrotic areas in cirrhotic livers (74). T cells that infiltrate into the liver during ALD are less diverse than in other liver diseases, which could be a result of recognizing antigens generated by protein adducts, which are byproducts of ethanol metabolism (47).

Th17 cells may contribute to liver injury. ALD patients have high levels of circulating IL-17, when compared to hepatitis C or autoimmune liver disease patients. IL-17+ cells are increased in areas of fibrosis in the livers of ALD, hepatitis C, and autoimmune patients. However, AH and autoimmune hepatitis patients had the highest number of IL-17+ cells in inflammatory infiltrates. The expression of IL-17 is co-localized with the expression of CD3 and MPO, which

indicates that T cells (Th17 cells) and neutrophils are producing IL-17, respectively. IL-17 promotes neutrophil infiltration into the liver, but in an indirect manner. HSCs express the receptor for IL-17 and upon stimulation with this cytokine, produce both IL-8 and Groα which induce neutrophil infiltration into the liver (75).

Natural killer cells are a type of lymphocyte that can produce cytokines and perform cytotoxic functions (76). NK cells have anti-fibrotic effects in chemical-induced fibrosis models via the killing of activated HSCs (39). Chronic alcohol decreases the number of NK cells in the liver in alcohol-fed mice and circulating NK cells are decreased in alcoholics (77-79). NK cells are also absent in the livers of ALD patients (74). Therefore, the alcohol-mediated decline in NK cells could promote the progression of fibrosis. The exact role of NK cells in alcoholic fibrosis remains unclear.

Natural killer T cells (NKT cells) reside in the liver and act as a bridge between the innate and adaptive immune response. NKT cells can respond to pathogen-associated molecular patterns (PAMPs) via toll-like receptors (TLRs) and antigens presented via CD1d. Activated NKT cells can then go on to act upon both innate and adaptive immune cells, including neutrophils and conventional T cells (80). KC production of IL-1β recruits invariant natural killer T-Cells (iNKT, also known as Type I NKT cells) to the liver in the NIAAA model (61). The iNKT cells, in turn, promote the infiltration of neutrophils. Genetic deletion or chemical inhibition of iNKT cells decreases neutrophil recruitment and

ameliorates liver injury, demonstrating that iNKT cells are crucial for alcohol induced liver injury and are a potential therapeutic target (61, 81, 82).

Similar to T cells, the number of circulating B cells is lower in alcoholics with active liver disease than those without or non-alcoholic control patients (72, 83). Despite this, ALD patients present with elevated serum immunoglobulin levels (72, 83). ALD patients also exhibit antibodies with specificity towards byproducts of ethanol metabolism like lipid peroxidation products, MDA, and 4-HNE (39, 43, 44). Antibody production towards these metabolism products suggests that endotoxin is not the sole immunogenic component in disease pathology. Further, ethanol metabolism itself can result in the activation of an immune response.

Pro-inflammatory cytokines and chemokines

ALD patients across various stages exhibit elevated circulating pro-inflammatory cytokine and chemokine levels. Circulating TNFα levels are higher in AH patients than healthy controls, alcoholics without liver injury, and alcoholic cirrhosis patients. This phenomenon is likely reflective of the higher levels of acute hepatocellular damage and necrosis in AH patients. Further, TNFα levels are approximately 2-fold higher in AH patients that died within six weeks of hospital admission when compared to AH patients who survived for that same duration (84). TNFα was one of the first pro-inflammatory cytokines to be associated with liver injury in ALD models. Ethanol exposure magnifies TNFα-mediated cell death in hepatocytes (33). TNFα also influences lipid metabolism in

hepatocytes. Stimulating hepatocytes with TNFα leads to the maturation and nuclear translocation of the lipogenic transcription factor SREBP-1c (85). Injecting mice with TNFα or LPS leads to hepatic steatosis, which can be prevented by treating with a TNFα neutralizing antibody (86). Treating alcohol-fed rats with antiserum to TNFα reverses liver injury and inflammation (87). This effect is mediated by the receptor TNF-R1, as alcohol-fed TNF-R1 knockout mice exhibit decreased liver injury, hepatic steatosis, and liver inflammation when compared to alcohol-fed WT mice (88).

Systemic MCP-1 (CCL2) is higher in severe AH patients versus alcoholic cirrhosis patients and healthy controls (89). *Ccl2*$^{-/-}$ mice are protected against alcohol-induced liver injury, inflammation, and steatosis. Interestingly, these effects are independent of its receptor, CCR2, because alcohol-fed *Ccr2*$^{-/-}$ exhibit liver injury and steatosis, similar to WT controls (90). There is evidence that MCP-1/CCL2 may be able to signal through another chemokine receptor, CCR10, but that has yet to be demonstrated in ALD models (91).

IL-17 production by neutrophils and T cells promotes infiltration of neutrophils into the liver via HSCs. ALD patients have higher levels of IL-17 in the blood, when compared to both healthy controls and hepatitis c patients. However, IL-17 is lower in AH patients than non-AH patients with ALD. This could be due to AH patients having fewer Th17 cells in circulation and a greater number of IL-17-expressing cells in the liver, when compared to non-AH patients

(75). Alcohol-fed mice also exhibit higher circulating IL-17. Treating alcohol-fed mice with an IL-17-specific antibody ameliorates hepatic steatosis (92).

IL-1β promotes the infiltration of iNKT cells into the liver, which, in turn, recruit neutrophils (61, 82). Circulating IL-1β is elevated in ALD patients compared to healthy controls (93). Alcohol boosts the production of IL-1β in liver mononuclear cells, which contributes to the rise of IL-1β in alcohol-fed mice. Alcohol-fed mice treated with IL-1Ra to counteract IL-1β signaling exhibited ameliorated liver injury, hepatic steatosis, and liver inflammation (61, 94).

Systemic IL-8, a neutrophil chemoattractant, is greatly elevated in AH patients, compared to both healthy controls and alcoholics without liver disease. IL-8 levels decline in AH patients overtime with alcohol abstinence and amelioration of liver injury (95-97). Alcohol elevates the levels of CXCL1, the murine homolog of human IL-8, in circulation and expression in the liver of mice (67-69, 98, 99). Genetic deletion of *Cxcl1* decreases neutrophil infiltration and liver injury, whereas treating mice with a CXCL1-neutralizing antibody can reverse liver injury (99). Antagonizing CXCL1 activity via blockade of its receptor reverses liver injury (98).

Anti-inflammatory cytokines

There are three anti-inflammatory cytokines with important roles in ALD: IL-6, IL-10, and IL-22, all of which exert their effects through STAT3 (39). The impact of STAT3 on the development of ALD is cell-type dependent. STAT3 expression in hepatocytes decreases alcohol-induced steatosis but contributes to

inflammation, whereas STAT3 expression in macrophages decreases inflammation (100). Circulating IL-6 levels are increased in ALD patients compared to healthy controls (93). IL-6 is crucial for liver regeneration, however chronic alcohol consumption impairs IL-6 mediated STAT3 activation in hepatocytes (101). Chronic alcohol exposure inhibits STAT3 serine and tyrosine phosphorylation. This occurs independent of JAK1 activation and tyrosine phosphatase activity, which activate or inactivate STAT3, respectively (102). It is unclear exactly how chronic alcohol exposure inhibits STAT3 activation, but IL-10 may also be involved, as *Il10*$^{-/-}$ mice have enhanced phosphorylated STAT3 when compared to WT mice (103). IL-6 also prevents apoptosis in hepatocytes exposed to ethanol and TNFα (104). IL-6-deficiency exacerbates alcohol-induced hepatic steatosis (104-106). Treating alcohol-fed mice with IL-6 reverses steatosis in both WT and *Il6*$^{-/-}$ animals (105, 107).

The role of IL-10 in ALD is not straightforward. It can inhibit both pro- and anti-inflammatory molecules (108). Alcohol increases IL-10 in both the liver and circulation in mice (94). Alcohol-fed *Il10*$^{-/-}$ mice have improved liver injury and steatosis when compared to alcohol-fed WT mice. However, the *Il10*$^{-/-}$ mice have a greater inflammatory response, including the production of IL-6 and increased STAT3 phosphorylation. The IL-6-STAT3 axis could be a compensatory mechanism mediating this improved liver injury and steatosis because both IL-6- and hepatocyte-specific STAT3-deficiency exacerbates liver injury in the *Il10*$^{-/-}$

mice (103). Interestingly, the TLR3-mediated production of IL-10 reduces alcohol-induced liver injury (109, 110).

IL-22 is a hepatoprotective cytokine that acts upon epithelial cells (111). It promotes hepatocyte proliferation via STAT3 and is important for liver regeneration (111). IL-22 administration alleviates liver injury in mice subjected to both acute alcohol and chronic-binge alcohol models (27, 112). IL-22 therapy may be a viable treatment for AH patients for two major reasons. First, the expression of the IL-22 receptor, IL-22R, is restricted to epithelial cells; this specificity could prevent side effects. Second, IL-22 treatment has been demonstrated to improve bacterial infection and kidney injury in mouse models, both of which contribute to AH fatality. At the time this dissertation was written, a clinical trial studying the effects of a recombinant fusion IL-22 protein on acute alcohol hepatitis patients was recruiting participants (NCT02655510)(39).

The development of liver inflammation in ALD is a complex process that involves many cell types from both the innate and adaptive immune system. The network of cytokines and chemokines that are modulated in response to chronic alcohol consumption is also crucial to disease progression. This, in part, has made developing targeted, effective treatments for ALD challenging.

Toll-like receptors

One group of proteins that has been of special interest in the development of ALD is the TLRs. The TLR family is a group of receptors that recognize foreign pathogens. TLRs are part of a larger group of pattern-recognition receptors

(PRRs) that detect PAMPs. Activation of TLRs ultimately results in the production of pro-inflammatory cytokines and/or Type I interferons, by signaling through the adaptor molecules MYD88 and TRIF, respectively. Each TLR recognizes a different type of PAMP. The TLRs expressed at the cell surface generally recognize PAMPs that make up the outermost part of bacteria and other microbes. Endosomal TLRs recognize PAMPs that are derived from foreign nucleic acids (113).

Toll-like receptor 4

TLR4 is the most well studied in the ALD field. It recognizes LPS, which is found on the outer wall of Gram-negative bacteria (113). TLR4 cannot bind to LPS alone. LPS binding protein (LBP) is a serum protein that binds to LPS and transfers it to CD14, a surface receptor. CD14 then transfers the LPS molecule to TLR4 and its co-receptor MD-2 (114). Endotoxemia occurs in ALD patients (20). As TLR4 is the receptor for endotoxin, it was hypothesized that it mediated the effects of endotoxemia in ALD pathogenesis. Many published studies support the hypothesis that TLR4 signaling impacts alcohol-induced liver injury. First it was discovered that TLR4-mutant mice subjected to the intragastric feeding model exhibit greatly reduced liver injury when compared to WT mice (115). This was also true for mice lacking either CD14 or LBP (116, 117). Subsequent studies using the TLR4-mutant mice or *Tlr4*$^{-/-}$ mice also produced the same results; alcohol-fed TLR4-deficient mice had decreased liver injury compared to WT mice, whether an intragastric feeding model or a Lieber-DeCarli diet was used

(64, 65, 118, 119). This effect can be attributed to different cell types and not just those of the innate immune system. Complementary bone marrow transplants studies reveal that the lack of TLR4 in either the hematopoietic or non-hematopoietic compartment leads to reduced liver injury (119). However, the role of TLR4 may not be as clear as initially discovered. Alcohol-fed *Tlr4*$^{-/-}$ mice exhibit WT levels of liver complement deposition and TNFα production (120). Moreover, a close examination yields that TLR4-deficiency only produces a modest relief of liver injury, or it only appears to inhibit pro-inflammatory signaling cascades (64, 118). These studies raise questions as to the exact role of TLR4 in early, alcohol-induced liver injury, as they use different models of liver injury. Moreover, what role TLR4 plays in later stages of liver injury remains to be determined. Careful analysis of the specific pathways impacted by TLR4-deficiency in each of these models will assist in providing more insight into this receptor.

Other TLR-family members

The roles of the other TLRs have not been fully explored in the ALD field. TLR2, which forms a heterodimer with either TLR1 and TLR6 to recognize triacylated lipopeptides or diacylated lipopeptides, respectively, has a controversial role in ALD models (113). In a five-week Lieber-DeCarli model, TLR2 was not required for liver injury. Alcohol-fed *Tlr2*$^{-/-}$ mice exhibited steatosis and pro-inflammatory cytokine production similar to alcohol-fed WT mice, which were absent in *Tlr4*$^{-/-}$ mice (64). However, in the NIAAA model, TLR2-deficient

mice are protected against liver injury, which was demonstrated by decreased serum ALT levels when compared to alcohol-fed WT controls. Interestingly, TLR2 is important to the production of neutrophil-specific chemokines, like CXCL1, and neutrophil accumulation in the liver (67). TLR3 recognizes double-stranded RNA and the synthetic ligand polyinosinic-polycytidylic acid (poly(I:C)), which makes it crucial for detecting viral infection (113). TLR3 does not have a direct role in alcohol-induced liver injury. When alcohol was administered via daily gavage on top of a high-fat diet, *Tlr3*$^{-/-}$ mice exhibited liver injury similar to WT mice; both genotypes had increased liver injury compared to isocaloric controls. However, when WT mice received injections of poly(I:C), liver injury is ameliorated via the production of IL-10 (109). TLR9 is an intracellular receptor which recognizes unmethylated CpG DNA from bacteria and viruses (113). Similar to TLR2, TLR9 is also required for neutrophil-mediated liver injury in the NIAAA model (67).

The development of new ALD mouse models has uncovered the complex roles of TLRs in ALD. TLR4 may be required for early, macrophage-driven injury, whereas TLR2 is dispensable (64, 115). On the other hand, TLR2 and TLR9 may be important for more advanced, neutrophil-driven liver injury (67). This would explain discrepancies in results, specifically those concerning TLR2, between the Lieber-DeCarli model and the NIAAA model (64, 67). Together, these studies highlight three things. First, macrophage- and neutrophil-mediated liver injury could be driven by distinct (yet still related) immune mechanisms. Second, the field needs to re-evaluate the importance placed on TLR4 as the only driver of

alcohol-induced liver inflammation and whether, instead, it has a very specific role in early stages of pathogenesis. Third, the other TLR family members not discussed in detail here warrant further study using the full range of animal models now available. This will deepen the understanding of TLR-related mechanisms in ALD pathogenesis.

Animal models of ALD

There are a number of different methods to use alcohol to induce liver damage in animals. Below, I will discuss those that administer alcohol via a liquid diet, as that is the method by which ALD patients consume alcohol. Table 1.1 provides a summary of the basic characteristics of each of these models.

Lieber-DeCarli

A breakthrough in animal models of ALD came with the development of the Lieber-DeCarli diet (121). This is an *ad libitum*, liquid diet, which is designed to be nutritionally adequate for rodents and to match the average human diet, based on calorie-consumption (18% protein, 35% fat, and 47% carbohydrates). The standard rodent chow diet is withheld from the rats or mice while this liquid diet is administered in order to overcome the aversion to consuming ethanol. The ethanol concentration in the diet is slowly increased to allow the animals to acclimate to consuming ethanol. A control group is given the same diet, but with the carbohydrate calories coming from maltose-dextrin instead of ethanol. After 24 days of up 50g/L of ethanol per day, hepatic steatosis is noted and the liver triglyceride content increased 5-fold (121). This diet has been modified further to

Table 1.1: Summary of ALD rodent models

Name	EtOH Administration	Duration	Liver injury	Challenges
Lieber-DeCarli	Liquid diet	4-6 weeks	-Steatosis -Mild inflammation	-Long-term -Early stage liver injury
NIAAA	Liquid diet Ethanol binge	3 weeks	-Steatosis -Mild Inflammation -Mild neutrophil infiltration	-Early stage liver injury
Chronic, multiple binge	Liquid diet Several ethanol binges	up to 8 weeks	-Steatosis -Fibrosis -Inflammation -Neutrophil infiltration	-Long-term -Many binges -High mortality rate
Tsukamoto -French	Intragastric	4-12 weeks	-Steatosis -Mild inflammation	-Difficult technique -Requires special equipment -Animals require a lot of care to maintain health

produce several iterations that have varying fat and protein content (122). While it was developed for rats, this model is widely used in mice, and a four-to-six-week long feeding with the Lieber-DeCarli diet is considered the standard for the ALD field (123). This model easily produces hepatic steatosis and elevated serum liver enzymes, but it fails to produce a robust inflammatory response in the liver (123). This diet serves as the basis for several models that more closely mimic human disease and are reviewed below.

NIAAA and Chronic, multiple-binge models

Recently, new models have emerged that incorporate alcohol binge events with chronic, *ab libitum* alcohol exposure. The purpose of the binge events is to recapitulate the drinking patterns of AH patients (124). The NIAAA model employs a single binge of ethanol (5g/kg bod weight) after 10 days of chronic alcohol consumption, using the Lieber-DeCarli model. This model has a shorter time span than the chronic feeding models which typically last four to six weeks and results in a greater induction of circulating ALT and AST levels (27, 123). It also shows signs of neutrophil infiltration into the liver, a hallmark of AH (67, 70). However, similar to the chronic feeding models, the NIAAA model produces early liver injury and does not result in fibrosis. A second model that uses multiple binges over a long period of time has been able to recapitulate some aspects of alcoholic fibrosis. Chronic, *ad libitum* alcohol feeding for eight weeks in conjunction with twice weekly ethanol binges produces more advanced liver injury. Neutrophil accumulation in the liver was described in this model. Both

α-SMA expression and Sirius Red staining in the liver, markers of fibrosis, were also observed in these mice (68). The authors also examined hepatitis and fibrosis markers in mice given a single ethanol gavage at the end of an eight-week chronic, *ad libitum* alcohol exposure. Similar to the multiple-binge model, neutrophils, α-SMA staining, and Sirius Red staining were all observed in these mice. However, the neutrophils had infiltrated the liver in a diffuse pattern, whereas the multiple-binge model produced discrete inflammatory foci, indicating that the pattern of drinking impacts liver inflammation (68).

Tsukamoto-French

The development of the intragastric alcohol feeding model, commonly referred to as the Tsukamoto-French model, enabled researchers to control the amount of ethanol delivered to animals (125). Central vein cannulation allows for continuous monitoring of BAC and inserting a cannula directly into the stomach enables the delivery of the liquid diet (126). Insertion of the catheter through the dorsal neck allows the animals to have unimpeded mobility throughout the duration of the experiment (127). This model is capable of inducing massive steatosis, but lacks the inflammatory component necessary to recapitulate human disease (128). It is also technically challenging and the animals require close, extensive monitoring throughout to maintain their health (127). This intragastric model has been built upon recently to design experiments to induce maximum liver damage. In one example, the authors used a combination of a solid Western diet (high cholesterol and high saturated fat), the liquid diet with

ethanol via intragastric cannulation, and weekly gavages of ethanol to induce liver damage. This combination resulted in steatosis, inflammatory infiltration, and liver fibrosis (129). This model is capable of generating massive liver injury, but its use should be carefully considered when studying ALD due to the complexity of the set up.

Adipose Tissue

Adipose tissue biology

Metabolic and endocrine functions

The primary function of adipose tissue is energy storage. Adipocytes store triglycerides, which can be broken down into glycerol and free fatty acids to be used as fuel by other tissues via the process of lipolysis (130). Adipocyte lipolysis is carried out in a step-wise manner by three enzymes: adipose triglyceride lipase (ATGL), hormone-sensitive lipase (HSL), and monoacylglycerol lipase (MGL) (130, 131). Lipolysis is tightly regulated and can be stimulated through glucocorticoid or β-adrenergic signaling and is inhibited by insulin signaling (130, 131).

Energy storage is not the only function of the adipose tissue. It also acts as an endocrine organ and produces a number of factors, most importantly adiponectin (132). The adipose tissue is comprised of many different cell types, including various immune cells, pre-adipocytes, and endothelial cells (132).

Adipose tissue immune cells

In parallel to KCs in the liver, the adipose tissue macrophage is the most-well studied immune cell with regards to adipose tissue inflammation, which is summarized in Figure 1.3. Pro-inflammatory macrophage accumulation is a hallmark in obesity-related adipose tissue inflammation (133). Macrophages infiltrate into the adipose tissue in obesity-models and upregulate expression of the M1 macrophage marker CD11c (134-138). M1, or classically activated macrophages, are typically activated by inflammatory cytokines like IFNγ or inflammatory molecules like LPS and other TLR ligands. They produce the pro-inflammatory cytokines TNFα, IL-6, IL-1β, and MCP-1 (133). In the adipose tissue, these M1 macrophages are localized to the inflammatory foci “crown-like structures”, which surround dead or dying adipocytes (139). Deleting CD11c-expressing cells reverses macrophage accumulation during obesity (140). On the other hand, MGL1-expressing M2 macrophages inhabit the space between adipocytes and do not localize to the crown-like structures (139). M2, or alternatively activated, macrophages can be further categorized into three general subsets: M2a macrophages participate in the wound healing response, M2b macrophages have immunoregulatory functions, and M2c macrophages are immunosuppressive (133, 141). M2 macrophages are polarized by cytokines IL-4, IL-13, or IL-10. They are categorized by a number of cell surface markers, including MGL1 and CD206, and produce anti-inflammatory cytokines or wound repairing cytokines like IL-10 and TGFβ (133, 141).

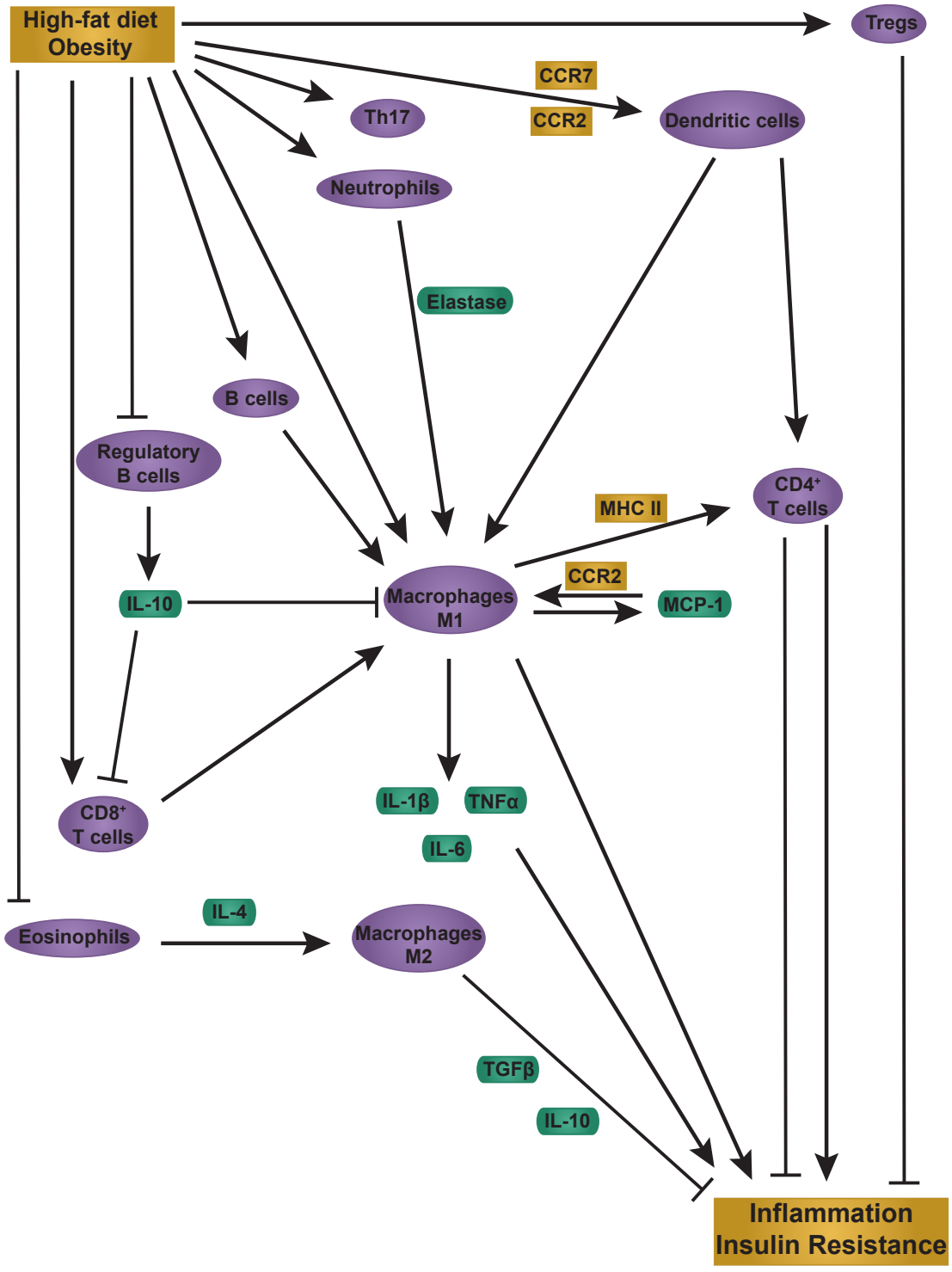
High-fat diet
Obesity
Tregs
CCR7
CCR2
Th17
Dendritic cells
Neutrophils
Elastase
B cells
Regulatory
B cells
CD4+
T cells
MHC II
CCR2
IL-10
Macrophages
M1
MCP-1
CD8+
T cells
IL-1β
TNFα
IL-6
IL-4
Eosinophils
Macrophages
M2
TGFβ
IL-10
Inflammation
Insulin Resistance

Figure 1.3: Adipose tissue inflammation in obesity and high-fat diet models. High-fat diet and obesity results in adipose tissue inflammation by regulating pro- and anti-inflammatory immune cells. M1 macrophages contribute to inflammation directly through the production of Il-1β, TNFα, and IL-6. MCP-1 production results in further macrophage infiltration, which is mediated by CCR2. Anti-inflammatory M2 macrophages control and resolve adipose inflammation through TGFβ and IL-10. High-fat diet and obesity inhibit M2 macrophages indirectly due to the decreased presence of eosinophils, which produce IL-4. Regulatory T cells (Tregs), which function to control inflammation are also reduced. High-fat diet increases the presence of Th17 cells. B cell accumulation leads to further macrophage accumulation, however regulatory B cells suppress M1 macrophages through the production of IL-10. IL-10 also suppresses $CD8^+$ T cells, which are required for macrophage infiltration. Elastase-producing neutrophils increase M1 macrophages. Dendritic cell (DC) accumulation is dependent on CCR2 and CCR7 and promotes the accumulation of M1 macrophages. Both macrophages and DCs interact with $CD4^+$ T cells to promote adipose tissue inflammation. $CD4^+$ T cells can promote or inhibit adipose tissue inflammation, depending on the specific subset.

Macrophage infiltration into the adipose tissue is thought to be dependent on MCP-1-CCR2 signaling, as *Ccr2*$^{-/-}$ mice fed a high-fat diet have fewer macrophages than their WT counterparts (142). Monocyte tracking experiments revealed that the expression of CCR2 in monocytes and MCP-1 in non-hematopoietic cells are both required for the infiltration of most, but not all, macrophages (138). A small number of macrophages do undergo proliferation in the adipose tissue in response to high-fat diet feeding, which demonstrates that macrophage accumulation in obesity is influenced by many factors (143-145). Adipose tissue macrophages also function as antigen presenting cells (APCs) for $CD4^+$ T cells, further promoting inflammation (146-148).

Another type of APC is the dendritic cell (DC). The number of adipose tissue DCs in mice increases when the animals are fed a high-fat diet. Isolated DCs from high-fat diet fed mice stimulate T-cell differentiation and proliferation *in vitro* (148, 149). Adipose tissue DCs may also be involved in macrophage recruitment. *Flt3*$^{-/-}$ mice, which lack DCs, accumulate fewer pro-inflammatory macrophages than WT mice when subjected to a high-fat diet (150). Similar to macrophages, DC accumulation in the adipose tissue is partially dependent on CCR2. CCR7 was identified to be expressed in adipose DCs and not macrophages and is also required for DC accumulation in the adipose tissue (148).

Neutrophils are primarily considered to be “first responders” to tissue damage during acute inflammation. As part of the resolution of acute injury,

necrotic and apoptotic neutrophils are cleared away by macrophages (69, 95). However recent studies in chronic inflammation in the obesity field have given evidence for this paradigm to be reconsidered (69). Neutrophils infiltrate into the adipose tissue within the first few days of a high-fat diet in mice, which is consistent with their role in responding to tissue damage (151, 152). Interestingly, they persist in the adipose tissue and produce neutrophil elastase in response to a prolonged, high-fat diet. High-fat diet-fed, neutrophil elastase-deficient mice have fewer M1 adipose macrophages than WT mice, which suggests that adipose neutrophils may be important for macrophage infiltration (152). Together, this suggests that neutrophils could be functioning in two ways during adipose tissue inflammation. First, they infiltrate early in the course of a high-fat diet in response to acute tissue damage. Second, they accumulate within the tissue, contributing to chronic inflammation.

B cells also contribute to adipose tissue inflammation. B-cell deficient mice fed a high-fat diet have fewer M1 macrophages than WT mice and improved insulin sensitivity (153). Interestingly, a population of regulatory B cells, which produce the anti-inflammatory cytokine IL-10, control adipose tissue inflammation. When mice that lack IL-10 expression in B cells are subjected to a high-fat diet, they accumulate more $CD8^+$ T cells and M1 macrophages in the adipose tissue, compared to WT mice. These mice also exhibit higher expression of the pro-inflammatory cytokine genes *Tnf*, *Il6*, and *Ccl2* and have greater insulin resistance (154).

Similar to macrophages, the role of T cells in adipose tissue inflammation is complex. Adipose tissue $CD4^+$ T cells proliferate in response to a high-fat diet in mice (147, 155). MHC II expression on pro-inflammatory, $CD11c^+$ adipose macrophages increases in response to a high-fat diet. Inhibiting MHC II activity decreases the ability of adipose macrophages to stimulate $CD4^+$ T cell proliferation (147). High-fat diet fed MHCII-deficient mice have fewer adipose tissue pro-inflammatory macrophages and $CD4^+$ T cells along with improved insulin sensitivity (146). On the other hand, *Rag1*$^{-/-}$ mice, which lack T cells, have aggravated insulin resistance. This is reversed with the transfer of $CD4^+$ T cells, but not $CD8^+$ T cells (155). Different subsets of $CD4^+$ T cells may serve different purposes in promoting or restraining adipose tissue inflammation.

Other T cell populations also contribute to adipose tissue inflammation. High-fat diet increases the number of $CD8^+$ T cells in the adipose tissue in mice, an event that precedes macrophage accumulation. Depleting $CD8^+$ T cells in high-fat diet-fed mice decreases pro-inflammatory macrophages, which suggests that $CD8^+$ T cells also influence macrophage accumulation in the adipose tissue (156). The presence of regulatory T cells in the adipose tissue declines as obesity progresses and *in vivo* expansion of this cell population improves insulin resistance (157). Obesity also increases the number of Th17 cells in mice (149).

High-fat diet also increases the number of natural killer (NK) cells in the adipose tissue. Depleting NK cells in high-fat diet-fed mice reduces the number of pro-inflammatory macrophages and improves insulin resistance (158).

Eosinophils help to maintain the M2 macrophage population via the cytokine IL-4, however their numbers in the adipose tissue are reduced by obesity (159).

In addition to adipocytes and immune cells, the adipose tissue is also comprised of endothelial cells, fibroblasts, and preadipocytes (132). These cell types also contribute to adipose tissue inflammation as they are capable of producing and responding to pro- and anti-inflammatory cytokines (132, 160, 161).

Adipose tissue cytokines and chemokines

The adipose tissue produces pro-inflammatory cytokines, chemokines, and adipokines during the progression of obesity and stops producing anti-inflammatory cytokines and adipokines (132). TNFα is expressed in the adipose tissue of obese rodents and neutralizing TNFα improves insulin-stimulated glucose uptake (162). IL-6 is a complicated cytokine because it demonstrates opposing roles in adipose inflammation in obesity models. IL-6 production by the adipose tissue, more specifically by adipocytes, directly impacts hepatic insulin resistance (163). On the other hand, *Il6*$^{-/-}$ mice subjected to a high-fat diet have a higher degree of hepatic insulin resistance than WT mice (164). High-fat diet-fed mice treated with sgp130FC, which partially blocks IL-6 signaling, have decreased pro-inflammatory macrophage accumulation in the adipose tissue, without any improvement in insulin sensitivity (165). However, neutralizing IL-6 increases the ratio of M1 macrophages to M2 macrophages in adipose tissue explants (145). The source of IL-6 and/or the mechanisms it signals through at its

target tissues could determine whether it is a beneficial or harmful consequence of adipose tissue inflammation. Expression of MCP-1 is also increased by obesity (166). High-fat diet-fed *Ccl2*$^{-/-}$ mice have fewer adipose macrophages than WT mice, as do mice deficient in the MCP-1 receptor, CCR2 (142, 166). Further, inhibiting CCR2 reverses adipose tissue macrophage accumulation in genetically obese mice (167). However, as with IL-6, MCP-1 also demonstrates inconsistent results. One study has demonstrated that *Ccl2*$^{-/-}$ mice are not protected against diet-induced adipose tissue inflammation (168).

Adiponectin is a hormone expressed exclusively by adipocytes (169). It has both metabolic and immune impacts on the liver. The expression of adiponectin is downregulated in the adipose tissue during obesity in both mice and humans (170). Adiponectin-deficient mice display severe insulin resistance when challenged with a high-fat, high-sucrose diet, which is rescued by the administration of an adenoviral vector expressing adiponectin (171). The insulin resistance that genetically obese mice display is greatly improved with the overexpression of adiponectin, and it also decreases the levels of circulating pro-inflammatory cytokines (172). Adiponectin polarizes macrophages towards the M2 phenotype; adipose tissue macrophages isolated from adiponectin-knockout mice have increased expression of M1 markers like *Tnf* and *Ccl2* and decreased expression of M2 markers like *Arg1* and *Clec10a* (173). Adiponectin also inhibits the production of TNFα in macrophages stimulated with LPS (174). Further, adiponectin inhibits the response of macrophages to TLR ligands, including LPS

(TLR4) and lipoteichoic acid (LTA, TLR2) (175). Treating genetically obese mice with exogenous adiponectin improves insulin sensitivity and hepatic steatosis (176).

Sexual dimorphism in adipose tissue inflammation

Obesity-related metabolic health complications also exhibit a sexual dimorphism. For example, pre-menopausal women have a much lower prevalence of cardiovascular disease then men in the same age group. However, post-menopausal women lose this protection (177). In humans, body fat is distributed differently between men and women. Typically, men have more abdominal adiposity whereas women have more gluteofemoral adiposity (178). Gluteofemoral adiposity is protective against the development of diabetes and cardiovascular disease. Women that have abdominal obesity develop metabolic disease similar to men. Post-menopausal women exhibit more abdominal adiposity, presumably due to the decline in estrogen levels, which could be one of the causes of a higher risk of cardiovascular disease in this group (178). A sexual dimorphism exists in rodent models of obesity; female animals are more resistant to the effects of diet-induced obesity than male animals (179). Male rats develop glucose intolerance when fed a high-fat diet, female rats do not. Additionally, high-fat diet fed male rats have greater expression of inflammatory markers in the adipose tissue compared to high-fat diet fed female rats (180). A direct comparison between male and female mice fed a high-fat diet reveals that male mice have greater adipose tissue inflammation; they have greater numbers

of crown-like structures as well as greater expression of pro-inflammatory cytokines. Male mice also have a much greater number of $CD11c^+$ adipose tissue macrophages (181). Male mice have worse glucose tolerance than their female counterparts, which is reversed when male mice are treated with 17, β-estradiol (182). Recently it was discovered that housing high-fat diet fed female mice at thermoneutral temperature greatly increases obesity, adipose tissue inflammation, and hepatic steatosis. Using the thermoneutral housing temperature will enable the use of female mice in high-fat diet and non-alcoholic fatty liver disease (NAFLD) studies, but how the higher housing temperature overcomes the sexual dimorphism in mice remains to be determined (183).

Adipose tissue in ALD

Alcohol impacts adipose tissue function in humans

In addition to affecting the liver and gut function described above, chronic alcohol consumption dysregulates adipose tissue function in humans. Serum adiponectin is increased in ALD patients in both men and women (184). When alcoholic cirrhosis patients are stratified, serum adiponectin levels are much higher in patients with more severe disease (185). Serum adiponectin levels are positively correlated with daily alcohol consumption and serum ALT levels, and they decrease over time with alcohol abstinence (186). The adipose tissue expression of the cytokines *TNF* and *IL10* is higher in acute AH patients than ALD patients without hepatitis (187). Cytokine mRNA expression in the adipose tissue correlates with liver injury scoring (187, 188). The expression of pro-

inflammatory markers in the adipose tissue is decreased in patients with mild liver lesions as early as one week of alcohol abstinence (188). Chronic alcohol consumption leads to inflammation in the adipose tissue, however the mechanisms through which this occurs are unknown. The elevation of adiponectin in ALD patients raises questions as to the function of this hormone in the protection against liver injury.

Adipose tissue function in ALD models

Inflammation

The current understanding of alcohol-induced adipose tissue inflammation is summarized in Figure 1.4. Alcohol increases the expression of pro-inflammatory markers in the adipose tissue of rodents. In rats, chronic alcohol consumption increases the expression of *Tnf*, *Il6*, and *Ccl2* in the adipose tissue (189-192). In mice, these pro-inflammatory cytokines increase as well as the expression of *Itgax* (CD11c) (193-195). Several mediators in alcohol-induced adipose tissue inflammation have been identified. The adipose tissue from alcohol-fed *Cyp2e1*$^{-/-}$ or *Bid*$^{-/-}$ mice do not exhibit the increase in *Tnf*, *Il6*, or *Ccl2* that occurs in their WT counterparts (194). Treating alcohol-fed mice with the PPARγ activator rosiglitazone reverses liver injury and normalizes expression of *Tnf*, *Il6*, and *Ccl2* in the adipose tissue (193, 195). Adiponectin is also important to alcohol-induced adipose tissue inflammation. Similar to obesity models, circulating adiponectin is decreased in alcohol-fed rodents (32, 176, 190, 191, 196). The lipid peroxidation product 4-HNE, a result of CYP2E1-mediated

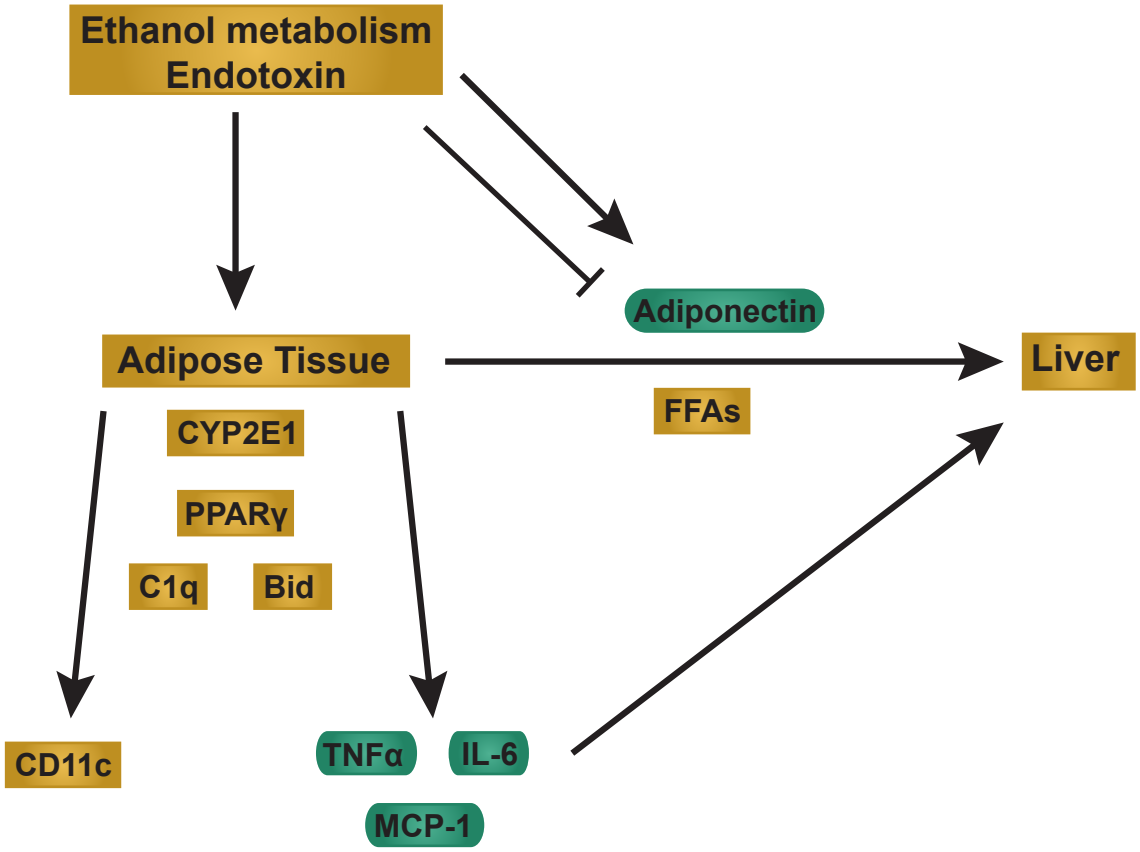

Figure 1.4: Current model of alcohol-induced adipose tissue inflammation. Ethanol metabolism and/or the presence of endotoxin in the adipose tissue results in the expression of TNFα, IL-6, and MCP-1, which can directly contribute to the inflammatory milieu in the liver, and CD11c, an M1 macrophage marker. The production of adiponectin is increased in ALD patients and is downregulated in rodent ALD models. The adipose tissue also releases FFAs, which may contribute to hepatic steatosis. CYP2E1, Bid, C1q, and PPARγ have all been demonstrated to mediate alcohol-induced adipose tissue inflammation.

ethanol metabolism, inhibits the release of adiponectin from differentiated adipocytes (197). Adipocytes isolated from the subcutaneous depot in alcohol-fed rats release less adiponectin than adipocytes from pair-fed controls (190). Administering full-length adiponectin to alcohol-fed mice reduces liver injury (176). This effect could be mediated in part by the impact of adiponectin on liver macrophages. Ethanol sensitizes macrophages to LPS-stimulated TNFα production. Pre-treating KCs isolated from alcohol-fed rats with adiponectin prior to LPS stimulation reverses this sensitization and decreases TNFα release (32, 198). Further, *ex vivo* adiponectin exposure shifts KCs isolated from alcohol-fed rats from a pro-inflammatory M1 phenotype to an anti-inflammatory, M2 phenotype (199). Interestingly, circulating adiponectin is increased in alcohol fed-mice that are fed a liquid diet high in saturated fats (200). Differences in nutritional intake in AH patients versus animal models could be one possible explanation for the discrepancy in the trends of circulating adiponectin

Metabolic Dysregulation

Alcohol has also been demonstrated to influence adipocyte metabolism. Alcohol-fed mice exhibit smaller adipocyte cell size, increased activation of HSL, and increased circulating glycerol or free fatty acids levels, indicating that the adipose tissue is actively undergoing lipolysis (193, 201, 202). A link between alcohol-induced adipose lipolysis and hepatic steatosis has been proposed. It was demonstrated, using deuterium-labeled lipids, that the presence of certain triacylglycerol species increases in the liver with a simultaneous decrease in the

adipose tissue. (203). Interestingly, using *in vitro* studies, it was determined that chronic alcohol exposure in fact inhibits stimulated lipolysis. Adipocytes isolated from alcohol-fed rats released less glycerol in response to β-adrenergic stimulation, compared to adipocytes from pair-fed rats (204, 205). Alcohol may be influencing lipolysis indirectly because it interferes with insulin-mediated suppression of lipolysis (204). Chronic alcohol consumption also results in increased hepatic glucose production and decreased insulin-stimulated glucose uptake in the adipose tissue, two indicators of the development of insulin resistance (189). The impact of alcohol on adipose tissue metabolism is unclear and requires further investigation.

Overview

Despite decades of research, there is a dearth of effective therapies for ALD patients. It is paramount to uncover how alcohol impacts other organs, particularly those that may contribute to liver injury, such as the adipose tissue. Adipose tissue inflammation is heavily involved in other disease, such as metabolic syndrome. Understanding the role of adipose tissue in ALD pathogenesis will deepen our understanding of this disease. This will facilitate the development of novel therapies. The overall goal of this thesis was to characterize adipose tissue inflammation in order to understand whether alcohol alters adipose tissue function. This will help to determine whether alcohol-induced adipose tissue inflammation impacts the liver, or whether it is collateral damage of liver injury and hepatic inflammation. In Chapter II, I establish that the

sexual dimorphism that occurs in response to chronic alcohol consumption is extended to the adipose tissue. Similar to what occurs in the liver, female mice have a higher degree of alcohol-induced adipose tissue inflammation than male mice. In Chapter III, I identify specific immune cell populations in the adipose tissue and determine how they are changed in response to alcohol consumption. Using a combination of germline and myeloid-specific TLR4 knockout mice, I demonstrate that alcohol polarizes adipose tissue macrophages to the M1 phenotype. This phenotype switch is dependent on the expression of TLR4 in cells of non-myeloid origin. Further, I discover that TLR4 is required for pro-inflammatory cytokine production in the liver, but not in the adipose tissue. Overall, this thesis characterizes alcohol-induced adipose tissue inflammation and uncovers a specific and limited role for TLR4.

CHAPTER II

Sexual dimorphism in alcohol induced adipose inflammation relates to liver injury

Introduction

ALD represents a spectrum of liver injury, starting with steatosis and progressing towards AH, fibrosis, cirrhosis, and HCC. ALD develops as a result of chronic, sustained drinking and is driven by both metabolic and immune insults (2, 34). Chronic alcohol exposure causes triglyceride accumulation in hepatocytes and promotes liver inflammation via endotoxin derived from the gut (30, 48, 53, 62, 63, 206).

In humans it is well established that women are more susceptible than men to develop ALD, despite consuming lower amounts of alcohol. For any amount of alcohol intake, women have a greater risk of developing ALD and progressing to cirrhosis than men (2, 13-16). Several factors have been proposed that may contribute to this phenomenon. First, women have a lower first pass metabolism (FPM) than men due to lower gastric alcohol dehydrogenase activity (17, 18). Second, women have a lower volume of distribution of alcohol than men due to lower total body water content and higher body fat content (17, 19). Third, estrogen can greatly influence alcohol-induced liver injury. Estrogens sensitize KCs to endotoxin injury (21, 22). Rodents exhibit this sexual dimorphism as well (23, 24, 27). Ovariectomized rats are protected from early alcohol-induced liver injury and supplementing with exogenous estrogen reverses this effect (25).

In addition to the direct metabolic and immune impacts on the liver, the influence of alcohol on adipose tissue inflammation is being studied. In both mice

and rats, chronic alcohol consumption induces expression of pro-inflammatory cytokines and chemokines in white adipose tissue (189-195). In humans, the production of cytokines in adipose tissue is correlated with acute AH score in a cohort of patients with ALD (187). Cytokine production in adipose tissue decreases in patients with mild liver lesions one week after cessation of drinking (188). Previous data has shown that chronic alcohol consumption decreases the production of adiponectin, a major adipokine, in rodent models (176, 207, 208). Infusing alcohol-fed mice with full-length recombinant adiponectin reverses liver injury (176). These studies demonstrate the impact of alcohol consumption on adipose tissue and the link between the adipose tissue and the liver. However, differences in body composition, with regards to women having higher body fat content, are not considered (19). Therefore, it remains to be determined whether sex-dependent consequences of alcohol consumption affect adipose tissue inflammation.

The aim of this study was to determine if adipose tissue inflammation also exhibits a sexually dimorphic response to alcohol consumption. Here we show that female mice have higher liver injury compared to male mice in a model of ALD. Using the clinically relevant NIAAA model of chronic-binge alcohol feeding we establish that alcohol-induced adipose tissue inflammation occurs to a higher degree in female mice, compared to male mice.

Results

The NIAAA ALD model induces greater liver injury in female mice despite lower alcohol consumption

In order to compare the extent of liver injury between male and female mice, ten-week old male and female C57BL/6J mice were subjected to the NIAAA model of chronic-binge alcohol feeding. Over the course of the experiment, male mice consumed higher amounts of the 5% alcohol diet than female mice (Figure 2.1 A). In support of higher alcohol consumption, male mice had a higher serum BAC than female mice at the end of the study (Figure 2.1 B). Regardless of the volume of alcohol that was consumed, male and female mice had similar increases in liver-to-body weight ratios (Figure 2.2 A). Furthermore, despite consuming lower amounts of alcohol, female mice had higher serum alanine aminotransferase (ALT) levels than their male counterparts (~2.3-fold) (Figure 2.2 B). Female mice also had elevated liver triglyceride content compared to male mice (Figure 2.2 C), which was confirmed by Oil Red O staining (Figure 2.2 D). Gene expression analysis of liver pro-inflammatory cytokines showed a significant upregulation of *Ccl2* mRNA in both male and female mice, however, female mice had greater *Ccl2* expression than male mice. *Il6* and *Tnf* expression were increased in female mice. The expression of the macrophage marker *Emr1* was decreased in both male and female mice, but the change was not significant. Interestingly, the expression of the monocyte marker *Ly6c1* was increased in male and female mice (Figure 2.2 E). Together, these

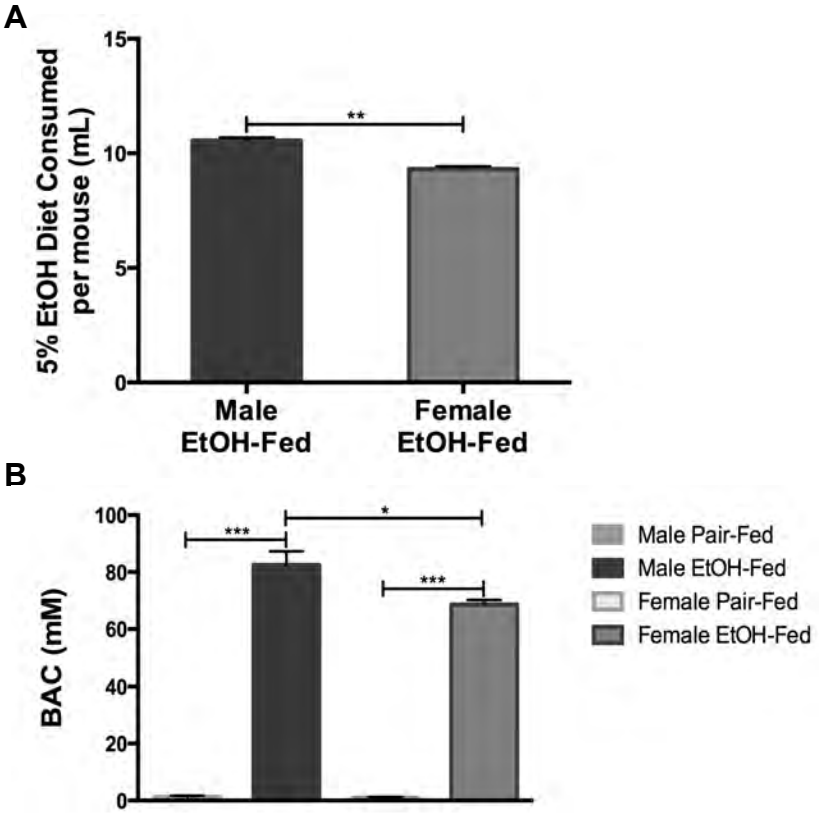

Figure 2.1: Male mice consume higher amounts of alcohol. Male and female mice were subjected to the NIAAA model. (A) Average daily consumption of the 5% Lieber-DeCarli diet per mouse. (B) Serum BAC at the time of sacrifice. * $p<0.05$, ** $p<0.01$, *** $p<0.001$. Data are represented as mean ± SEM. EtOH-fed: Alcohol-fed.

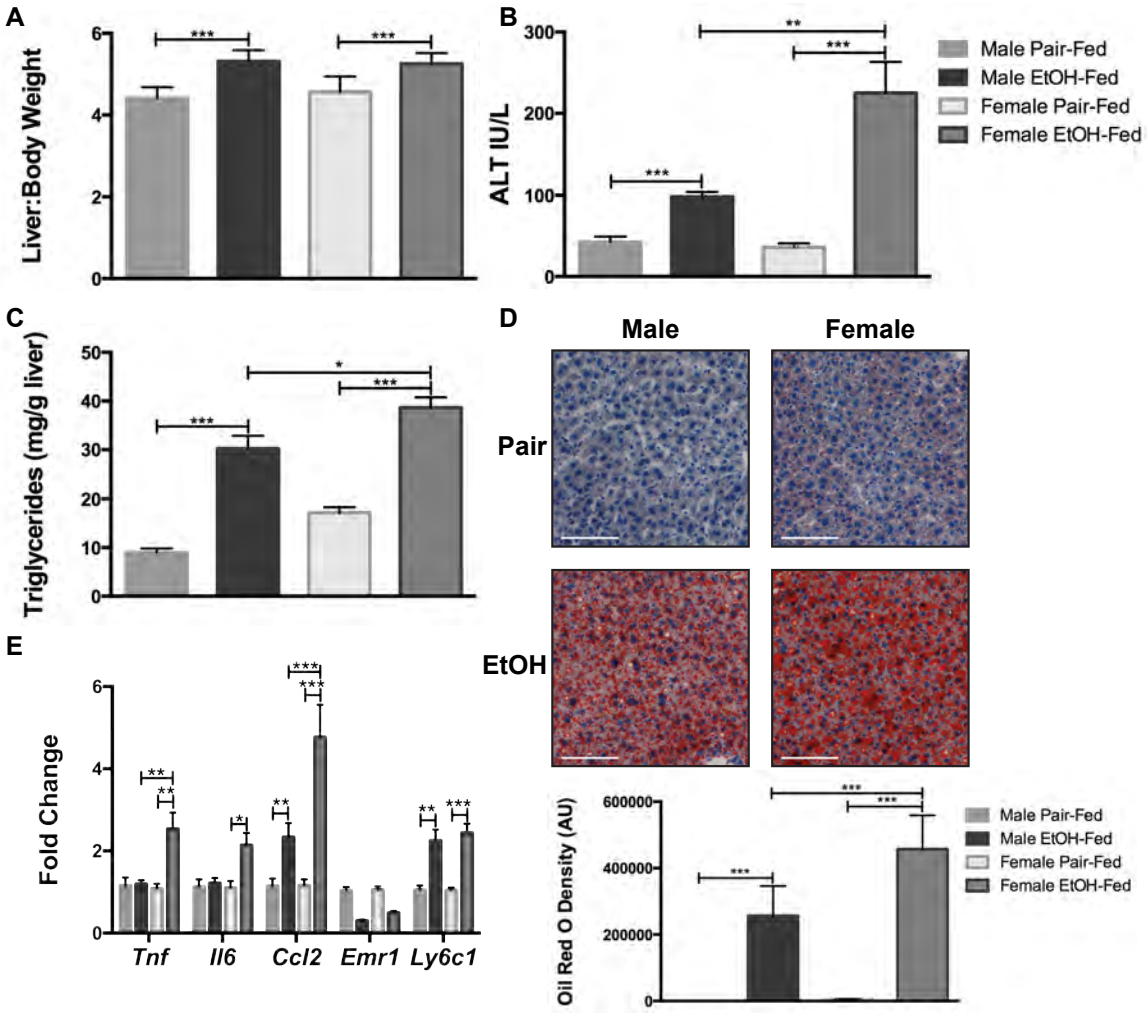

Figure 2.2: Female mice have more severe liver injury than male mice. (A) Liver-to-body weight ratio. (B) Serum (ALT) levels at the time of sacrifice. (C) Liver triglyceride content. (D) Representative Oil Red O staining of liver sections. Scale bar is set to 100 μm and magnification is at 100x. Quantitation was done with Fiji. (E) Liver mRNA levels of *Tnf*, *Il6*, *Ccl2*, *Emr1*, and *Ly6c1* were quantified by qPCR. * p<0.05, ** p<0.01, *** p<0.001. Data are represented as mean ± SEM.

data show that female mice exhibit a higher degree of alcohol-induced liver injury than male mice.

Chronic-binge alcohol feeding induces greater adipose tissue inflammation in female mice than in male mice

Considering the sex-dependent differences in human body fat composition, we wanted to determine if adipose tissue also exhibits a sexually dimorphic response to chronic-binge alcohol exposure. Perigonadal adipose tissue was collected and analyzed for expression of pro-inflammatory cytokines, chemokines, and immune cell markers. Pro-inflammatory cytokines and chemokines exhibited a sexually dimorphic profile, wherein there was a highly significant increase in expression of *Il6* mRNA in male mice and a trend of increase noted in female mice. On the other hand, *Ccl2* mRNA was increased only in female mice. *Tnf* mRNA levels were unchanged in male adipose tissue but female adipose tissue showed a trend towards increased expression (Figure 2.3 A). Alcohol consumption increased the expression of the macrophage marker *Emr1* and the activation markers *Cd68*, *Itgam*, and *Itgax* in female, but not male mice, without any effect on *Ccr2* (Figure 2.3 B). Histological analysis showed no overt differences in adipose tissue morphology between the sexes (Figure 2.3 C). Unexpectedly, the NIAAA model did not reduce serum adiponectin levels. Here, alcohol increased adiponectin production in both male and female mice, with higher levels in female mice (Figure 2.3 D). Overall, these results show that the

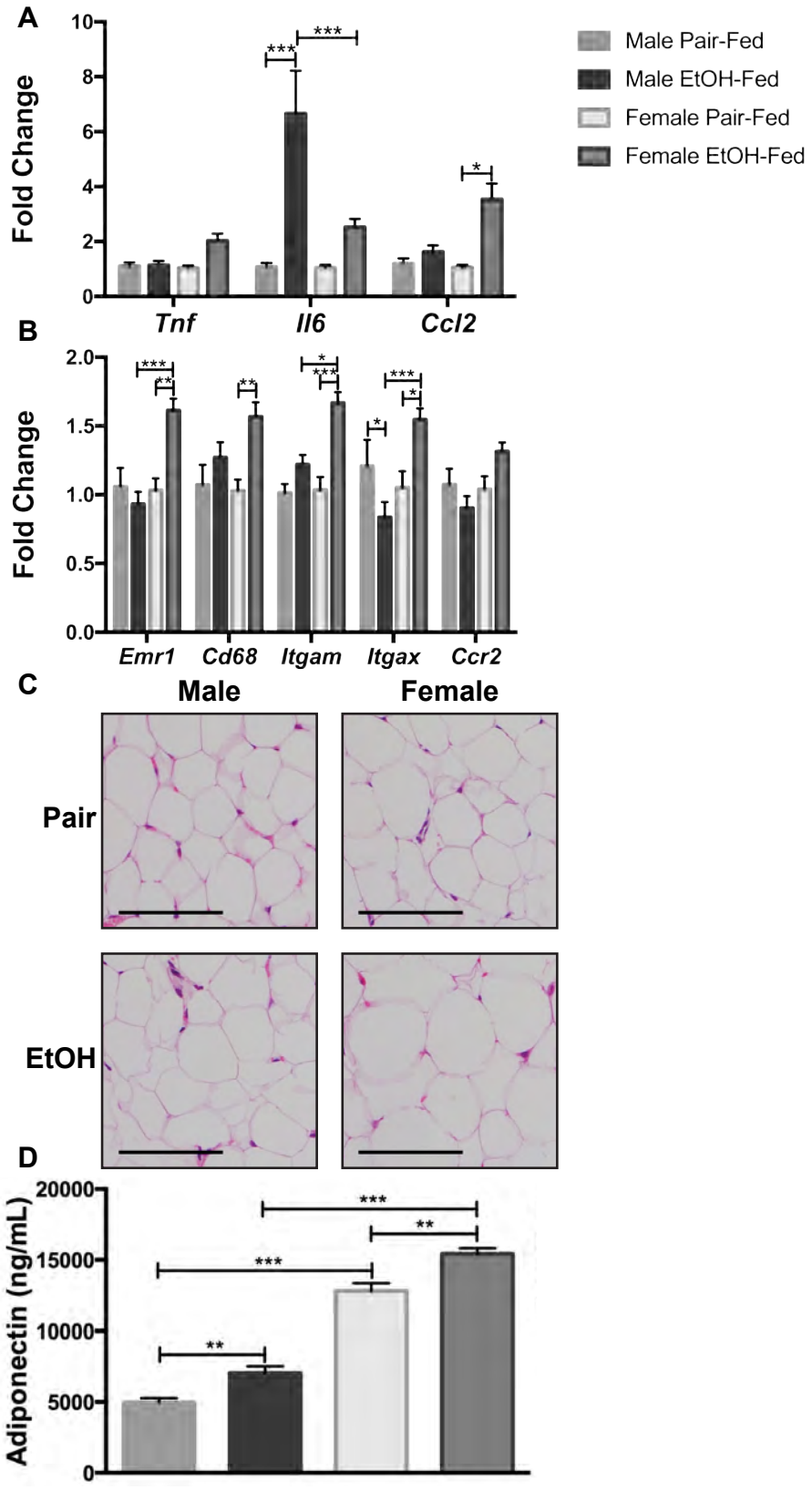
A
Fold Change
10
8
6
4
2
0
***
***
***
*
Tnf
Il6
Ccl2
Male Pair-Fed
Male EtOH-Fed
Female Pair-Fed
Female EtOH-Fed
B
Fold Change
2.0
1.5
1.0
0.5
0.0
Emr1
Cd68
Itgam
Itgax
Ccr2
C
Male
Female
Pair
EtOH
D
Adiponectin (ng/mL)
20000
15000
10000
5000
0
***
**
***
**

Figure 2.3: Female mice have a higher degree of adipose tissue inflammation. Perigonadal adipose tissue mRNA levels of (A) *Tnf*, *Il6*, and *Ccl2* and (B) *Emr1*, *Cd68*, *Itgam*, *Itgax*, and *Ccr2* were quantified by qPCR. (C) H&E staining of perigonadal adipose tissue. Scale bar is set to 100 μm and magnification is at 100x. (D) Serum adiponectin levels were measured by ELISA. * $p<0.05$, ** $p<0.01$, *** $p<0.001$. Data are represented as mean ± SEM.

NIAAA model induces adipose tissue inflammation in female mice concomitant to higher liver injury.

Chronic-binge alcohol feeding increases circulating endotoxin and innate immune activation markers in female mice

Alcohol sensitizes macrophages to endotoxin/LPS stimulation, due to alcohol-induced oxidative stress (32). To determine whether macrophages are sensitized to alcohol in a sexually dimorphic manner, we exposed bone marrow derived macrophages (BMDMs) from male and female mice *in vitro* to chronic alcohol and analyzed cytokine expression to a subsequent challenge by LPS. Female derived BMDMs produced more TNFα than male derived BMDMs in response to LPS, in the presence or absence of alcohol (Figure 2.4 A). However, alcohol sensitized male and female BMDMs equally significantly; alcohol increased LPS-induced TNFα production to 1.7-fold in male BMDM and 1.5-fold in female BMDMs, compared to LPS alone (Figure 2.4 A).

Since alcohol-induced macrophage sensitization to LPS stimulation did not differ between male and female macrophages, we wanted to determine if there were sex-dependent differences in circulating LPS, the expression of TLRs that are important in its recognition, or both (209, 210). Previous data in models of ALD show higher circulating endotoxin in female rodents, compared to their male counterparts (23, 24). We show that serum endotoxin levels are unchanged in alcohol-fed male mice compared to pair-fed male mice, whereas a trend of increase in alcohol-fed female mice (approximately 1.4-fold) compared to pair-fed

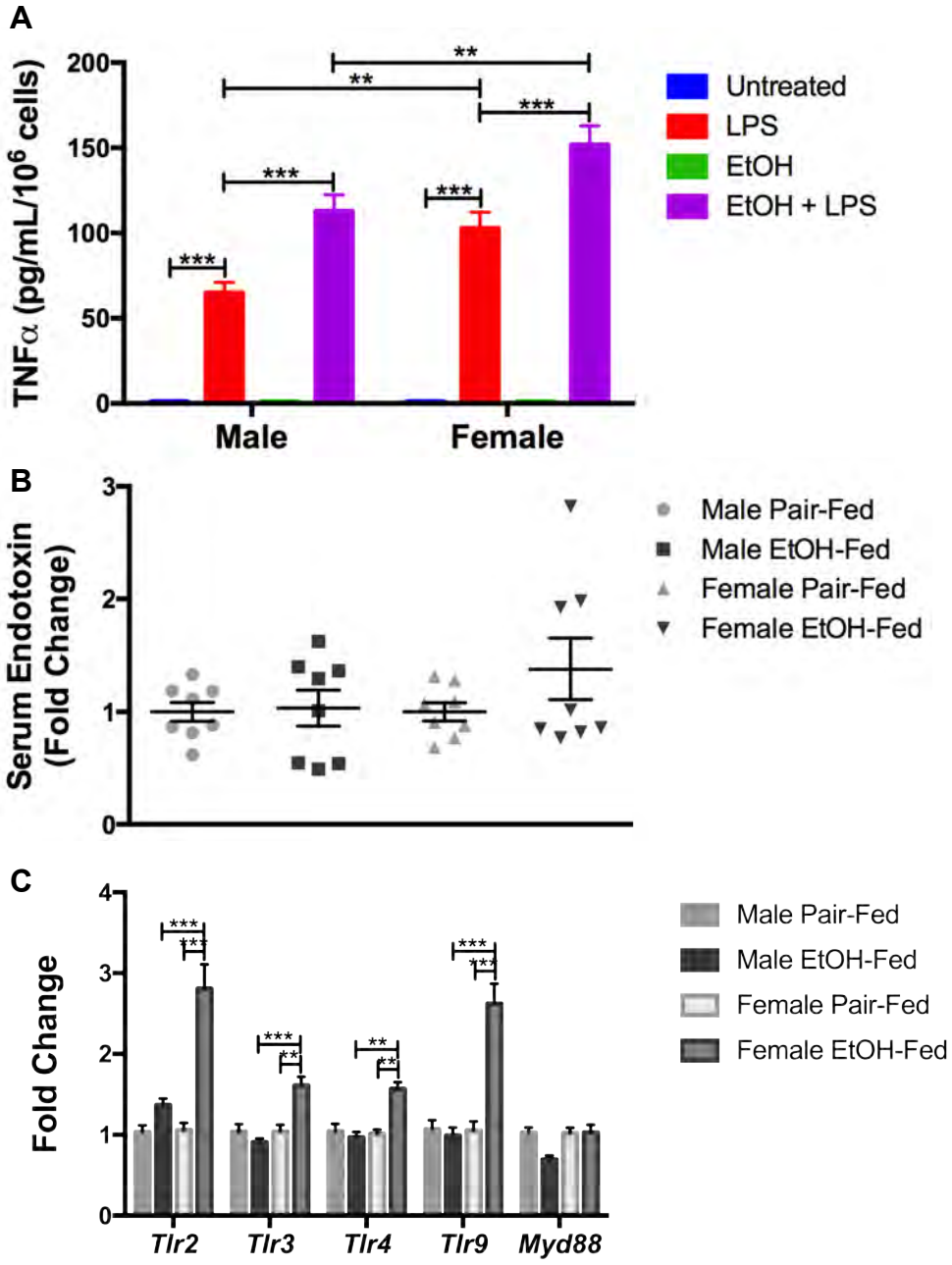

Figure 2.4: Increased adipose tissue inflammation is due to *Tlr* expression. (A). BMDMs were cultured in the presence of 25mM ethanol for 5 days and then stimulated with 100ng/mL LPS for 18 hours. TNFα was measured in the cell supernatants by ELISA. (B) Serum endotoxin levels at time of sacrifice. (C) Perigonadal adipose tissue mRNA levels of *Tlr2*, *Tlr3*, *Tlr4*, *Tlr9*, and *Myd88* were quantified by qPCR. * $p<0.05$, ** $p<0.01$, *** $p<0.001$. Data are represented as mean ± SEM.

female mice was noted (Figure 2.4 B). Further, female adipose tissue, but not male adipose tissue, showed an increase in several *Tlr* genes: *Tlr2*, *Tlr3*, *Tlr4*, and *Tlr9,* indicating either an upregulation of these genes in resident adipose tissue cells or an increased number of TLR-expressing cells in alcohol-fed female mice (Figure 2.4 C). Expression of another common adaptor gene *Myd88* was unchanged in both sexes. These data shows that while alcohol does not sensitize macrophages in a sex-dependent manner, circulating endotoxin and increased expression of TLRs in female mice could be potential mechanisms contributing to the sexual dimorphism in alcohol-induced adipose tissue inflammation.

Summary

In this chapter, I explored the differences between male and female mice in response to the NIAAA model. A previously published study using the same model only described the differences in circulating liver enzyme levels in male and female mice (27). The work I present here builds upon that to develop a more detailed analysis of the sexual dimorphism that occurs in mice in response to this specific model. Further, I uncovered that this sexual dimorphism extends to the adipose tissue; female mice have greater liver injury and adipose tissue inflammation despite consuming less alcohol. Lastly, I demonstrate that female mice have higher expression of innate immune cell markers in the adipose tissue in response to the NIAAA model, indicating a role for innate immune cells in alcohol-induced adipose tissue inflammation.

Materials and Methods

Animals and experimental models

Ten-week old male and female C57BL/6J mice were purchased from Jackson Laboratories (Bar Harbor, ME). Mice were subjected to the NIAAA model, which recapitulates the chronic-binge drinking patterns of AH patients, as described earlier (123). Briefly, a total of 18 mice per sex were divided into two groups (n=9 per group). One group was fed a 5% ethanol (v/v) Lieber-DeCarli diet (Bio-Serv, Flemington, NJ.) for 10 days, following a one-week ramp up period. On the eleventh day, mice received an ethanol gavage (5 g/kg body weight, 31.5% ethanol) and were sacrificed nine hours later. The other group was fed an isocaloric control diet during the feeding and a maltose dextrin (Bio-Serv, Flemington, NJ.) gavage was administered nine hours before sacrifice. Blood was collected for serum isolation. Perigonadal adipose tissue was chosen as a representative depot for visceral adipose tissue because it is associated with metabolic disease (211). The adipose tissue was excised and fixed in 10% buffered formalin or snap frozen. Livers were excised and snap frozen, preserved in RNA*later* RNA Stabilizing Reagent (Qiagen GmbH, Hilden, Germany), fixed in 10% buffered formalin for histological analysis, or frozen in O.C.T. Compound (Tissue-Tek, Sakura Finetek USA, Inc., Torrance, CA).

Ethics statement

All animals received proper care in accordance with the *Guide for the Care and Use of Laboratory Animals* from the National Institutes of Health. The

protocol was approved by the Institutional Animal Care and Use Committee of the University of Massachusetts Medical School (protocol number A-2393-15). Animals were euthanized by carbon dioxide asphyxiation followed by cervical dislocation.

Serum analysis

BAC was measured in serum using the Alcohol Reagent and the AM1 Alcohol Analyzer (Analox Instruments Ltd., London, UK). Serum alanine aminotransferase levels were measured using the Liquid ALT reagent set (Pointe Scientific Inc., Canton, MI). Serum adiponectin levels were measured using the Mouse Adiponectin/Acrp30 Quantikine ELISA kit (R&D systems, Minneapolis, MN). Serum endotoxin was measured using the Limulus Amebocyte Lysate (LAL) QCL-1000 kit (Lonza Walkersville, Inc., Walkersville, MD).

Liver triglycerides

Liver triglycerides were extracted and quantified as follows: liver tissue was homogenized in a 5% NP-40 solution. Samples were heated to 95°C for five minutes, cooled on ice, and then subsequently heated to 95°C for another five-minute incubation. Samples were spun at 14,000 rpm in a room temperature centrifuge, and supernatants were used to quantify triglycerides with the L-Type TG M kit (Wako Diagnostics, Wako Life Sciences Inc., Mountain View, CA).

Histological analysis

Sections of formalin-fixed adipose tissue samples were embedded and stained with hematoxylin and eosin and were analyzed for histological features.

Frozen liver sections were stained with Oil Red O. Images were captured using an Olympus BX51 microscope (Olympus, Waltham, MA) and NIS-Elements Advance Research software (Nikon Instruments Inc., Melville, NY). Oil Red O quantitation was performed using Fiji software (Schneider 2012 Nat Methods, Schindelin 2012 Nat Methods).

RNA extraction, cDNA synthesis, and qPCR analysis

Total RNA was extracted from RNA*later* preserved livers and flash frozen adipose tissue using the RNeasy Mini Kit (Qiagen GmbH, Hilden, Germany), according to manufacturer's instructions. Adipose tissue was homogenized in QIAzol (Qiagen GmbH, Hilden, Germany) and subjected to a chloroform extraction before proceeding with RNA isolation. RNA concentration was measured with a NanoDrop 2000 (ThermoScientific, Wilmington, DE). Adipose tissue cDNA was synthesized using the Reverse Transcription System (Promega, Madison, WI) and liver cDNA was synthesized using the iScript Reverse Transcription Supermix for RT-qPCR (Biorad Laboratories, Hercules, CA). mRNA transcript levels were quantified using iTAQ Universal SYBR Green Supermix and CFX Connect Real-Time PCR Detection System (Biorad Laboratories, Hercules, CA) and normalized to *18s* ribosomal RNA. Primer sequences are listed in Table 2.1. *Ly6c1* expression was quantified using QuantiTect Primer assay #QT00247604 (Qiagen GmbH, Hilden, Germany).

Bone marrow-derived macrophages

Bone marrow was harvested from the femurs of 10-week old male and female C57BL/6J mice. Bone marrow cells were plated in RMPI 1640 (Thermo Fisher Scientific, Waltham, MA) supplemented with 10% Fetal Bovine Serum (Gemini Bio-Products, West Sacramento, CA), 1% Penicillin Streptomycin (Thermo Fisher Scientific, Waltham, MA), and 1% L-glutamine 200mM (Thermo Fisher Scientific, Waltham, MA) ("complete RPMI") onto non-tissue culture treated 10 cm plates in the presence of 50 ng/mL Recombinant Murine Macrophage Colony Stimulating Factor (M-CSF) (Peprotech, Rocky Hill, NJ) to induce differentiation. On day four of differentiation, cells were supplemented with fresh complete RMPI with 50 ng/mL M-CSF. On day 6, cells were harvested in 1mM EDTA in PBS and seeded in 6-well plates at a density of one million cells per well, in the presence of 50 ng/mL M-CSF and allowed to adhere overnight. After adherence, cells were cultured in the presence of 5 ng/mL M-CSF. To mimic chronic alcohol conditions, BMDMs were cultured in 25 mM ethanol in humidified chambers for 5 days as described previously by our group (212). Cells were stimulated with 100 ng/mL LPS (Sigma-Aldrich Corp., St. Louis, MO) for 18 hours, at which point supernatants were collected and BMDMs were counted for ELISA analysis. The BD OptEIA Mouse TNFα (Mono/Mono) ELISA set (BD Biosciences, San Diego, CA) was used to measure TNFα protein in cell supernatants. TNFα protein concentration was normalized to cell number.

Statistical analysis

Data are represented as mean ± SEM. All statistical analysis was performed using Graphpad Prism 6.0. Student's t-test was used to determine the difference between two groups; Two-way ANOVA was used to determine the difference between four groups.

Table 2.1: List of primer sequences 5'-3'

Gene	Sequence
18s forward	GTAACCCGTTGAACCCCATT
18s reverse	CCATCCAATCGGTAGTAGCG
Ccl2 forward	CAGGTCCCTGTCATGCTTCT
Ccl2 reverse	TCTGGACCCATTCCTTCTTG
Ccr2 forward	GTGTACATAGCAACAAGCCTCAAAG
Ccr2 reverse	CCCCCACATAGGGATCATGA
Cd68 forward	CCCACAGGCAGCACAGTGGAC
Cd68 reverse	TCCACAGCAGAAGCTTTGGCCC
Emr1 forward	TGCATCTAGCAATGGACAGC
Emr1 reverse	GCCTTCTGGATCCATTTGAA
Il6 forward	ACAACCACGGCCTTCCCTACTT
Il6 reverse	CACGATTTCCCAGAGAACATGTG
Itgam forward	ATGGACGCTGATGGCAATACC
Itgam reverse	TCCCCATTCACGTCTCCCA
Itgax forward	CTGGATAGCCTTTCTTCTGCTG
Itgax reverse	GCACACTGTGTCCGAACTCA
Myd88 forward	AGAACAGACAGACTATCGGCT
Myd88 reverse	CGGCGACACCTTTTCTCAAT
Tlr2 forward	ACAATAGAGGGAGACGCCTTT
Tlr2 reverse	AGTGTCTGGTAAGGATTTCCCAT
Tlr3 forward	AATCCTTGCGTTGCGAAGTG
Tlr3 reverse	ACCCCGGGGAGAACTCTTTA
Tlr4 forward	GCCTTTCAGGGAATTAAGCTCC
Tlr4 reverse	AGATCAACCGATGGACGTGTAA
Tlr9 forward	TCCCAACATGGTTCTCCGTC
Tlr9 reverse	GGTGGTGGATACGGTTGGAG
Tnf forward	GAAGTTCCCAAATGGCCTCC
Tnf reverse	GTGAGGGTCTGGGCCATAGA

CHAPTER III

Alcohol-induced adipose tissue macrophage phenotype switching is independent of myeloid toll-like receptor 4 expression

Introduction

ALD is a spectrum of liver injury that occurs due to chronic alcohol consumption. The liver is the primary site of pathogenesis, wherein the early stage of fatty liver, steatosis, can progress to more severe forms of liver injury, fibrosis and cirrhosis, with continued heavy drinking. This injury results from a combination of pathogenic events including inflammation in the liver, which is driven by immune cells including the resident macrophages, KCs, and storage of excess lipids in hepatocytes (2, 34). In addition to the liver, the adipose tissue has been considered as a secondary site of pathogenesis in ALD. Similar to the liver, chronic alcohol consumption drives adipose tissue inflammation and may also affect adipocyte metabolism (34, 189-195, 201, 213). Using different models of chronic alcohol exposure, several groups have established that alcohol causes an increase in the expression of pro-inflammatory cytokines and immune cell markers in the adipose tissue (189-195, 213). Factors including PPARγ, CYP2E1, Bid, and C1q have all been suggested as potential mediators of adipose tissue inflammation (193-195). However, specific immune cell types involved and related mechanisms that drive alcohol-induced adipose tissue inflammation remain largely unknown.

Adipose tissue inflammation has well been characterized in obesity models. As obesity progresses, pro-inflammatory immune cells, most importantly M1 macrophages, accumulate within the adipose tissue and drive the expression of pro-inflammatory cytokines and chemokines (133-136, 139, 146-153, 155,

156, 159, 211, 214). Concurrently, anti-inflammatory or immunosuppressive cell types and cytokines are decreased in adipose tissue (136, 139, 154, 157). Ultimately, this results in a shift to pro-inflammatory state within the adipose tissue that contributes to metabolic dysfunction, impacting the adipose tissue and the liver (132, 133, 159, 211, 214).

The role of TLRs, more specifically TLR4, has been investigated in both ALD and obesity models. TLR4 is the receptor for endotoxin/LPS and drives pro-inflammatory cytokine production (113). Endotoxemia is considered to be a key driver of ALD pathogenesis (2, 34). TLR4-deficient mice are protected against alcohol-induced liver injury (65, 115, 118, 119). Global TLR4 knockout (TLR4KO) mice exhibit protection against high-fat diet-induced adipose tissue inflammation and insulin resistance (215-217). The impact of TLR4 expression on alcohol-induced adipose tissue inflammation is unknown. Here we use both germline and tissue-specific deletion of *Tlr4* in mice to determine the role of TLR4 in adipose tissue inflammation in a model of chronic, multiple-binge alcohol exposure. In this model, WT mice show an increase in the number of M1 macrophages and DCs as well as inflammatory cytokine production following alcohol exposure. DC accumulation is prevented in both global and myeloid-specific TLR4KO mice. In contrast, global, but not myeloid-specific, TLR4KO mice are protected against M1 macrophage phenotype switching, whereas cytokine and chemokine production occurs independent of TLR4. Further, changes in the neutrophil and $CD8^+$ T cell populations are independent of TLR4. Our results suggest that TLR4 is one part

of a large network, which involves cells other than those of myeloid origin, to drive alcohol-induced adipose tissue inflammation.

Results

Alcohol induces adipose macrophage phenotype switching through TLR4

TLR4 has been implicated in both alcohol-induced liver inflammation and high-fat diet-induced adipose tissue inflammation (65, 115, 118, 119, 215-217). In order to identify TLR4-driven mechanisms that contribute to alcohol-induced adipose tissue inflammation we subjected female, C57BL/6J (WT) mice and global TLR4 knockout mice (TLR4KO) to the chronic, multiple-binge model of alcohol exposure, which is a model representative of alcoholic steatohepatitis (ASH) (68). Previously we have shown that the NIAAA model of chronic, single-binge alcohol exposure causes adipose tissue inflammation in female mice, which includes increased expression of pro-inflammatory cell markers (213). Here, we used flow cytometry in order to identify the specific cell populations that contribute to alcohol-induced adipose inflammation. The stromal vascular fraction (SVF) was isolated from perigonadal white adipose and stained for flow cytometry analysis. $CD45^+$ leukocytes were identified and separated into myeloid and lymphoid populations (Figure 3.1 A). Macrophages ($CD11b^+F4/80^+$) were identified in the myeloid population (Figure 3.1 B). The number of total macrophages ($CD11b^+F4/80^+$) relative to the total number of SVF cells was unchanged in WT and TLR4KO alcohol-fed mice, compared to their respective pair-fed controls (Figure 3.1 C).

In obesity models, adipose tissue macrophage phenotype switching occurs wherein CD11c-expressing M1 macrophages become the predominant

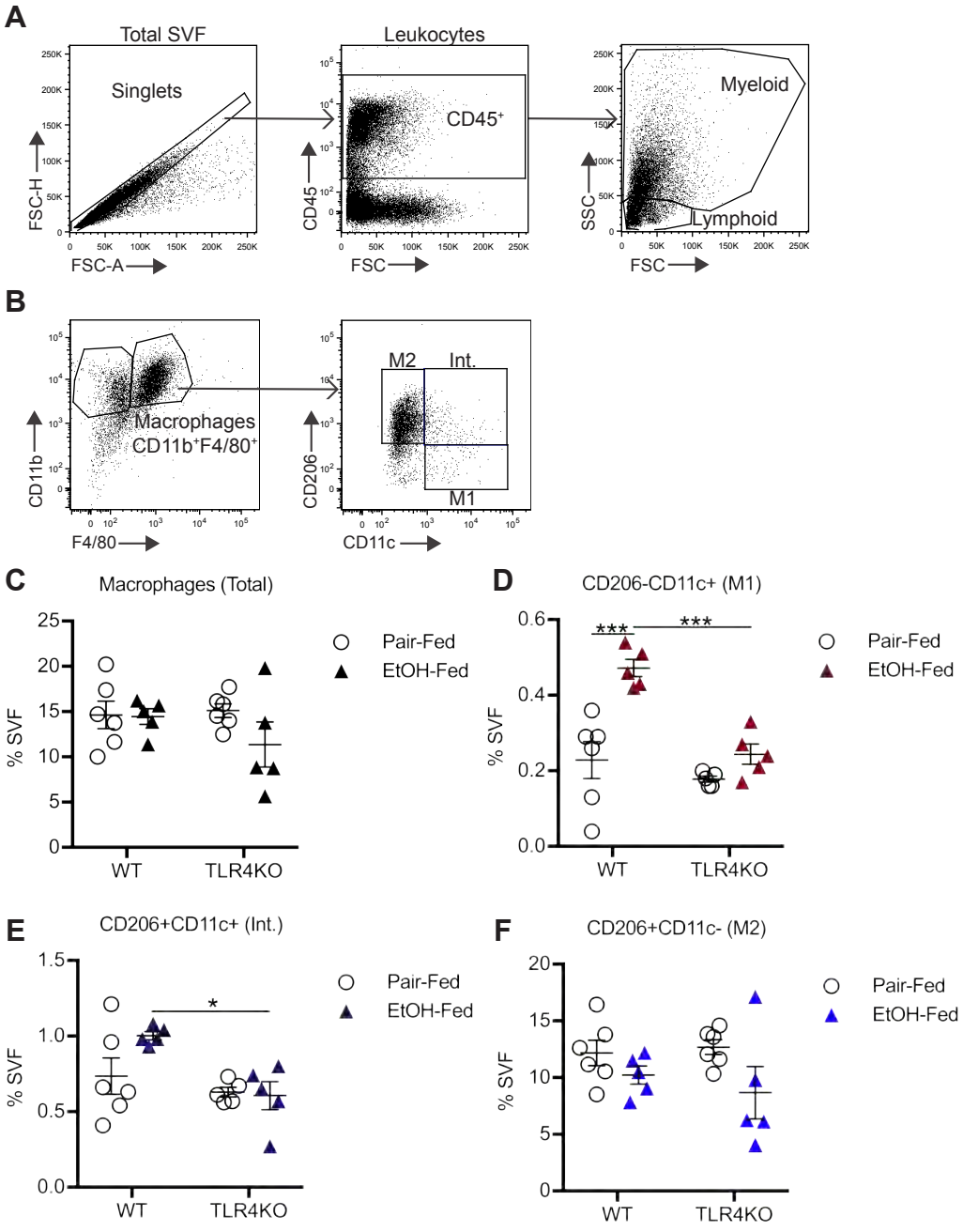
A
Total SVF
Singlets
FSC-H
FSC-A
Leukocytes
CD45+
CD45
FSC
Myeloid
Lymphoid
SSC
FSC
B
Macrophages
CD11b+F4/80+
CD11b
F4/80
M2
Int.
M1
CD206
CD11c
C
Macrophages (Total)
% SVF
Pair-Fed
EtOH-Fed
WT
TLR4KO
D
CD206-CD11c+ (M1)
***
***
% SVF
Pair-Fed
EtOH-Fed
WT
TLR4KO
E
CD206+CD11c+ (Int.)
*
% SVF
Pair-Fed
EtOH-Fed
WT
TLR4KO
F
CD206+CD11c- (M2)
% SVF
Pair-Fed
EtOH-Fed
WT
TLR4KO

Figure 3.1: Chronic, multiple-binge alcohol increases adipose M1 macrophages in WT but not TLR4KO mice. WT (C57BL/6J) and TLR4KO mice were subjected to the chronic, multiple-binge alcohol model and the SVF isolated from perigonadal adipose tissue was analyzed by flow cytometry. (A-B) Representative gating strategy. (A) Total SVF cells are defined as singlets (*left*), leukocytes as $CD45^+$ cells (*middle*), and myeloid and lymphoid populations were identified based on forward- and side-scatter (*right*). (B) The myeloid population was gated on CD11b and F4/80 to identify total macrophages ($CD11b^+F4/80^+$) (*left*) and macrophages were further gated on CD206 and CD11c to identify M2 macrophages ($CD206^+CD11c^-$), intermediate macrophages ($CD206^+CD11c^+$), and M1 macrophages ($CD206^-CD11c^+$) (*right*). Quantification of (C) total macrophages, (D) M1 macrophages, (E) Intermediate macrophages, and (F) M2 macrophages as a percentage of total SVF cells. n=5-6. Data are represented as mean ± SEM, * $p < 0.05$, ** $p < 0.01$, ***$p < 0.001$, **** $p < 0.0001$.

cell type over CD206-expressing M2 anti-inflammatory macrophages (133, 136, 139, 159, 214). Here, we identified three different macrophage phenotypes along this spectrum: M1 ($CD206^{-}CD11c^{+}$), an intermediate (Int.), mixed phenotype ($CD206^{+}CD11c^{+}$), and M2 ($CD206^{+}CD11c^{-}$) (Figure 3.1 D-F). Chronic, multiple-binge alcohol exposure increased the number of M1 macrophages in WT, but not TLR4KO mice, compared to pair-fed controls (Figure 3.1 D). The number of intermediate and M2 macrophages were both unchanged in alcohol-fed WT and TLR4KO mice (Figure 3.1 E and F). Alcohol-fed TLR4KO mice had fewer intermediate macrophages than alcohol-fed WT mice (Figure 3.1 E).

Alcohol changes the immune cell composition of adipose tissue

Adipose tissue inflammation is not dependent solely on macrophages; other immune cell types such as DCs, neutrophils, B, and T cells have been implicated in the inflammatory process (159, 211, 214). We analyzed the SVF for the presence of these immune cell populations (Figure 3.2 A and Figure 3.3 A). Alcohol increased the number of DCs ($F4/80^{-}CD11b^{+}CD11c^{+}$) in WT, but not TLR4KO mice, similar to M1 macrophages (Figure 3.2 B). The number of neutrophils ($F4/80^{-}CD11b^{+}Gr1^{+}$) showed a trend of increase in both alcohol-fed WT and TLR4KO mice when compared to pair-fed mice (Figure 3.2 C). Both macrophages and DCs act as APCs in the adipose tissue by engaging the adaptive immune response (146, 147, 149). We quantified the number of B and T cells to assess whether this model results in the activation of the adaptive immune system in the adipose tissue (Figure 3.3 A). The number of B cells

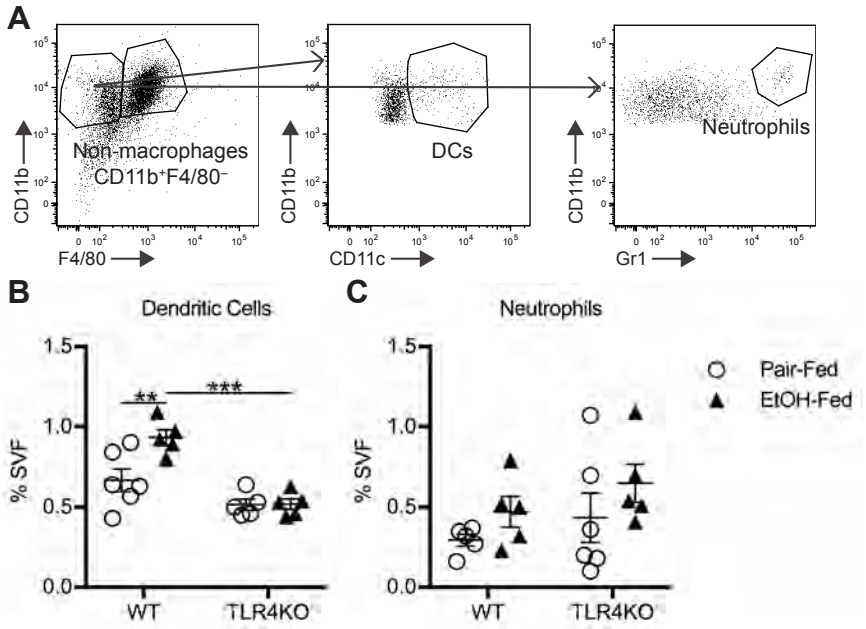

Figure 3.2: Chronic, multiple-binge alcohol increases adipose DCs in WT but not TLR4KO mice. WT (C57BL/6J) and TLR4KO mice were subjected to the chronic, multiple-binge alcohol model and the SVF isolated from perigonadal adipose tissue was analyzed by flow cytometry. (A) Representative gating strategy. Non-macrophage myeloid cells ($CD11b^{+}F4/80^{-}$) (*left*) were gated on CD11b and CD11c to identify DCs ($CD11b^{+}CD11c^{+}$) (*middle*) and CD11b and Gr1to identify neutrophils ($CD11b^{+}Gr1^{+}$) (*right*). Quantification of (B) DCs and (C) Neutrophils as a percentage of total SVF cells. n=5-6. Data are represented as mean ± SEM, * p <0.05, ** p <0.01, ***p<0.001, **** p<0.0001.

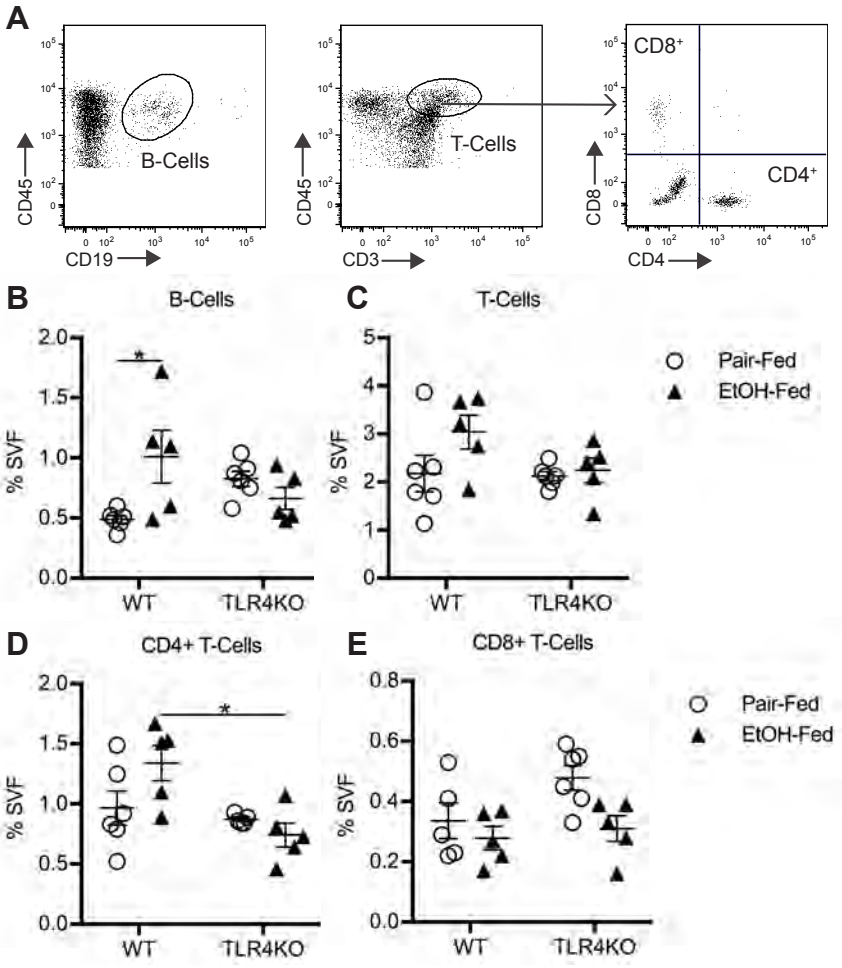

Figure 3.3: Chronic, multiple-binge alcohol increases adipose B-cells in WT but not TLR4KO mice. WT (C57BL/6J) and TLR4KO mice were subjected to the chronic, multiple-binge alcohol model and the SVF isolated from perigonadal adipose tissue was analyzed by flow cytometry. (A) Representative gating strategy. Lymphoid cells were gated on CD45 and CD19 to identify B-cells ($CD45^+CD19^+$) (*left*) or CD45 and CD3 to identify total T-cells ($CD45^+CD3^+$) (*middle*). T-cells were further gated on CD4 and CD8 to identify $CD4^+$ ($CD4^+CD8^-$) or $CD8^+$ ($CD4^-CD8^+$) T-cells (*right*). Quantification of (B) B-cells, (C) T-cells, (D) $CD4^+$ T-cells, and (E) $CD8^+$ T-cells as a percentage of total SVF cells. n=5-6. Data are represented as mean ± SEM, * p <0.05, ** p <0.01, ***p<0.001, **** p<0.0001.

($CD45^+CD19^+$) increased in alcohol-fed WT mice, but this elevation was absent in alcohol-fed TLR4KO mice (Figure 3.3 B). There was a trend of increase in the number of T cells in alcohol-fed WT mice ($CD45^+CD3^+$), more specifically $CD4^+$ T cells when both populations are compared to their respective pair-fed controls, but this was not significant (Figure 3.3 C and D). On the other hand, these populations were unchanged in alcohol-fed TLR4KO mice. However, the number of $CD4^+$ T cells in alcohol-fed TLR4KO was significantly lower than alcohol fed WT mice (Fig 3.3 D). Alcohol did not change the number of $CD8^+$ T cells in WT or TLR4KO mice (Figure 3.3 E). Together, this data shows that in addition to macrophage phenotype switching, increases in DCs, and to some extent B cells and T cells, also contribute to alcohol-induced adipose inflammation.

Alcohol induces the expression of pro-inflammatory cytokines and chemokines in the SVF

To assess whether the M1 macrophages and other cell types in the adipose tissue produce cytokines during alcohol-induced inflammation, we measured the expression of pro-inflammatory cytokines and chemokines important to adipose inflammation (133). Chronic, multiple-binge alcohol increased the expression of both *Il6* and *Ccl2* in the SVF of WT and TLR4KO mice compared to pair-fed controls (Figure 3.4 A and B). This is similar to previous data obtained using the NIAAA model from whole adipose tissue analysis (213). Alcohol did not increase the expression of *Il1b* in WT or TLR4KO SVF (Figure 3.4 C). CXCL1 is a chemokine important for neutrophil chemotaxis

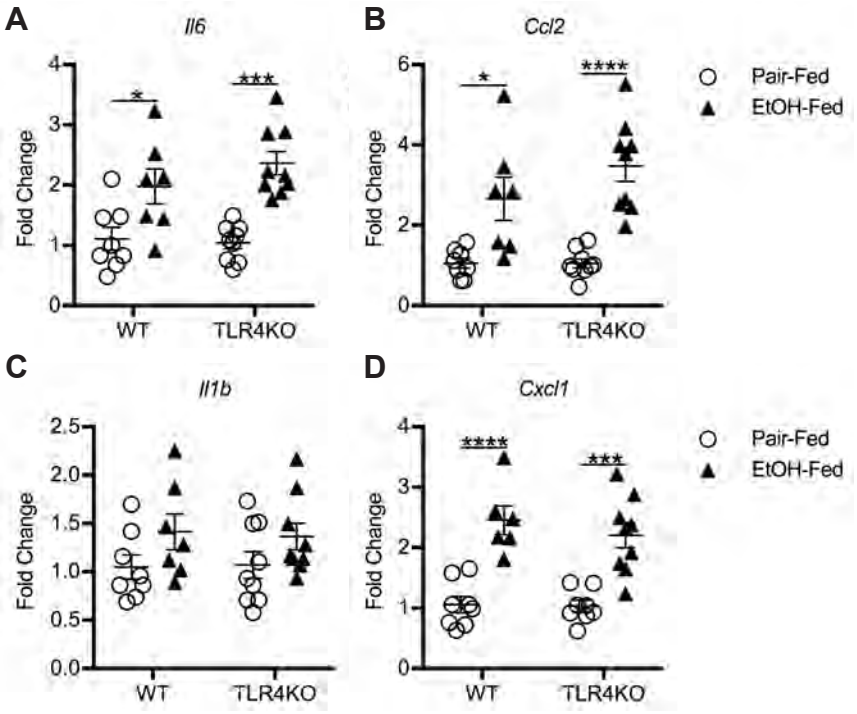

Figure 3.4: TLR4KO mice are not protected against inflammatory cytokine production. WT (C57BL/6J) and TLR4KO mice were subjected to the chronic, multiple-binge alcohol model and the SVF isolated from perigonadal adipose tissue was analyzed qPCR. mRNA expression of (A) *Il6*, (B) *Ccl2*, (C) *Il1b*, and (D) *Cxcl1*. Each genotype is normalized to respective pair-fed controls. n=7-9, some data points are the result of pooling SVF from two individual mice. Data are represented as mean ± SEM, * p <0.05, ** p <0.01, ***p<0.001, **** p<0.0001.

and recent studies in the ALD field have demonstrated the importance of neutrophils in alcohol-induced liver inflammation (67, 68, 70). Alcohol increased the expression of *Cxcl1* in the SVF of WT and TLR4KO mice (Figure 3.4 D). Together, our data shows that alcohol-induced cytokine/chemokine expression in the adipose tissue occurs independent of TLR4 and likely involves cells other than myeloid cells.

Characterization of myeloid-specific TLR4 knockout mice

In order to further understand how TLR4 expression on myeloid cells contributes to alcohol-induced adipose tissue macrophage phenotype switching, we generated myeloid-specific TLR4 knockout (M-TLR4KO) mice. Mice expressing the myeloid-specific Cre recombinase, *LysMCre*$^{+/+}$, were crossed to mice with exon 3 of the *Tlr4* gene flanked by *LoxP* sites (*Tlr4*$^{f/f}$) to generate myeloid-specific TLR4 knockout (*LysMCre*$^{+/-}$*; Tlr4*$^{f/f}$; M-TLR4KO) mice (218, 219). TLR4 was absent at the cell surface of peritoneal macrophages isolated from M-TLR4KO (Figure 3.5 A-C). Additionally, peritoneal macrophages from M-TLR4KO mice had a greatly reduced TNFα response when stimulated with LPS compared to macrophages isolated from WT littermates (*LysMCre*$^{-/-}$*;Tlr4*$^{f/f}$). M-TLR4KO macrophages maintained WT level responses to a TLR2 ligand, Pam_3CSK_4 (Figure 3.5 D and E). Further, intracellular staining revealed that peritoneal neutrophils isolated from M-TLR4KO also had decreased TNFα production in response to LPS compared to WT littermate neutrophils, but maintained TNFα production in response to Pam_3CSK_4 (Figure 3.5 F-H). Thus, both macrophages

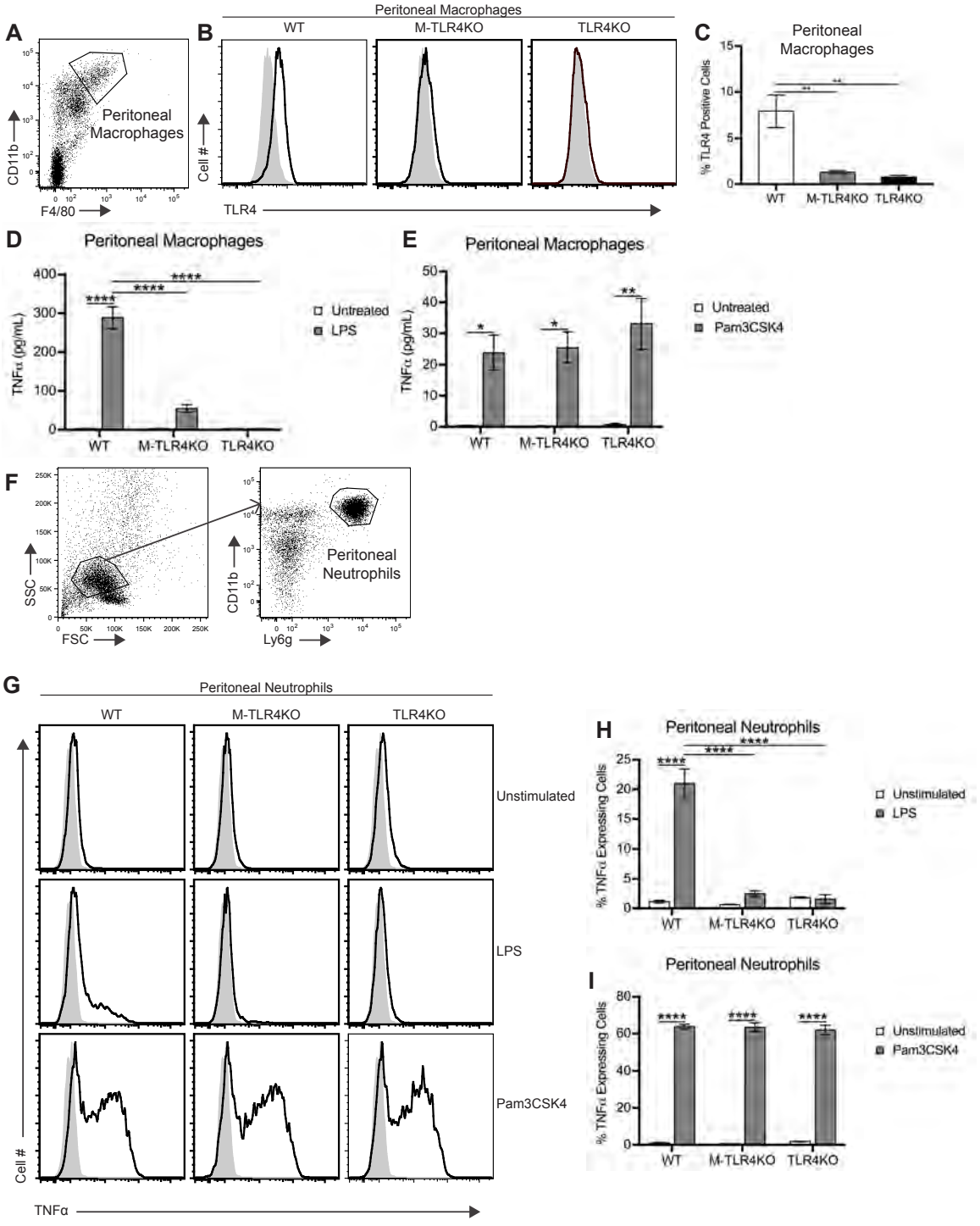
A
Peritoneal Macrophages
CD11b
F4/80
B
Peritoneal Macrophages
WT
M-TLR4KO
TLR4KO
Cell #
TLR4
C
Peritoneal Macrophages
% TLR4 Positive Cells
WT
M-TLR4KO
TLR4KO
D
Peritoneal Macrophages
TNFα (pg/mL)
Untreated
LPS
WT
M-TLR4KO
TLR4KO
E
Peritoneal Macrophages
TNFα (pg/mL)
Untreated
Pam3CSK4
WT
M-TLR4KO
TLR4KO
F
SSC
FSC
CD11b
Ly6g
Peritoneal Neutrophils
G
Peritoneal Neutrophils
WT
M-TLR4KO
TLR4KO
Unstimulated
LPS
Pam3CSK4
Cell #
TNFα
H
Peritoneal Neutrophils
% TNFα Expressing Cells
Unstimulated
LPS
WT
M-TLR4KO
TLR4KO
I
Peritoneal Neutrophils
% TNFα Expressing Cells
Unstimulated
Pam3CSK4
WT
M-TLR4KO
TLR4KO

Figure 3.5: TLR4 is deleted in macrophages and neutrophils from M-TLR4KO mice. (A) Representative gating of elicited peritoneal macrophages, which were first gated on singlets. (B) Representative surface staining of TLR4 on elicited peritoneal macrophages from WT littermate (WT), Myeloid-TLR4 knockout (M-TLR4KO), and global TLR4 knockout (TLR4KO) mice. (C) TLR4 surface expression of WT, M-TLR4KO, and TLR4KO mice, n=3 for each genotype. (D) TNFα ELISA of cell supernatants from elicited peritoneal macrophages that were stimulated 2 μg/mL LPS, n=3 for each genotype. (E) TNFα ELISA of cell supernatants from elicited peritoneal macrophages that were stimulated with 1 μg/mL Pam_3CSK_4, n=3 for each genotype. (F) Representative gating of elicited peritoneal neutrophils. The granulocyte population was identified by gating singlets on forward and side scatter (*left*) and then was gated on CD11b and Ly6g to identify neutrophils ($CD11b^+Ly6g^+$) (*right*). (G) Representative intracellular TNFα staining of elicited peritoneal neutrophils stimulated with either LPS or Pam_3CSK_4 in WT, M-TLR4KO, and TLR4KO mice. (H) Intracellular TNFα in peritoneal neutrophils of WT, M-TLR4KO, and TLR4KO mice stimulated with 1 μg/mL LPS, n=3 for each genotype. (I) Intracellular TNFα in peritoneal neutrophils of WT, M-TLR4KO, and TLR4KO mice stimulated with 1 μg/mL Pam_3CSK_4, n=3 for each genotype. Data are represented as mean $\pm$ SEM, * $p < 0.05$, ** $p < 0.01$, ***$p < 0.001$, **** $p < 0.0001$.

and neutrophils from M-TLR4KO are unresponsive to LPS stimulation due to the absence of TLR4.

Myeloid-TLR4 does not regulate alcohol-induced macrophage phenotype switching

To determine whether myeloid-specific TLR4-deficiency directly impacts macrophage phenotype switching, the M-TLR4KO mice and their WT littermates were subjected to the chronic, multiple-binge alcohol exposure model and the SVF was isolated and stained for flow cytometry analysis. The number of total macrophages was unchanged in alcohol-fed WT littermates or M-TLR4KO mice, compared to their respective pair-fed controls (Figure 3.6 A). Interestingly, the M-TLR4KO mice were not protected against the alcohol-induced M1 phenotype switch; alcohol-fed M-TLR4KO mice had a greater number of M1 macrophages compared to pair-fed mice, which is in contrast to the global TLR4KO mice (Figure 3.6 B). The number of intermediate and M2 macrophages were not increased in alcohol-fed WT littermates or alcohol-fed M-TLR4KO mice when compared to pair-fed WT littermates or M-TLR4KO mice, respectively (Figure 3.6 C and D). This suggests that adipose tissue macrophage phenotype switching is independent of myeloid TLR4 and that TLR4 expression on cells other than myeloid cells may be important.

The number of DCs, neutrophils, B cells, and T cells were also quantified in these mice. We observed differences in the immune cell composition of alcohol-fed C57BL/6J WT mice and alcohol-fed WT littermates of M-TLR4KO

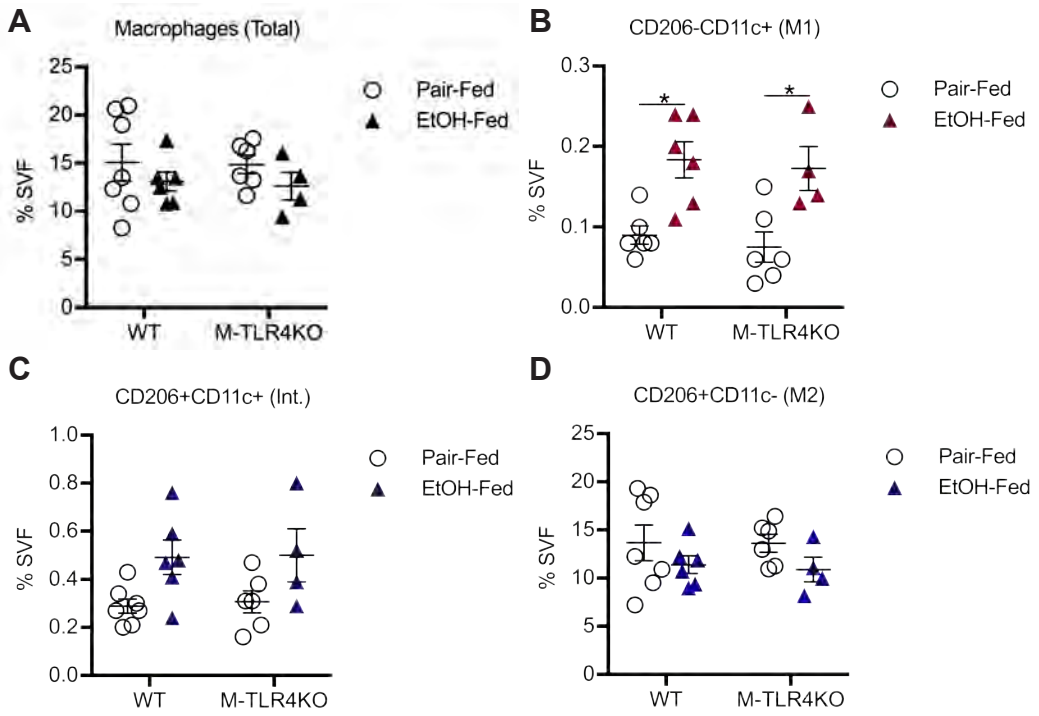

Figure 3.6: M-TLR4KO mice are not protected against adipose macrophage phenotype switching. WT littermates and M-TLR4KO mice were subjected to the chronic, multiple-binge alcohol model and the SVF isolated from perigonadal adipose tissue was analyzed by flow cytometry. Quantification of (A) total macrophages, (B) M1 macrophages, (C) Intermediate macrophages, and (D) M2 macrophages as a percentage of total SVF cells. n=4-7. Data are represented as mean ± SEM, * p <0.05, ** p <0.01, ***p<0.001, **** p<0.0001.

mice, which could be attributed to *LoxP* sites inserted in the *Tlr4* gene (219). Similar to the C57BL/6J WT mice (Figure 3.2 B), the number of DCs in alcohol-fed WT littermates showed a trend of increase, whereas DCs from alcohol-fed M-TLR4KO did not increase compared to the pair-fed controls (Figure 3.7 A). Neutrophil numbers were increased in alcohol-fed WT littermates, and there was a trend of increase in the alcohol-fed M-TLR4KO mice when compared to pair-fed controls but this was not significant (Figure 3.7 B). This differs slightly from the alcohol-fed WT C57BL/6J mice, which exhibit a trend of increase in adipose neutrophils (Figure 3.2 C). The number of B cells, total T cells, and $CD4^+$ T cells did not exhibit significant changes in alcohol-fed WT littermates and M-TLR4KO mice (Figure 3.7 C, D, and E). On the other hand, $CD8^+$ T cells were decreased in both alcohol-fed WT littermates and M-TLR4KO mice, compared to their respective pair-fed controls (Figure 3.7 F). Together, this data shows that chronic, multiple-binge alcohol modulates the immune cell composition of the adipose tissue and leads to the increased number of M1 macrophages, DCs, and neutrophils, but fewer $CD8^+$ T-cells. *Tlr4* is required for macrophage phenotype switching and the increase in DCs, but the mechanism is independent of myeloid TLR4 expression. Interestingly, neutrophil accumulation and the decrease in $CD8^+$ T cells are both independent of TLR4 expression.

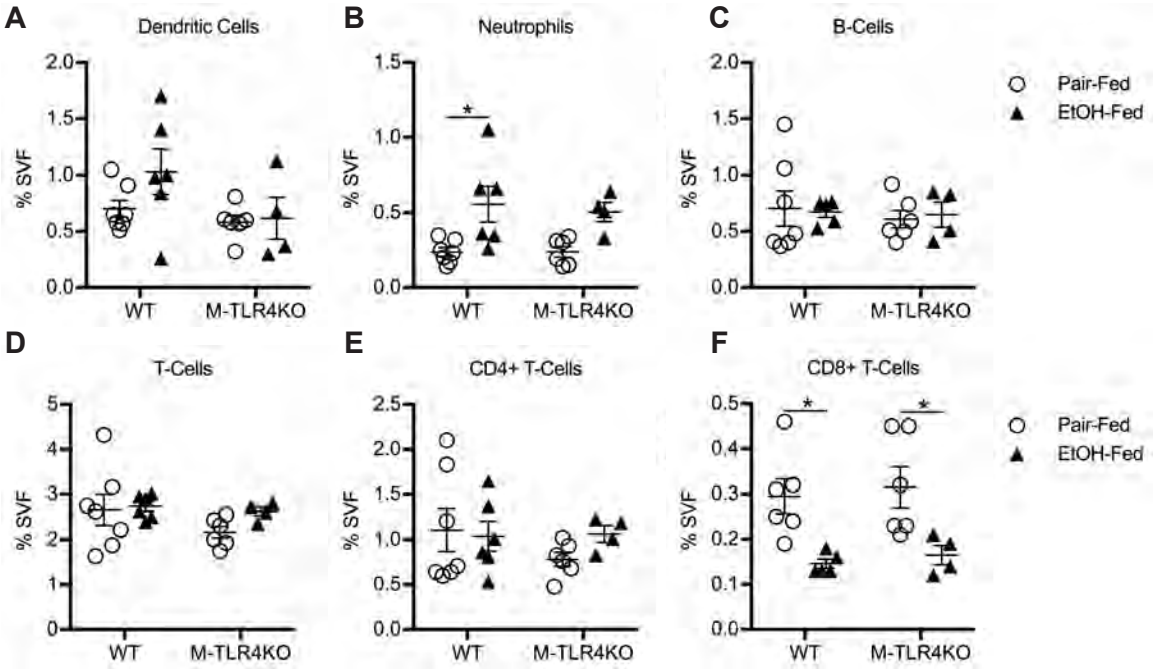

Figure 3.7: Chronic, multiple-binge alcohol decreases CD8$^+$ T-cells in WT and M-TLR4KO mice. WT littermates and M-TLR4KO mice were subjected to the chronic, multiple-binge alcohol model and the SVF isolated from perigonadal adipose tissue was analyzed by flow cytometry. Quantification of (A) DCs, (B) neutrophils, (C) B-cells, (D) T-cells, (E) CD4$^+$ T-cells, and (F) CD8$^+$ T-cells as a percentage of total SVF cells. n=4-7. Data are represented as mean ± SEM, * p <0.05, ** p <0.01, ***p<0.001, **** p<0.0001.

TLR4 partially mediates hepatic inflammation, but not steatosis, in the chronic, multiple-binge model.

In order to determine whether TLR4 mediates liver injury in the chronic, multiple-binge model, we assayed several parameters of liver injury in WT and global TLR4KO mice. Serum ALT and AST levels were elevated in alcohol-fed WT and TLR4KO mice, when compared to their respective pair-fed controls. Both ALT and AST levels were reduced in alcohol-fed TLR4KO compared to alcohol-fed WT mice (Figure 3.8 A and B). Hepatic triglycerides were also elevated in both alcohol-fed WT and TLR4KO mice, however there was no difference between those two groups (Figure 3.8 C). Next, we wanted to determine whether TLR4-deficiency impacts liver inflammation in this model by measuring the expression of pro-inflammatory cytokines and chemokines. The expression of *Il6* and *Ccl2* were elevated in alcohol-fed WT, but not alcohol-fed TLR4KO mice, compared to pair-fed controls (Figure 3.8 D and E). The expression of *Il1b* was induced in alcohol-fed WT and alcohol-fed TLR4KO mice compared to their respective pair-fed controls, but the expression in alcohol-fed TLR4KO mice is much lower compared to alcohol-fed WT mice (Figure 3.8 F). Together, this demonstrates that TLR4KO mice are protected against liver inflammation, but not hepatic steatosis, in the chronic, multiple-binge model and they have reduced overall liver injury.

In order to determine whether myeloid TLR4 mediates the reduced cytokine expression seen the livers of alcohol-fed global TLR4KO mice, we

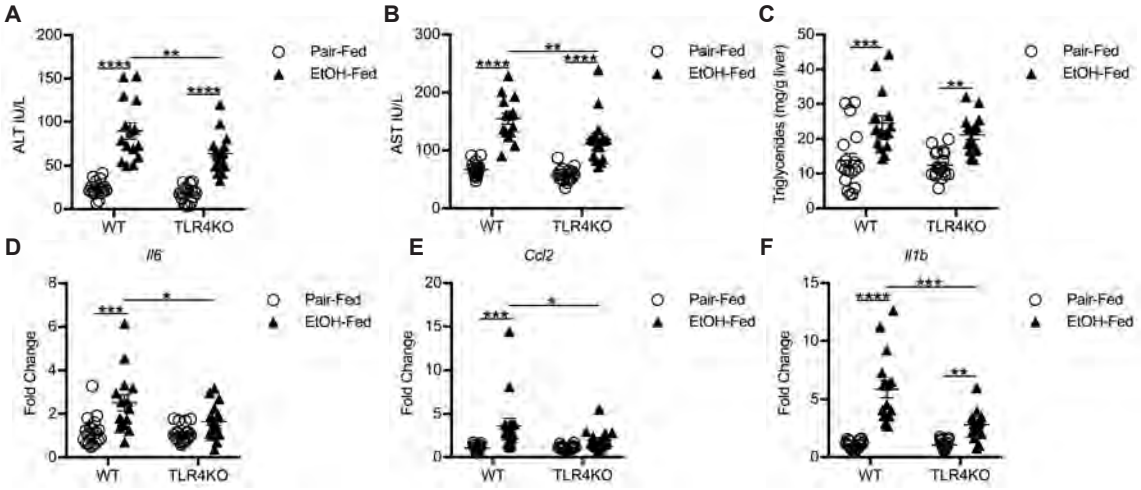

Figure 3.8: TLR4 partially mediates liver injury. WT and TLR4KO mice were subjected to the chronic, multiple-binge alcohol model. Blood and liver were collected. Serum was used to quantify (A) ALT and (B) AST levels. (C) Liver triglyceride quantification. qPCR was used to quantify liver mRNA expression of (D) *Il6*, (E) *Ccl2*, and (F) *Il1b*. Each genotype is normalized to respective pair-fed controls. n=15-19 from three independent experiments. Data are represented as mean ± SEM, * p <0.05, ** p <0.01, ***p<0.001, **** p<0.0001.

assayed liver injury parameters in M-TLR4KO mice and their WT littermates. Serum ALT levels were elevated in alcohol-fed WT littermates compared to pair-fed WT littermates, but not in alcohol-fed M-TLR4KO mice (Figure 3.9 A). Serum AST levels were elevated in both alcohol-fed WT littermates and alcohol-fed M-TLR4KO compared to their respective pair-fed controls, but there was no difference between the two groups (Figure 3.9 B). Hepatic triglycerides were elevated in alcohol-fed WT littermates compared to pair-fed WT littermates. There is a trend of increase in alcohol-fed M-TLR4KO mice compared to pair-fed M-TLR4KO mice, but this was not significant. This could be due to the increased level of triglycerides in the pair-fed M-TLR4KO mice (Figure 3.9 C). Expression of *Il6* is unchanged in both alcohol-fed WT littermates and alcohol-fed M-TLR4KO mice (Figure 3.9 D). Similar to the global TLR4KO mice, expression of *Ccl2* is induced in alcohol-fed WT littermates, but not alcohol-fed M-TLR4KO mice, when compared to pair-fed controls (Figure 3.9 E). Expression of TLR4 on myeloid cells impacts hepatic inflammation but does not influence hepatic steatosis or overall liver injury in the chronic, multiple-binge model.

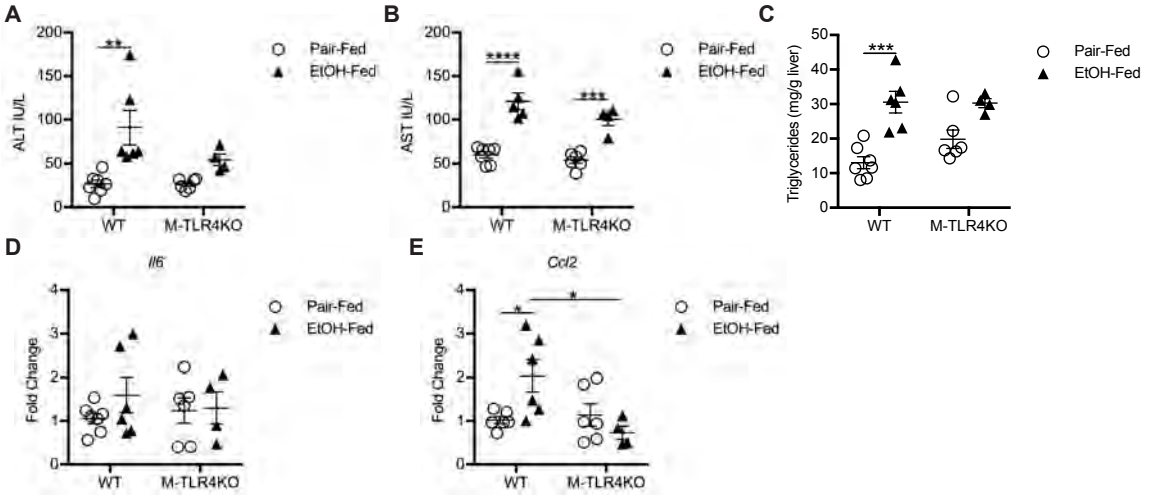

Figure 3.9: Myeloid TLR4 partially mediates liver injury. WT and M-TLR4KO mice were subjected to the chronic, multiple-binge alcohol model. Blood and liver were collected. Serum was used to quantify (A) ALT and (B) AST levels. (C) Liver triglyceride quantification. qPCR was used to quantify liver mRNA expression of (D) *Il6* and (E) *Ccl2*. Each genotype is normalized to respective pair-fed controls. n=4-7. Data are represented as mean ± SEM, * p <0.05, ** p <0.01, ***p<0.001, **** p<0.0001.

Summary

In this chapter, I used flow cytometry to identify specific immune cell populations and determined whether they changed in response to the chronic, multiple binge model. Previous analysis of adipose tissue inflammation was limited to gene expression analysis and immunohistochemistry. The data I presented here builds upon this work and confirms the presence of pro-inflammatory M1 macrophages in the adipose tissue. Moreover, I demonstrated that the chronic, multiple-binge alcohol model also modulates adipose tissue DCs, neutrophils, and $CD8^+$ T cells. Additionally, I established that TLR4 influences alcohol-induced adipose tissue macrophage phenotype switching, but surprisingly, through cells other than macrophages and neutrophils. Lastly, I determined that TLR4 has a limited role in liver injury in this model and that pro-inflammatory cytokine production depends on TLR4 in the liver but not in the adipose tissue.

Materials and Methods

Animals and experimental models

Experiments were approved by the Institutional Animal Care and Use Committee of the University of Massachusetts Medical School and conducted in accordance with the *Guide for the Care and Use of Laboratory Animals* from the National Institutes of Health. To generate the myeloid-specific *Tlr4* knockout mice, *LysMCre*$^{+/+}$ mice purchased from The Jackson Laboratory (strain 004781) were crossed to *Tlr4*$^{f/+}$ mice, which were provided by the University of Cincinnati Gene Targeting Mouse Core Facility, to produce *LysMCre*$^{+/-}$;*Tlr4*$^{f/+}$ (219). The resulting offspring were interbred to produce *LysMCre*$^{+/-}$;*Tlr4*$^{f/f}$ (M-TLR4KO) and wild-type (WT) littermates; *LysMCre*$^{-/-}$;*Tlr4*$^{f/f}$. For the chronic alcohol consumption experiments, nine- to ten-week old female C57BL/J mice were purchased from The Jackson Laboratory (strain 000664). Conventional TLR4KO mice (global TLR4KO) on the C57BL/6 background were maintained in house (220, 221). Eight- to 16-week old female mice were subjected to a chronic, multiple-binge model of alcohol exposure modified from an early stage alcoholic steatohepatitis model (68). Mice were assigned to two groups. The first group had *ad libitum* access to a 5% ethanol (v/v) Lieber-DeCarli diet (Bio-Serv, #F1258SP) for five weeks, following a one-week period of ethanol acclimatization. After 10 days of 5% ethanol, mice received an ethanol gavage (5 g/kg body weight, 31.5% ethanol), as reported in the NIAAA model once per week for the duration of the feeding for a total number of five gavages (123). The second group were an

isocaloric Lieber-DeCarli control diet (Bio-Serv, #F1259SP) and received an isocaloric gavage of maltodextrin (Bio-Serv, #3585). Mice were euthanized nine hours after the final gavage by CO_2 inhalation followed by cervical dislocation. Perigonadal adipose tissue was excised and stored at 37°C in HBSS (Gibco, #14025) supplemented with 3% (w/v) bovine serum albumin (Sigma, #A7030). For peritoneal cell experiments, 15-19-week old female, M-TLR4KO, their WT littermates, and TLR4KO mice were injected intraperitoneally with 1 mL of a 4% thioglycollate medium brewer modified solution (Becton Dickinson, #211716). Mice were euthanized by CO_2 inhalation followed by cervical dislocation four hours later to harvest elicited neutrophils and four days later to harvest elicited macrophages.

Adipose tissue fractionation

Adipose tissue was minced and digested with a 1 mg/mL collagenase solution (Sigma, #C6885) in a 37°C shaking water bath for one hour. The collagenase was deactivated by adding 10% (v/v) FBS (Gemini Bio-Products, #100-500). Samples were filtered through a 100 μm cell strainer (Corning, #352360) and centrifuged at 800 xg for six minutes at room temperature. The adipocyte layer was collected, washed, and lysed in QIAzol Lysis Reagent (Qiagen, #79306). The pelleted stromal vascular fraction was treated with ACK Lysing buffer (Gibco, #A10492-01) and lysed in RLT lysis buffer and homogenized via QIAshredder (Qiagen, #79654) for RNA extraction or washed in staining media (1 mM EDTA (Corning, #46-034-CI) and 3% FBS in HBSS (Gibco, #14175)) for flow cytometry.

The SVF was blocked with anti-mouse CD16/32 Clone 2.4G2 (Bio X Cell, #CUSTOM24G2) for 15 minutes at 4°C and then was subsequently incubated with primary antibodies or isotype controls for 20 minutes at 4°C in the dark. Antibodies and isotype controls used are listed in Table 3.1. The SVF was washed and fixed with 1% formaldehyde (ThermoScientific, #28908) for 20 minutes at 4°C in the dark. After fixation, the cells were washed and analyzed on a BD LSRII Cytometer (BD Biosciences). Data was analyzed using FlowJo (Tree Star, Inc.). In some experiments, Zombie Aqua Fixable Viability kit (Biolegend) was used to exclude dead cells. Gates were set based on fluorescence minus one (FMO) and isotype controls.

Peritoneal macrophages

Four days after thioglycollate injection, macrophages were collected as previously described (222). Briefly, macrophages were harvested by washing the peritoneal cavity with DPBS (Gibco, #14190) and treated with ACK Lysing Buffer. For flow cytometry analysis, cells were washed in staining media, blocked, and incubated with primary antibodies or isotype controls as described above. Antibodies and isotype controls used are listed in Table 3.2. Data was analyzed as described above. For the TLR ligand experiment, cells were washed in DMEM/F12 (Gibco, #11320) supplemented with 10 mM L-glutamine (Gibco, #25030) and 100 U/mL penicillin/100 μg/mL streptomycin (Gibco, #15140) and plated at $3x10^5$/well in 12-well plates in media with 10% FBS and rested for 2 hours. Media was changed and cells were stimulated with 2 μg/mL LPS-EB

Ultrapure (Invivogen, #tlrl-3pelps) or 1 μg/mL Pam_3CSK_4 (Invivogen, #tlrl-pms) for five hours. Cell supernatants were collected and the BD OptEIA Mouse TNFα (Mono/Mono) ELISA set (BD Biosciences, #555268) was used to quantify TNFα production.

Peritoneal neutrophils

Four hours after thioglycollate injection, neutrophils were collected as previously described (223). Briefly, the peritoneal cavity was washed with cold RPMI (Gibco, #11875). Neutrophils were treated with ACK Lysing Buffer and then washed in RPMI. Neutrophils were aliquoted to 5 mL polypropylene cell culture tubes at a density of $6x10^5$/mL in RPMI supplemented with 10% (v/v) FBS, 100 U/mL penicillin/100 μg/mL streptomycin, and 2 mM L-glutamine (Gibco, #25030) at a final volume of 0.5 mL. Cells were incubated with 1 μg/mL LPS-EB Ultrapure or 1 μg/mL Pam_3CSK_4 for 10 minutes and then treated with GolgiPlug (BD Biosciences, #555028) for 2 hours. Neutrophils were stained for intracellular TNFα as previously described (224). Briefly, cells were washed with staining media, blocked, and incubated with primary antibodies as described above. Antibodies and isotype controls used are listed in Table 3.3. Neutrophils were washed and then fixed and permeabilized with BD Cytofix/Cytoperm Plus (BD Biosciences, #555028) according to the manufacturer's instructions and then washed again. Cells were incubated with either the TNFα antibody or the isotype control for 30 minutes on ice. Cells were washed in staining media and analyzed as described above.

RNA extraction and Real-Time qPCR

Adipocyte RNA was extracted using the RNeasy Lipid Tissue Mini Kit (Qiagen, #74804) and SVF RNA was extracted using the RNeasy Mini Kit (Qiagen, #74104) following the manufacturer's instructions. RNA concentration was measured with a NanoDrop 2000 (ThermoScientific) and cDNA was synthesized using the Reverse Transcription System (Promega, #A3500) or the iScript Reverse Transcription Supermix (Bio-Rad, #1708841). mRNA transcript levels were assayed using the iTAQ Universal SYBR Green Supermix (Bio-Rad, #172-5121) and the CFX Connect Real-Time PCR Detection System (Bio-Rad). All data was normalized to *18s* ribosomal RNA. Primer sequences are listed in Table 3.4.

Statistical analysis

Data are presented as mean ± SEM. ANOVA was used to determine differences between groups. Grubbs' test was used to exclude outliers. All statistical analysis was performed using GraphPad Prism 7 (GraphPad).

Table 3.1: List of flow cytometry antibodies for SVF

Antibody	**Company**	**Catalog #**	**Clone**
CD45-APC/Fire 750	Biolegend	103154	30-F11
CD11b-PerCP/Cy5.5	Biolegend	101228	M1/70
F4/80-Brilliant Violet 650	Biolegend	123149	BM8
CD206-Brilliant Violet 421	Biolegend	141717	C068C2
CD11c-PE	Biolegend	117307	N418
Ly6G (Gr-1)-APC	eBioscience	17-5931-81	RB6-8C5
CD3-PerCP/Cy5.5	Biolegend	100218	17A2
CD4-PE	Biolegend	100512	RM4-5
CD8α-Brilliant Violet 421	Biolegend	100753	53-6.7
CD19-APC	BD Biosciences	561738	1D3
Isotype	**Company**	**Catalog #**	**Clone**
APC/Fire 750 Rat IgG2b	Biolegend	400669	RTK4530
PerCP/Cy5.5 Rat IgG2b	Biolegend	400631	RTK4530
Brilliant Violet 650 Rat IgG2a	Biolegend	400542	RTK2758
Brilliant Violet 421 Rat IgG2a	Biolegend	400535	RTK2758
PE Armenian Hamster IgG	Biolegend	400907	HTK888
APC Rat IgG2b	eBioscience	17-4031-81	eB149/10H5
PE Rat IgG2a	eBioscience	12-4321-41	eBR2a
APC Rat IgG2a	Biolegend	400511	RTK2758

Table 3.2: List of flow cytometry antibodies for peritoneal macrophages

Antibody	**Company**	**Catalog #**	**Clone**
CD11b-PerCP/Cy5.5	Biolegend	101228	M1/70
F4/80-Brilliant Violet 650	Biolegend	123149	BM8
TLR4-PE	Biolegend	145403	SA15-21
Isotype	**Company**	**Catalog #**	**Clone**
PerCP/Cy5.5 Rat IgG2b	Biolegend	400631	RTK4530
Brilliant Violet 650 Rat IgG2a	Biolegend	400542	RTK2758
PE Rat IgG2a	eBioscience	12-4321-41	eBR2a

Table 3.3: List of flow cytometry antibodies for peritoneal neutrophils

Antibody	**Company**	**Catalog #**	**Clone**
CD11b-PerCP/Cy5.5	Biolegend	101228	M1/70
Ly6g-APC	Biolegend	127613	1A8
TNFα-PE	Biolegend	506306	MP6-XT22
Isotype	**Company**	**Catalog #**	**Clone**
PerCP/Cy5.5 Rat IgG2b	Biolegend	400631	RTK4530
APC Rat IgG2a	Biolegend	400511	RTK2758
PE Rat IgG1	Biolegend	400407	RTK2071

Table 3.4: List of primer sequences 5'-3'

Gene	**Sequence**
18s forward	GTAACCCGTTGAACCCCATT
18s reverse	CCATCCAATCGGTAGTAGCG
Ccl2 forward	CAGGTCCCTGTCATGCTTCT
Ccl2 reverse	TCTGGACCCATTCCTTCTTG
Cxcl1 forward	TGCACCCAAACCGAAGTC
Cxcl1 reverse	GTCAGAAGCCAGCGTTCACC
Il6 forward	ACAACCACGGCCTTCCCTACTT
Il6 reverse	CACGATTTCCCAGAGAACATGTG

CHAPTER IV

Discussion

Sexual dimorphism in liver injury and adipose tissue inflammation

The sexual dimorphism in human ALD is well known; women are more likely than men to develop ALD, despite consuming less alcohol (2, 13-16). Human studies and rodent models indicate differences in first-pass metabolism, body water content, and hormones may contribute to the sexual dimorphism in ALD (17-19, 21, 22). Whether sexual differences play an important part in alcohol mediated adipose tissue inflammation and its impact on liver disease is not yet considered. The studies presented in Chapter II of this thesis show that chronic alcohol consumption causes adipose tissue inflammation in a sex-dependent manner.

Here I provide an analysis of the sexual dimorphism in adipose inflammation that occurs in mice when subjected to the NIAAA model of chronic-binge alcohol exposure. This model employs a single binge of alcohol delivered at the end of the study, which mimics a binge event common in AH patients (123). My studies show that male mice consume higher volumes of the 5% alcohol diet and had a higher BAC than their female counterparts on an *ad libitum* diet. Despite this, female mice have greater liver injury, as shown by elevated serum ALT and high liver triglycerides, similar to previous studies from Ki and colleagues (27). From these studies, it is apparent that increased serum ALT and triglycerides occur despite lower alcohol consumption and BAC in female mice.

The production of pro-inflammatory cytokines and chemokines in the liver has been reported in male and female mice subjected to the NIAAA model (27, 70, 225). Here I show a direct comparison of cytokine, chemokine, and monocyte/macrophage marker mRNA expression between male and female mice. I report an increase in *Tnf*, *Il6*, and *Ccl2* mRNA in alcohol-fed female mice whereas alcohol-fed male mice exhibit an increase in *Ccl2* mRNA. Furthermore, alcohol-fed female mice have greater *Ccl2* expression than alcohol-fed male mice in the liver. Previous studies using male mice have shown minimal or lack of expression of *Tnf*, *Il6*, and *Ccl2* mRNA in the liver (226, 227). Expression of the macrophage marker *Emr1* is decreased in both male and female livers. This decrease has been reported in other chronic alcohol models and is likely a result of the resident KCs undergoing apoptosis (70, 228). *Ly6c1* mRNA, a marker of pro-inflammatory monocytes, is increased in alcohol-fed male and female livers, indicating that there is infiltration of monocytes into the livers of these mice. This is in agreement with previous studies showing that chronic alcohol consumption increases the presence of Ly6C-expressing monocytes in mouse livers and that this increase is enhanced further with the administration of an ethanol binge (60). Overall, my results show that alcohol-fed female mice exhibit higher expression of pro-inflammatory cytokines than male mice.

Adipose tissue biology has been extensively studied in the context of obesity. Low-grade adipose tissue inflammation is linked to the development of metabolic disorders, namely Type 2 diabetes. Adipose tissue inflammation is

characterized by the increased presence of pro-inflammatory macrophages and the production of pro-inflammatory adipokines (132). Similar to studies on obesity, studies in ALD models have shown that chronic alcohol consumption can induce pro-inflammatory responses in the adipose tissue. Female mice on an *ad libitum* alcohol diet produce cytokines in the adipose tissue and exhibit increased expression of the pro-inflammatory macrophage marker *Itgax* (CD11c) (194). In other chronic ALD models, male rats fed alcohol *ad libitum* for four weeks exhibit increased *Tnf*, *Il6*, and *Ccl2* production in adipose tissue (189, 190). Male mice fed alcohol for four to eight weeks also reveal increases in adipose tissue cytokine production (193, 195). My data show higher expression of *Tnf*, *Il6*, and *Ccl2* in female adipose tissue, whereas increased *Il6* but not *Tnf* or *Ccl2* is observed in male adipose tissue using the NIAAA model of chronic-binge alcohol feeding. It is likely that pro-inflammatory cytokine induction in male adipose tissue may further increase with a prolonged (four to eight weeks) alcohol-feeding regimen. Although previously published studies provide evidence for chronic alcohol consumption-mediated adipose tissue inflammation, they have not explored whether sex-dependent differences exist in alcohol-induced adipose tissue inflammation.

I report for the first time that alcohol-induced adipose tissue inflammation occurs in a sex-dependent manner. Male and female adipose tissues have a distinctly different cytokine signature in response to the NIAAA model: male mice express high *Il6* mRNA, whereas female mice express elevated *Ccl2* mRNA. The

role of IL-6 in adipose tissue function is controversial; evidence exists in support of both its pro- and anti-inflammatory functions (132, 229). It is likely that the increase in *Il6* expression in male adipose tissue exerts an anti-inflammatory response. On the other hand, increased *Ccl2* in female adipose tissue could be indicative of a pro-inflammatory state, which is consistent with obesity-related adipose tissue inflammation (132). Increased *Ccl2* expression in male adipose tissue, but not female, correlates to a higher degree of inflammation in high fat diet models, in which male mice have more severe metabolic dysfunction (181). Interestingly, I observe an opposite paradigm; females exhibit higher *Ccl2* and are more susceptible than males to liver injury. In mouse models of obesity, there is increased numbers of pro-inflammatory macrophages in the adipose tissue (134, 136, 137, 139). In this data, female mice show an increase in the expression of a number of macrophage markers (*Emr1*, *Cd68*, *Itgam*, and *Itgax*). This indicates either an increase in the number of macrophages within the adipose tissue or increased expression of these markers, suggesting that resident adipose macrophages likely acquire a pro-inflammatory phenotype. Interestingly, H&E staining of adipose tissue sections show that adipocyte morphology remains unchanged between the sexes and pair-and alcohol-fed groups. There is an absence of crown-like structures, which indicates that macrophage activation is occurring without a significant change in macrophage numbers by alcohol (132).

Consistent with previous results, female mice have higher serum adiponectin in control animals than male mice (208). In contrast to previous rodent studies using long-term chronic alcohol consumption models, the NIAAA model employed here did not show reduced serum adiponectin levels (32, 176, 191). Serum adiponectin is increased in both male and female mice, likely due to a compensatory mechanism. Studies in ALD patients report increased serum adiponectin levels when compared to healthy controls or hepatitis C patients. Serum adiponectin is positively correlated with severity of liver injury (184-186). One possible explanation for the discrepancy between the mouse models could be the difference in drinking patterns because the NIAAA model includes a binge, whereas other models do not. This model is reflective of the drinking patterns in AH patients, suggesting that future studies on serum adiponectin alcohol models employing a binge are needed (123).

I sought to identify the underlying mechanism that contributes to the sexual dimorphism in adipose tissue inflammation. Chronic alcohol exposure increases the sensitivity of macrophages to endotoxin-mediated TNFα production and estrogen also sensitizes liver macrophages to endotoxin injury (21, 32). Here I investigated the effect of chronic alcohol exposure on male- and female-derived BMDMs. BMDMs exposed to chronic alcohol conditions *in vitro* increased LPS-induced TNFα production; however, the extent of increase due to alcohol exposure is similar between both male- and female-derived BMDMs. It is likely that the increased expression of macrophage markers in the adipose tissue is

regulated to some extent by the infiltration of bone marrow-derived immune cells during alcohol exposure. Furthermore, circulating endotoxin show higher trends in alcohol-fed female mice compared to male counterparts. The increased endotoxin could contribute to adipose inflammation in female mice. Moreover, the expression of several *Tlr* genes is increased in the adipose tissue of female, but not male mice. This indicates either an increased presence of *Tlr*-expressing cells or an upregulation of these genes in resident macrophages in females but not in males. The exact mechanism of sex-dependent upregulation of TLRs during alcohol exposure remains to be further explored. Overall my data provides some insights regarding how the propensity of increased circulating endotoxin in alcohol-fed female mice could lead to greater adipose tissue inflammation, dependent on mechanisms that are associated with increased TLR expression and/or macrophage activation.

There are other factors related to biological sex that could contribute to the sexual dimorphism in ALD and ALD rodent models. Estrogen signaling in the adipose tissue of female, but not male, mice could contribute to the differential expression of *Il6* (Figure 2.3 A). 17, β-estradiol inhibits IL-6 production in response to IL-1β and TNFα stimuli (230). This inhibition is also demonstrated in macrophages isolated from mice subjected to a thermal injury combined with ethanol exposure; 17, β-estradiol treatment decreased the production of IL-6 (231). There may also be sex-dependent differences in the gut microbiome that could influence alcohol-induced adipose tissue and liver inflammation. The gut

microbiota composition differs between male and female mice on both chow and high-fat diets (232). In humans, the gut microbiota composition is influenced by gender (233). There has been recent interest in examining the relationship between the gut microbiome and the liver within the context of ALD, but it is unknown whether biological sex impacts this axis (234-236).

This work highlights the role of adipose tissue inflammation within the context of sexual dimorphism that is observed in human ALD. In conjunction with the studies presented here, it will be imperative that all forthcoming alcohol studies carefully consider biological sex as an experimental variable. This will be important particularly in interpreting current and future studies that attempt to target adipose tissue as a means of resolving alcohol-induced liver injury. It is crucial that therapeutic strategies for AH patients are designed considering appropriate targets and the biologic sex of the patient.

Since the publication of Chapter II as a manuscript, there have been no new studies exploring the sexual dimorphism in ALD to report. A recent epidemiological study confirmed that being female is an independent risk factor for mortality in decompensated ALD patients and those with ASH (237).

Using the correct pre-clinical model for developing new ALD treatments will be crucial for making progress in the search for new and effective therapies. In Chapter II of this thesis, I demonstrate that the sexual dimorphism in mice that occurs in response to alcohol consumption extends to the adipose tissue. Three therapeutic strategies related to the adipose tissue have been tested in rodent

models of ALD to reverse liver injury. Exogenous adiponectin administration reverses liver injury in alcohol-fed mice (176). Taurine supplementation prevents the alcohol-mediated production of *Il6* and *Ccl2* mRNA in the adipose tissue of rats, as well as the alcohol-mediated decrease in circulating adiponectin. This also coincides with a reversal of hepatic steatosis and TNFα production in the liver (191). Rosiglitazone, a PPARγ agonist, improves liver injury, circulating adiponectin, and adipose tissue inflammation in alcohol-fed mice (193, 195). Together, these studies help to support the connection between alcohol-induced adipose tissue inflammation and liver injury. They also provide evidence for targeting adipose-related mechanisms to alleviate alcohol-induced liver injury. However, only male animals were used to test these therapies. It remains to be determined how efficacious adiponectin, taurine, and rosiglitazone are in female animals, which have a much higher burden of injury than male animals. This will help to determine the overall effectiveness of these strategies and whether they will be suitable for potential use in human patients.

Adipose macrophage phenotype switching is independent of TLR4 expression in myeloid cells

Adipose tissue inflammation is well-characterized in obesity models, but is an emerging area of investigation in ALD. Previous studies from our lab and others, have reported that alcohol increases the presence of innate immune cells within the white adipose tissue, using gene expression analysis and immunohistochemical staining (189, 194, 213). In Chapter III of this thesis, I

employed flow cytometry to identify and characterize both innate and adaptive adipose immune cells using a model of ASH established by Xu and colleagues (68). My studies report for the first time that alcohol increases the number of pro-inflammatory M1 macrophages and DCs in the perigonadal adipose tissue. I also report that alcohol impacts other immune cell populations, such as neutrophils and $CD8^+$ T cells. These mechanistic studies reveal that while TLR4 signaling is required globally for macrophage phenotype switching, myeloid TLR4 signaling is dispensable. Interestingly, alcohol mediated adipose inflammatory cytokine induction is independent of TLR4, as is the change in neutrophils and $CD8^+$ T cells (Figure 4.1). These studies suggest alcohol mediated adipose inflammation is independent of myeloid TLR4 expression and future studies will be required to determine whether this inflammation involves non-immune cells, such as adipocytes, pre-adipocytes, or endothelial cells.

During high-fat diet driven inflammation, the adipose tissue becomes populated with pro-inflammatory immune cells, specifically M1 macrophages that express CD11c (133-136, 139, 211). Depleting CD11c-expressing cells ameliorates adipose tissue inflammation (140). Alcohol-induced adipose tissue inflammation has been characterized by the increased expression of pro-inflammatory cytokines as well as innate immune cell markers, including CD11c (*Itgax*) (189-195, 213). Recently it has been demonstrated that DCs, which also express CD11c, contribute to obesity-related adipose inflammation, but it is unknown if chronic alcohol exposure can modulate the DC population in the

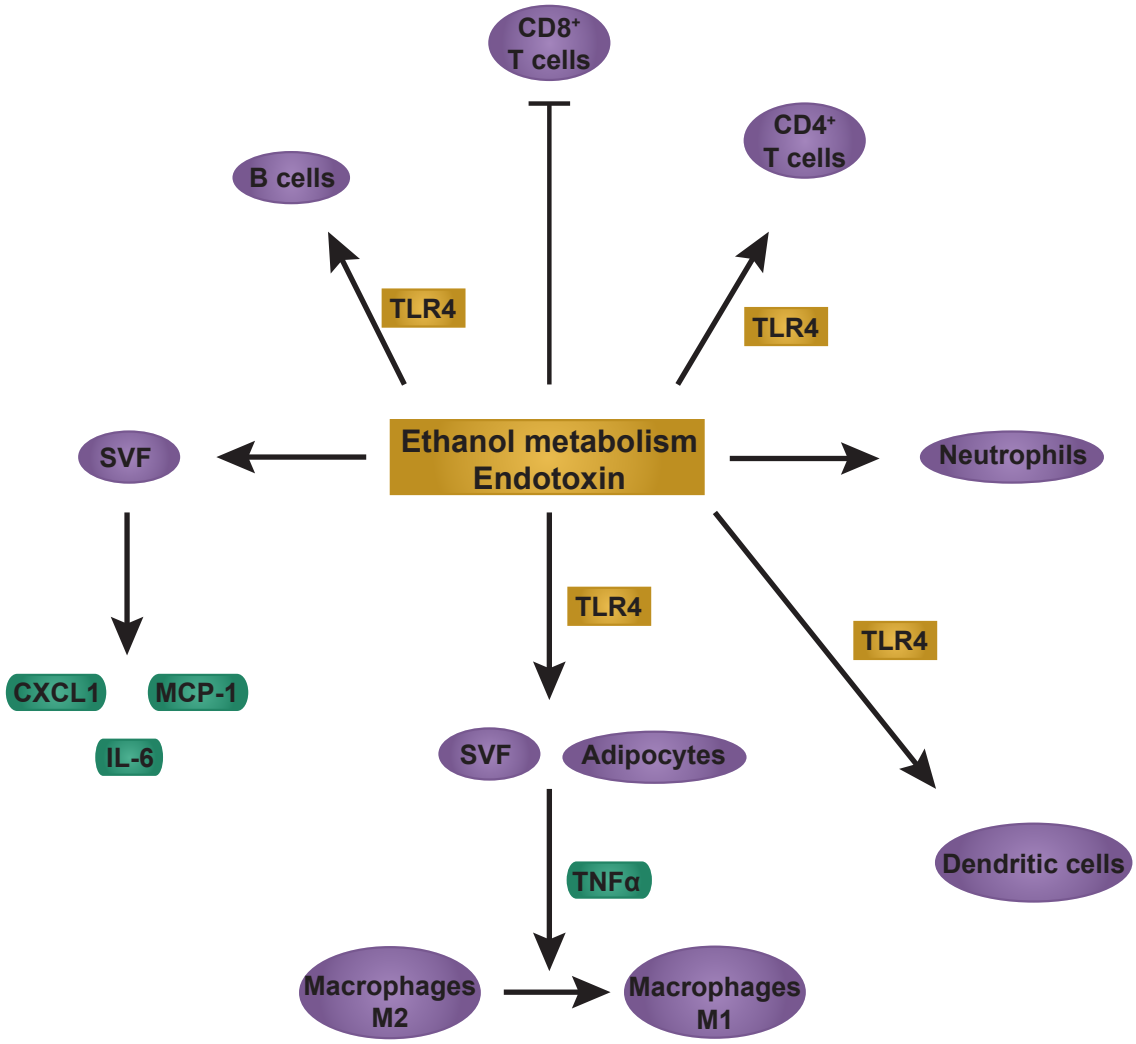

Figure 4.1: Alcohol-induced adipose tissue inflammation is partially mediated by TLR4. Ethanol metabolism and/or the presence of endotoxin results in the expression of CXCL1, MCP-1, and IL-6 in the SVF. TLR4 expression on the SVF and/or adipocytes results in macrophage phenotype switching to the M1 macrophage, which could be mediated by TNFα. Dendritic cell (DC), B cell, and $CD4^+$ T cell accumulation are mediated by TLR4; neutrophil accumulation occurs independently of TLR4. The number of $CD8^+$ T cells decreases, independent of TLR4.

adipose tissue (148-150). Previous studies from our lab have shown that moderate alcohol exposure impairs peripheral DC function and induces T-cell anergy (238). Here I show that in addition to the increased numbers of pro-inflammatory M1 macrophages, DCs are also increased in alcohol-fed WT mice. On the other hand, global TLR4-deficiency prevents an increase in either M1 macrophages or DCs when compared to pair-fed controls. Notably, the deletion of TLR4 from myeloid cells, including macrophages and neutrophils, in alcohol-fed mice does not impact the number of M1 macrophages when compared to pair-fed mice, but inhibits the accumulation of DCs.

Reports indicate that neutrophils increase in adipose tissue during high-fat diet-induced inflammation, at both early and late time points (151, 152). Here, I observe that alcohol increases the number of neutrophils in the adipose tissue of WT littermates. There is also a trend of increase in alcohol-fed WT (C57BL/6J), TLR4KO, and M-TLR4KO mice compared to their respective pair-fed controls, but this was not significant. Germline deletion of TLR4 did not impact the alcohol-induced expression of pro-inflammatory cytokines, which indicates that innate immune cells are not the sole producers of pro-inflammatory cytokines in the SVF. The SVF is comprised of a number of different cell types, including immune cells, endothelial cells, and preadipocytes, all of which can produce cytokines or other inflammatory mediators that activate immune cells (132, 160, 161). Other adipose tissue cell types, including adipocytes, preadipocytes, and endothelial cells express *Tlr4* (217, 239-241). My data suggests that the interplay between

these resident adipose cell types and immune cells is important for macrophage phenotype switching to the M1 phenotype, as well as the recruitment of DCs and neutrophils.

Lymphocytes are also involved in adipose tissue inflammation during obesity. Pro-inflammatory B cells increase in the adipose tissue of mice subjected to a high-fat diet, while a population of regulatory B cells, which produce IL-10, are decreased (153, 154). Alcohol increased the number of B cells in WT C57BL/6J mice compared to their pair-fed controls, but alcohol-fed TLR4KO and M-TLR4KO mice do not experience this increase. In a paradigm similar to macrophages, specific subsets of T cells are involved in either the progression or control of adipose inflammation. Generally, $CD4^+$ T cells in the adipose tissue are associated with pro-inflammatory macrophages (146, 147, 155). However, the presence of regulatory T cells, which are immunosuppressive, is decreased by the progression of obesity (157). There may also be a role for regulatory T cells in maintaining the M2 macrophage population via the production of IL-10 (242). The number of $CD4^+$ T cells is increased in alcohol-fed WT C57BL/6J but not TLR4KO or M-TLR4KO mice, when compared to their respective pair-fed controls. Macrophages and DCs can act as APCs for $CD4^+$ T cells in the adipose tissue (146, 147, 149). The alcohol-induced increase in the number of adipose tissue $CD4^+$ T cells appears to mirror the increase seen in DCs and not M1 macrophages.

$CD8^+$ T cell numbers are decreased in alcohol-fed WT littermates and alcohol-fed M-TLR4KO mice, with similar trends in alcohol-fed WT C57BL/6J and global TLR4KO mice. This is opposite to what occurs in obesity models; $CD8^+$ T cell accumulation precedes and is required for macrophage accumulation in adipose tissue during high-fat diet-induced adipose inflammation (156). One explanation for this discrepancy for the role of $CD8^+$ T cells is that the experimental model we use here involves repeated, acute alcohol insults during chronic alcohol exposure. This could change the timing of $CD8^+$ T cell accumulation. Time course studies to determine when $CD8^+$ T cells appear in the adipose tissue in relation to acute alcohol gavages may provide some insights as to whether or not they are required for alcohol-induced M1 macrophage accumulation.

How, exactly, TLR4 controls macrophage phenotype switching remains to be determined. TLR4 promotes phenotype switching, but in an indirect manner because expression of TLR4 on macrophages themselves is dispensable for this switch. A likely scenario is that another adipose cell type, like adipocytes or endothelial cells, which express TLR4, generate the pro-inflammatory milieu that leads to M1 phenotype switching (217, 240, 241). For example, TLR4 activation in adipocytes or endothelial cells results in the production of TNFα (217, 241). TNFα, in turn, promotes M1 macrophage polarization (243). Therefore, in WT mice subjected to the chronic, multiple-binge model, adipocytes or endothelial cells produce the TNFα molecules which promote adipose tissue macrophage

phenotyping switching. This scenario is disrupted in the global TLR4KO mice, but remains intact in the M-TLR4KO mice. Whether TLR4 or TNFα expression in adipocytes and/or endothelial cells is required for this process could be tested by deleting *Tlr4* or *Tnf* specifically in either cell type (219, 244). Mice expressing *Cre* under the control of the *Adipoq* promoter or the *Cdh5* promoter could be used to delete these genes in adipocytes or endothelial cells, respectively (245, 246). If TLR4 expression on these cells is required for M1 phenotype switching in the chronic, multiple-binge model, there would be no increase in $CD11c^+$ macrophages in either the adipocyte- or endothelial cell-specific TLR4KO mice, similar to the results in the global TLR4KO mice. The same result would hold true if TNFα is mediating the phenotype switch; there would be no increase in the number of $CD11c^+$ macrophages in the adipocyte- or endothelial cell-specific TNFαKO mice.

The impact of TLR4 on liver and adipose tissue inflammation in the chronic, multiple-binge model

TLR4 is a key innate immune receptor and when it binds to endotoxin (LPS), a major component of the outer layer of gram-negative bacteria. Following binding to TLR4, a signaling cascade results in the production of pro-inflammatory cytokines (113). Generally, TLR4-deficient mice are protected against alcohol-induced liver injury (65, 115, 118, 119). This effect can be attributed to both hematopoietic and non-hematopoietic cells, as bone marrow transplant studies with WT and *Tlr4*$^{-/-}$ mice show partial protection against liver

injury (119). However, in some studies the role is less clear as *Tlr4*$^{-/-}$ are not protected against early complement deposition or TNFα production in the liver, or the role of TLR4 is confounded when only a modest reduction in liver injury is seen (64, 120). Here, I demonstrate that TLR4KO mice have reduced liver injury in the chronic, multiple-binge model, when compared to WT mice. In the chronic, multiple-binge model alcohol-fed TLR4KO mice display a degree of liver injury, as indicated by elevated serum ALT and AST levels, when compared to pair-fed TLR4KO mice. This is in contrast to the studies which in which TLR4-deficient mice were completely protected from alcohol-induced injury, suggesting TLR4 is absolutely crucial for liver injury (65, 115, 119). However, the studies I present here show that the degree of injury in TLR4KO mice is less than that of the alcohol-fed WT mice. Alcohol-induced pro-inflammatory cytokine production is absent in the alcohol-fed TLR4KO mice; however, these animals display the same degree of steatosis as the alcohol-fed WT mice. These data suggest that in the chronic, multiple-binge model, TLR4 expression impacts only certain aspects of injury, such as hepatic inflammation, while others are TLR4-independent, such as hepatic steatosis. This partial requirement for TLR4 has also been demonstrated in the Lieber-DeCarli model, wherein TLR4 is dispensable for early complement deposition and TNFα production in the liver (120). The limited role of TLR4 in alcohol-induced liver injury in the more advanced chronic, multiple-binge model is supported by the use of the M-TLR4KO mice, in which TLR4 signaling is absent in macrophages and neutrophils. Alcohol-fed M-TLR4KO mice have

reduced hepatic *Ccl2* production, but not serum AST levels when compared to alcohol-fed WT littermates. Together, these data demonstrate that the role of TLR4 in mediating alcohol-induced liver injury is restricted to the induction of pro-inflammatory cytokines in the chronic, multiple-binge model.

There is also a varied response to high-fat diet insult in TLR4-deficient mice as well. Overall, TLR4-deficient mice exhibit some degree of protection against diet-induced adipose inflammation (215-217). However, in some experiments this protection is limited because both high-fat died fed WT and TLR4-mutant mice exhibit signs of macrophage infiltration into the adipose tissue, but TLR4-mutant mice have lower expression of *Tnf* and higher circulating adiponectin (247). Further, some studies demonstrate either a modest protective effect, or they are protected only on a modified high-fat diet, while others only demonstrate that *Tlr4*$^{-/-}$ mice have more M2 adipose macrophages (248-250). Myeloid-specific *Tlr4* knockout mice exhibit no change in the expression of several pro-inflammatory cytokines and cell markers in the adipose tissue when subjected to a high-fat diet. Surprisingly, these mice displayed elevated circulating pro-inflammatory cytokines, which the authors attribute to upregulated TLR4 expression in other SVF cell types (251). My data also demonstrate that the role for TLR4 in tissue inflammation may not be as straightforward as initially hypothesized. Here, I demonstrate that alcohol-induced pro-inflammatory cytokine production in the adipose tissue is independent of TLR4. This differs from previously published studies that use TLR4-deficient mice in high-fat diet

models. Expression of the innate immune cell markers CD11b (*Itgam*) and CD11c (*Itgax*) as well as the cytokines TNFα (*Tnf*) and IL-6 (*Il6*) were all blunted in the adipose tissue of TLR4-mutant mice fed subjected to a short-term high-fat diet (215). High-fat diet fed *Tlr4*$^{-/-}$ mice also displayed reduced expression of TNFα (*Tnf*), IL-6 (*Il6*), and MCP-1 (*Ccl2*), compared to high-fat diet fed WT mice (217). Bone marrow transplant studies revealed that the adipose tissue from high-fat diet fed mice that lack TLR4 expression in hematopoietic cells have decreased production of IL-6 and TNFα, as well as fewer crown-like structures (216). I show that alcohol-induced phenotype switching to an M1 macrophage is dependent on global, but not myeloid, TLR4 expression. Further, global TLR4-deficiency does not increase the number of M2 macrophages, as it does for mice fed a high-fat diet enriched with saturated fats (249). Overall, differences in the requirement for TLR4 in adipose tissue inflammation between high-fat diet and alcohol models are beginning to emerge. This suggests that high-fat diet and alcohol may be functioning through different mechanisms to drive adipose inflammation.

The varied responses seen in both ALD and obesity models could be attributed to several aspects, including differences in diet composition. Recently, it was established that housing temperature greatly influences high-fat diet-induced obesity. Mice in which TLR4 was deleted from the hematopoietic compartment exhibit protection against diet-induced liver damage at the higher, thermoneutral temperature, but not at the standard housing temperature (183).

Housing temperature likely also contributes to the varied results reported in the literature that use TLR4-deficient mice in both alcoholic and non-alcoholic liver injury models. The animals used for the work presented in this thesis were housed consistently at the standard temperature, however the influence of thermoneutral housing on ALD models has not yet been examined.

The role of TLR4 in alcohol and diet-induced inflammation is complex; previously published data reveal that TLR4 contributes to inflammation in some, but not all, instances which may be influenced by housing conditions. Chronic, multiple-binge alcohol consumption drives the expression of pro-inflammatory cytokines and chemokines independent of TLR4 signaling. M1 macrophage phenotype switching occurs, but this is dependent on the expression of TLR4 in a non-myeloid cell type. Alcohol-induced DC accumulation is absent when TLR4 is deleted globally and from myeloid cells. Both neutrophil accumulation and $CD8^+$ T cell depletion are independent of TLR4. The work presented in Chapter III is the first to characterize the SVF in a model of chronic, multiple-binge alcohol-induced adipose tissue inflammation by identifying specific immune cell populations. I have shown that similar to obesity-related inflammation, alcohol increases pro-inflammatory cytokine/chemokine expression as well as pro-inflammatory cell types in the adipose tissue. Differences from diet-induced adipose inflammation are beginning to emerge, as 1) alcohol produces cytokines independent of TLR4 and 2) macrophage accumulation does not appear to depend on $CD8^+$ T cells. These findings help to establish a role for adipose

tissue inflammation in ALD and to distinguish alcohol-induced adipose inflammation from high-fat diet-induced adipose tissue inflammation.

Caveats and future directions

In generating the M-TLR4KO mice and their WT littermates, the use of both LPS and Pam_3CSK_4 was valuable in confirming the deletion of *Tlr4*. Macrophages and neutrophils isolated from M-TLR4KO mice did not respond to the TLR4 ligand LPS, as expected. The same cells did respond to Pam_3CSK_4, which is the ligand for the TLR2/TLR1 heterodimer. This demonstrates that *Tlr4*, and not another *Tlr* family member, such as *Tlr1* or *Tlr2*, was deleted from macrophages and neutrophils.

As noted above, there were differences observed in the immune cell composition between the C57BL/6J WT mice and the WT littermates (*LysMCre*$^{-/-}$;*Tlr4*$^{f/f}$). One factor mentioned above that could be contributing to these differences is the differences in genetic backgrounds between the two sets of mice. The C57BL/6J mice are considered to be true WT mice, whereas the WT littermates have sequence changes at the *Tlr4* locus due to the insertion of the *LoxP* sites (219). Future experiments should include *LysMCre*$^{+/-}$;*Tlr4*$^{+/+}$ littermates. This will assist in controlling for any off-target effects caused by the insertion of the *Cre* sequence in the *M lysozyme* gene (218).

Another potential contributor to these differences are the housing conditions, and ultimately the microbiome of the WT strains. The C57BL/6J mice were ordered from The Jackson Laboratory shortly before starting the

experiments. The WT littermates were bred and maintained in house. ALD is particularly sensitive to the status of the gut microbiome; the translocation of endotoxin and endotoxemia are key events in disease pathogenesis. Additionally, chronic alcohol consumption changes colonic mucosal microbiota in ALD patients and some of these changes can be reversed with alcohol abstinence. Rodents also exhibit intestinal dysbiosis when subjected to a chronic alcohol model (236). Therefore, in order to ensure that mice used in future experiments are all housed under the same conditions, the C57BL/6J mice should be bred in house, as are the WT littermates. If that is not feasible, mice ordered from The Jackson Laboratory should be allowed to acclimate to their new housing conditions and develop an intestinal microbiota similar to the animals maintained in house. Additionally, to help facilitate a direct comparison between alcohol-fed germline TLR4KO and M-TLR4KO mice, these animals should be subjected to the chronic, multiple-binge model at the same time. This will eliminate any effects caused by differences in the diet and water composition. Together, these steps will help to eliminate the variability observed between the C57BL/6J WT mice and WT littermates.

Is adipose tissue inflammation a cause or consequence of liver injury?

In this thesis, I have presented data relating alcohol-induced liver injury to adipose tissue inflammation. This work was done in the pursuit of the answer to this question: does adipose tissue inflammation impact liver injury or does liver inflammation impact the adipose tissue? While it is clear that alcohol

consumption, whether chronic, acute, or both, does impact both the liver and the adipose tissue, what is unclear is how these two organs interact within the context of ALD. As the liver is the primary site of ethanol metabolism, it would be easy to assume that liver injury and inflammation occur first in disease pathogenesis. The resulting pro-inflammatory mediators, such as TNFα, MCP-1, and IL-1β, that are released into circulation would activate the resident adipose immune cells, like macrophages, and would initiate adipose tissue inflammation. However, adipocytes also express CYP2E1, the enzyme that metabolizes ethanol and produces ROS. Chronic alcohol consumption increases the expression of CYP2E1 in the adipose tissue in a time-dependent manner (194, 197). When mice lacking CYP2E1 (*Cyp2e1*$^{-/-}$) are fed alcohol, the adipose tissue does not produce pro-inflammatory cytokines (194). Further, enhanced expression of CYP2E1 in differentiated 3T3-L1 cells, a murine adipocyte cell line, inhibits the release of adiponectin in the presence of ethanol (197). Therefore, liver inflammation and adipose tissue inflammation could develop simultaneously in response to chronic alcohol consumption. The resulting pro-inflammatory milieu in each tissue then promotes inflammation in the other by elevated circulating pro-inflammatory cytokines and decreased circulating anti-inflammatory cytokines. Careful time course studies will need to be carried out in order to confirm that inflammation, due to ROS production, develops simultaneously in both organs.

In addition to ethanol metabolism, circulating endotoxin could be another factor that impacts both the liver and adipose tissue. As detailed in Chapter III, TLR4 is required for alcohol-induced cytokine production in the liver and macrophage phenotype switching in the adipose tissue. It is unclear whether this effect is mediated by endotoxin exposure in both organs. Gut endotoxin translocates to the liver via the portal vein (252). It remains to be determined if any endotoxin not cleared by the liver reaches the adipose tissue directly via circulation. It could be possible for LPS to reach the adipose tissue through its incorporation into lipoproteins and subsequent uptake into adipose macrophages and adipocytes (253). LPS tracking studies, such as those employing FITC-labelled LPS, in ALD models will need to be carried out in order to understand whether endotoxin directly impacts the adipose tissue in addition to the liver (254).

Potential mediators of adipose-liver crosstalk

The purpose of characterizing alcohol-induced adipose tissue inflammation was to understand how alcohol impacts adipose tissue function, with the goal of understanding how adipose tissue function impacts liver injury. A deeper understanding of alcohol-induced liver injury will enable the development of effective therapies for ALD. Ultimately, the mediators of alcohol-induced adipose-liver crosstalk need to be identified. Inflammatory cytokines and chemokines, like TNFα, MCP-1, IL-1β, and IL-6 are the first group of potential mediators. These cytokines and chemokines are produced by cells in both the

adipose tissue and liver. What remains to be determined is how cytokines produced in the adipose tissue specifically impact the liver, and vice versa. For example, IL-6 produced in the adipose tissue can cause hepatic insulin resistance in mice with diet-induced obesity (163). However, it is unknown how adipose IL-6 impacts the liver in alcohol-fed mice. Alcohol-induced IL-6 signaling through STAT3 has different impacts on different liver cells types; STAT3 in hepatocytes promotes inflammation and STAT3 in macrophages prevents inflammation (100). It is unknown whether the alcohol-IL-6-STAT3 axis also has different effects on the different cell types that make up the adipose tissue. Further, the receptors for IL-6 are expressed on many different cell types, so using IL-6 to alleviate alcohol-induced inflammation through hepatic macrophages is not an ideal strategy (255). MCP-1 promotes alcohol-induced liver inflammation, but does so independent of its receptor CCR2, thus, the exact mechanism through which MCP-1 functions remains to be determined (90). Targeting one specific cytokine or chemokine may not be sufficient to treat ALD or AH. Treatments that target TNFα have been largely unsuccessful (37, 38). Clinical trials are currently underway for inhibiting IL-1 in AH patients (39). However, a successful therapeutic regimen may require targeting more than one cytokine, or a combination of cytokines and other mediators, which are discussed below.

The role of adiponectin as a mediator of adipose-liver crosstalk has been extensively studied. However, there is a stark difference in adiponectin

production in response to alcohol consumption between human studies and animal models of ALD. In humans, circulating adiponectin is increased in ALD patients and is higher in patients with more severe cirrhosis, but declines with alcohol abstinence (184-186). Moderate alcohol intake also elevates circulating adiponectin in men (256, 257). On the other hand, chronic alcohol consumption decreases the production of adiponectin in animal models (32, 176, 190, 191, 196). In Chapter II, I presented data demonstrating that the NIAAA model increases serum adiponectin, similar to human ALD patients, which could be a compensatory mechanism due to the binge event in this model. A closer study of how acute ethanol administration on top of chronic alcohol consumption regulates adiponectin production will help to determine if drinking pattern impacts adiponectin. Both *in vivo* and *in vitro* data demonstrate that adiponectin is capable of alleviating liver injury in ALD models. Exogenous adiponectin administration reverses alcohol-induced liver injury in mice (176). This may be due to its impact on KCs. Adiponectin can reverse the sensitization of KCs to LPS by ethanol exposure and it also shifts KCs to an M2, anti-inflammatory phenotype, due to the downregulation of TLR4 expression (32, 198, 199, 258). Adiponectin may also reverse alcohol-induced liver injury through modulating lipid metabolism by shifting away from lipogenesis and towards β-oxidation (208). Exogenous overexpression of adiponectin downregulates SREBP-1c (*Srebpf1*) mRNA in rat livers (259). Adiponectin increases the response of PPARα-responsive promoters in the presence of ethanol in a rat hepatoma cell line (200).

While adiponectin appears to be a potential therapeutic target for animal models of ALD, its practicality for use in humans is debatable, because ALD patients have elevated adiponectin levels.

The free fatty acids and glycerol released by adipocytes during lipolysis are another set of candidates for mediating adipose-liver crosstalk. Alcohol consumption enhances adipose tissue lipolysis in mouse models of ALD (193, 201, 202). The elevated levels of circulating free fatty acids presumably contribute to hepatic steatosis. Wei and colleagues demonstrate that the presence of specific lipid species in the adipose tissue declines with alcohol consumption. This coincides with the increase of lipid species in the liver. However, this study did not uncover a direct link between alcohol-induced adipose tissue lipolysis and hepatic steatosis (203). The extent to which adipose tissue lipolysis contributes to hepatic steatosis remains to be determined. In addition to contributing to steatosis, the elevated serum free fatty acids and glycerol could also be causing inflammation in the liver. Inhibiting lipid accumulation in KCs decreases the production of pro-inflammatory cytokines in a NAFLD mouse model (260). Whether lipid storage in KCs of alcohol-fed mice also contributes to pro-inflammatory cytokine production remains to be determined. The excess circulating free fatty acids and glycerol could also be acting locally within the adipose tissue to promote inflammation. Adipose tissue macrophages store lipids, and impairing their ability to do so can impact hepatic metabolism (261). Adipose tissue lipolysis induced by fasting leads to an influx of

macrophages (262). Whether adipose macrophage lipid storage occurs in ALD models and what impacts this has on liver injury remains to be determined.

FGF21 is an example of a potential liver to adipose tissue mediator. FGF21 is highly expressed in the liver, and has been demonstrated to improve the metabolic dysfunction caused by obesity (263). FGF21 stimulates the release of adiponectin from adipocytes. Injecting high-fat diet fed mice with FGF21 elevates circulating adiponectin and improves insulin resistance (264). FGF21 makes for an interesting target, not only due to its metabolic impacts, but also because FGF21 transgenic mice have a greatly decreased preference for ethanol over their WT counterparts (265) An FGF21 therapeutic could possibly act to improve liver injury and deter alcohol consumption, however whether FGF21 modulates human drinking preferences remains to be determined. Recently, an FGF21 analog, PF-05231023, was demonstrated to reduce body weight and food intake in obese, non-human primates. Further, the same drug reduced body weight and improved circulating triglyceride and cholesterol levels in overweight and obese patients with Type 2 diabetes (266). However, FGF21 may have an opposite role in ALD. FGF21 knockout mice (FGF21 KO) subjected to the NIAAA model have reduced adipose tissue lipolysis and hepatic steatosis. However, the alcohol-fed FGF21 KO mice have similar inductions of circulating ALT and AST levels, compared to alcohol-fed WT mice (201). Whether FGF21 deficiency improves alcohol-induced hepatic inflammation in the NIAAA model remains to be determined. Further, the role of FGF21 in later stage ALD models,

such as the chronic, multiple-binge model is unexplored. Most importantly, how FGF21 deficiency modulates alcohol-induced adipose tissue inflammation will be useful in determining how FGF21 regulates adipose tissue function in ALD models.

Reconsidering TLR4 in ALD pathogenesis

In Chapter III I have shown that TLR4 has different roles for mediating alcohol-induced liver injury and adipose tissue inflammation. For example, hepatic pro-inflammatory cytokine production is dependent on TLR4. In the adipose tissue, pro-inflammatory cytokine production is independent of TLR4. If endotoxin is in fact an important mediator in ALD pathogenesis, then TLR4 may be more important for injury in the liver than the adipose tissue. The interplay of the other mediators mentioned above, like FGF21 and adiponectin, could also contribute to why TLR4-deficiency has a greater impact on liver injury than adipose tissue inflammation.

One question raised by my work is: what is the true role of TLR4 in ALD pathogenesis? TLR4 signaling in the liver is considered to be absolutely crucial for disease pathogenesis, but the work I present here contradicts this model. The answer to the above question could be that TLR4 is important for early stage ALD models, but not for later stage models. The initial studies exploring TLR4 employ the Tsukamoto-French model or a five-week Lieber-DeCarli model (64, 65, 115, 118, 119). Both of these models are excellent for inducing steatosis and mild inflammation, but fail to reproduce the neutrophil infiltration in AH or collagen

deposition in fibrosis (68, 123, 127, 128). Using the chronic, multiple-binge model, which represents a later stage liver injury, I demonstrate that TLR4 plays a limited role both in liver injury and adipose tissue inflammation. In the liver, pro-inflammatory cytokine production, but not steatosis, is absent in both the global TLR4KO mice and M-TLR4KO mice. In the adipose tissue, pro-inflammatory cytokine production is independent of TLR4, but macrophage phenotype switching is not. TLR4 is important for some, but not all, parameters of liver injury in this model.

TLR2 is another example of a TLR family member that has different roles in different ALD models. With a five week Lieber-DeCarli diet, alcohol-fed *Tlr2*$^{-/-}$ mice exhibit hepatic steatosis and hepatic inflammation similar to alcohol-fed WT mice (64). In contrast, using the NIAAA model, alcohol-fed *Tlr2*$^{-/-}$ mice have reduced liver injury and hepatic inflammation, when compared to alcohol-fed WT mice (67). This demonstrates a different requirement for TLR2 in different ALD models.

With the introduction of models for more advanced liver injury, the roles of TLRs, more specifically TLR4, should be re-evaluated. Additionally, the two downstream signaling pathways common to the TLR family also need to be re-examined. TLR3 signals through the TRIF-dependent pathway, TLR4 signals through both the MYD88- and TRIF-dependent pathways, and all other TLR members signal exclusively through the MYD88-dependent pathway (113, 267). Alcohol-induced liver injury occurs independently of the adaptor MYD88 in a five-

week Lieber-DeCarli model and requires the transcription factor IRF3, which is downstream of the adaptor TRIF (64, 110). Additionally, TRIF is required for liver injury in mice fed alcohol and injected with LPS (268). If the other members of the TLR family have greater roles in later stage ALD models, this should be reflected in the downstream signaling molecules as well. Interestingly, both TLR signaling pathways display cell-type specific effects in ALD models. Myeloid specific MYD88 knockout mice are protected against alcohol-induced liver injury and inflammation (66). On the other hand, bone marrow transplant studies reveal that while global IRF3 knockout mice are protected against liver injury, alcohol-fed mice that lack IRF3 in parenchymal cells have aggravated liver injury and inflammation (110). Therefore, it is important to understand how TLR signaling in different cell types changes in the later stage ALD models. Employing models that represent the full spectrum of ALD will help to uncover the role of TLR4, as well as the other TLRs, in disease pathogenesis.

Conclusion

In this body of work, I have characterized adipose tissue inflammation in two models of ALD. I have shown that alcohol impacts several immune cell populations in the adipose tissue and that alcohol-induced adipose tissue inflammation occurs in a sex-dependent manner. Further, I have shown that, in contrast to others, TLR4 is important for certain stages of liver injury. The requirement for TLR4 is restricted to specific cell populations in the adipose tissue. This characterization lays the groundwork for understanding how alcohol

impacts the adipose tissue. Uncovering the underlying mechanisms for alcohol-mediated adipose tissue dysfunction, in conjunction with how the adipose tissue impacts liver injury will broaden our understanding of ALD. This knowledge will help to uncover novel therapeutic targets, so that effective therapies can be developed to treat this disease.

Appendix A

Flow cytometry analysis

SVF Gating Strategy

Here, I describe the gating strategies used to analyze the data presented in Chapter III. During collection of the adipose tissue, a single spleen was collected from a WT, alcohol-fed mouse to use as a guide for leukocyte gating. The spleen was homogenized on a 70 μM filter, washed, and treated with ACK Lysing buffer alongside SVF samples as described in Chapter III. Splenocytes were stained, fixed, and acquired alongside SVF samples as described in chapter III.

The SVF gating strategy to identify macrophages and other adipose immune cells is based on previous studies using flow cytometry to analyze the adipose tissue (143, 269-271). First doublets are excluded by gating on singlets (Figure A1 D). Next, $CD45^+$ cells, leukocytes, are selected (Figure A1 E). Myeloid and Lymphoid populations are identified based on forward and side scatter properties (Figure A1 F). Here, the spleen is especially useful in delineating between these two populations (Figure A1 C).

The myeloid population was gated on the markers CD11b and F4/80 to identify macrophages ($CD11b^+F4/80^+$) (Figure A2 A and D). In spleen, this analysis revealed an absence of macrophages and a predominance of $CD11b^+F4/80^-$ cells (Figure A2 B and C). Fluorescence minus one (FMO) controls were used to gate on SVF macrophages (Figure A2 E and F). Once macrophages were identified, the phenotype was determined using CD206 and CD11c (Figure A2 G). Again, FMO controls were used to identify the three

distinct macrophage phenotypes, M1 ($CD206^{-}CD11c^{+}$), the intermediate, mixed phenotype ($CD206^{+}CD11c^{+}$), and M2 ($CD206^{+}CD11c^{-}$) (Figure A2 H and I).

In order to determine which cell types make up the $CD11b^{+}F4/80^{-}$ non-macrophage population, Gr-1 and CD11c were used to identify neutrophils and DCs, respectively. In the SVF, non-macrophages (Figure A3 D) were gated on CD11b and Gr-1 (Figure A3 E) to find neutrophils, with the aid of an FMO control (Figure A3 G). Interestingly, using the same gating in spleen (Figure A3 A and B) reveals that SVF neutrophils have higher expression of CD11b than neutrophils in the spleen. SVF DCs were also found in the non-macrophage population (Figure A3 F) using an FMO control (Figure A3 H).

From the lymphoid population, SVF B-cells were identified by gating on $CD45^{+}CD19^{+}$ cells (Figure A4 C and D) and using the CD19 FMO control (Figure A4 E), similar to the spleen (Figure A4 A and B). SVF T-Cells (total) were identified by gating the lymphoid population on $CD45^{+}CD3^{+}$ cells (Figure A5 D and E) by following the gating used for spleen (Figure A5 A and B). Total T-Cells were then separated into $CD8^{+}$ and $CD4^{+}$ T-Cells (Figure A5 G), using the same gating scheme as the spleen (Figure A5 C) as well as FMO controls (Figure A5 H and I).

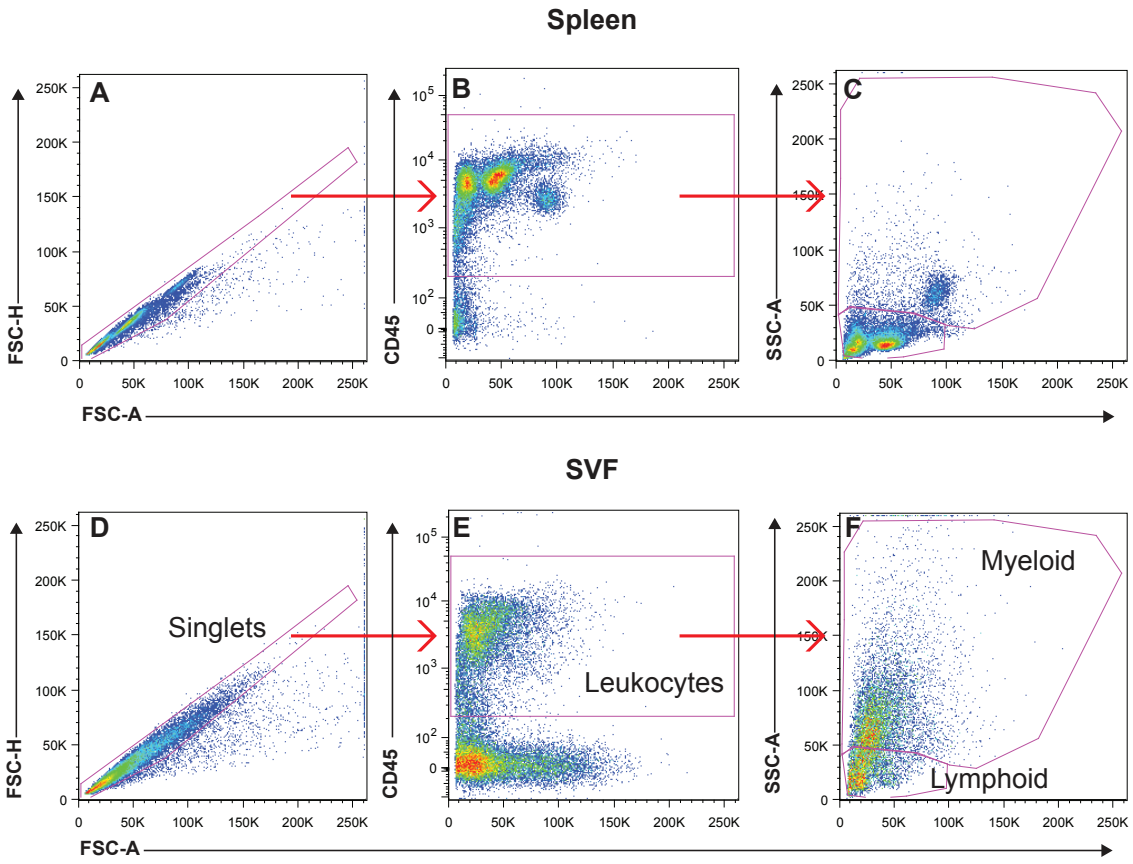

Figure A1: Gating scheme to identify SVF myeloid and lymphoid populations. The gating scheme for splenocytes (A) Singlets, (B) $CD45^+$ leukocytes, and (C) myeloid and lymphoid populations was applied to SVF samples to identify (D) singlets, (E) $CD45^+$ leukocytes, and (F) myeloid and lymphoid cells.

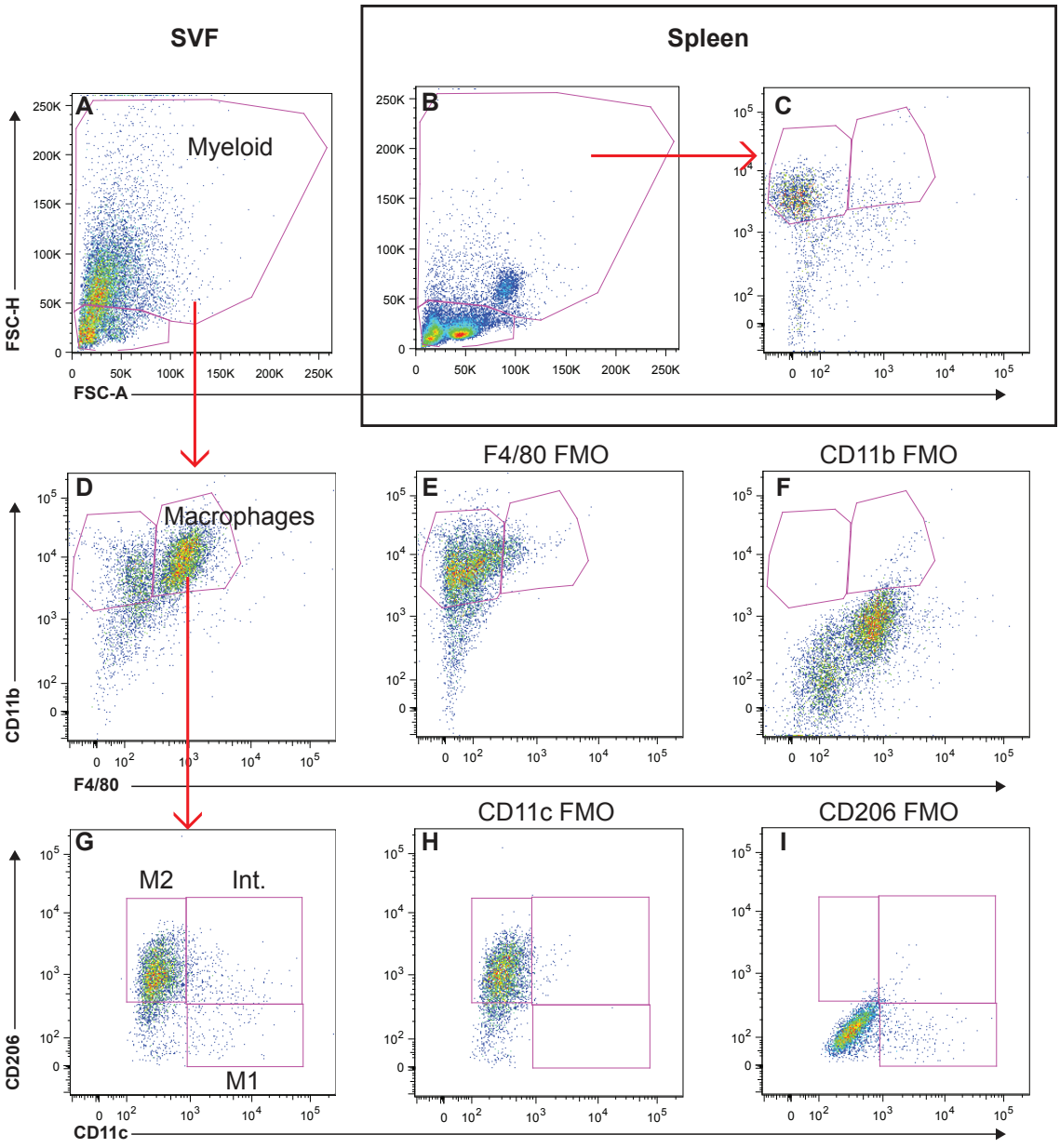

Figure A2: Gating scheme to identify SVF macrophages. (A) The SVF myeloid cell population. Splenocyte (B) myeloid cell population and (C) CD11b and F4/80 staining for reference. SVF myeloid cells were gated on CD11b and F4/80 to identify (D) $CD11b^{+}F4/80^{+}$ macrophages. (E) F4/80 FMO control for macrophages. (F) CD11b FMO control for macrophages. (G) SVF macrophages were stained for CD11c and CD206. (H) CD11c FMO control for macrophages (I) CD206 FMO control for macrophages.

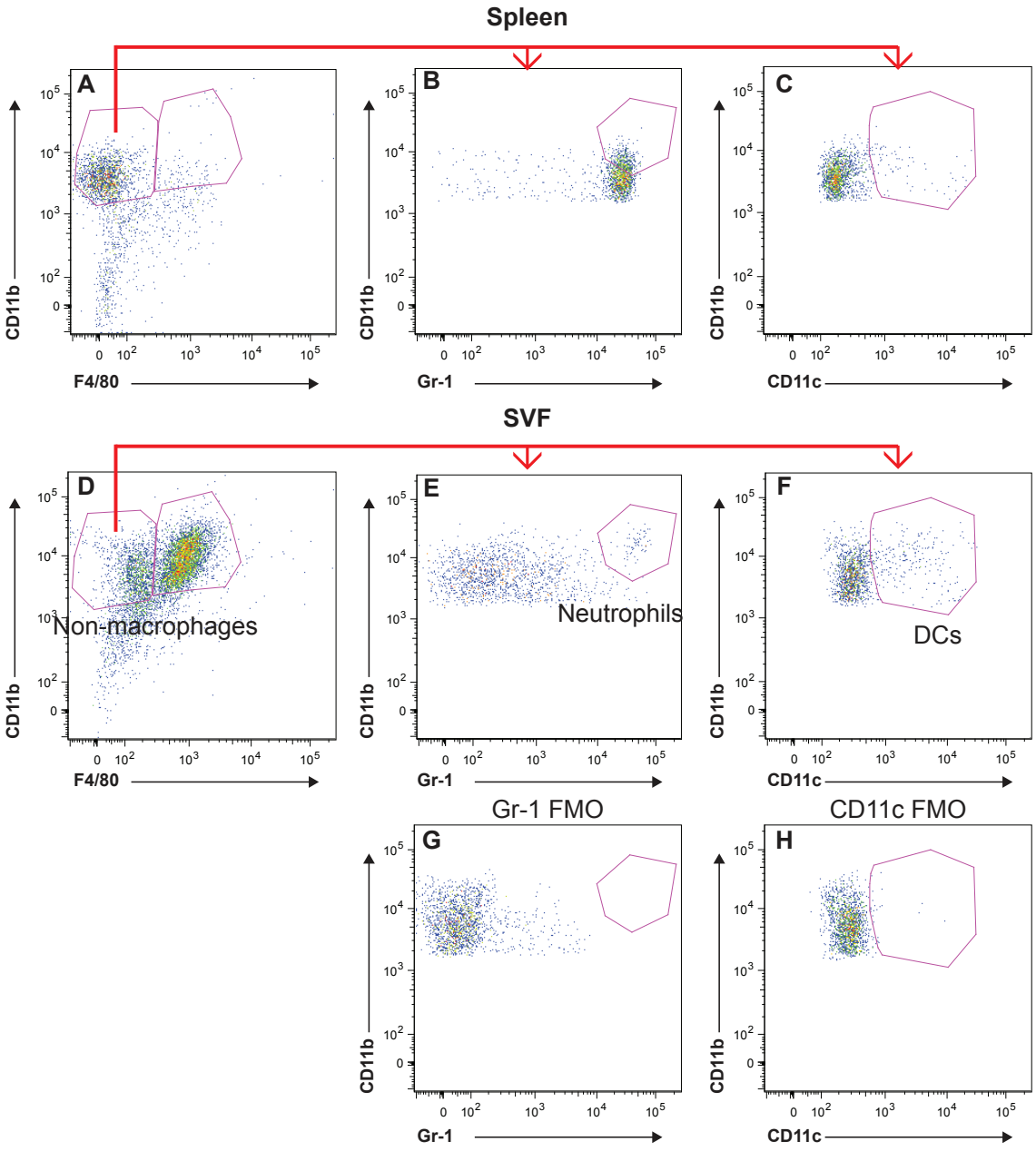

Figure A3: Gating scheme to identify SVF neutrophils and DCs. (A) Spleen $CD11b^{+}F4/80^{-}$ cells were gated on (B) CD11b and Gr-1 for neutrophils and (C) CD11b and CD11c for DCs. (D) SVF $CD11b^{+}F4/80^{-}$ non-macrophages were gated on (E) CD11b and Gr-1 for neutrophils and (F) CD11b and CD11c for DCs. (G) Gr-1 FMO control for neutrophils (H) CD11c FMO control for DCs.

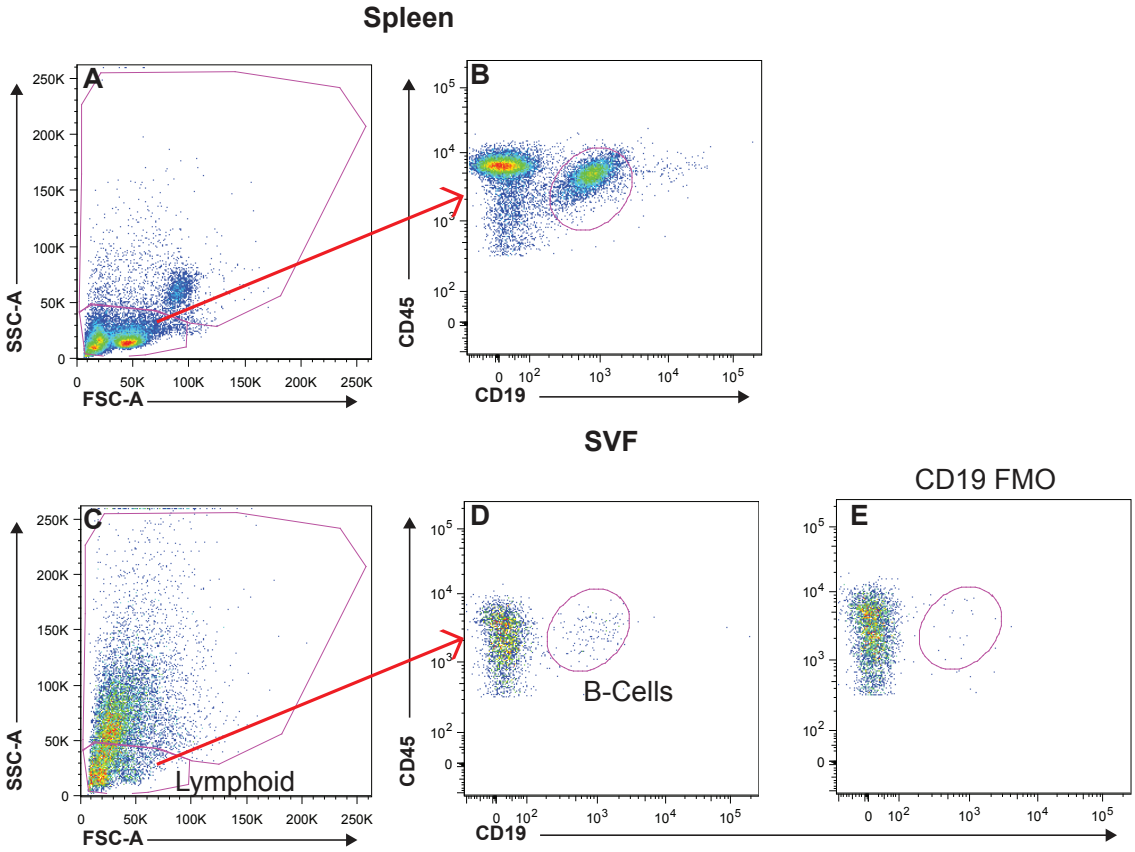

Figure A4: Gating scheme to identify SVF B-Cells. (A) Spleen lymphoid^{-} cells were gated on (B) CD45 and CD19 to for B-Cells (C) SVF lymphoid cells were gated on (D) CD45 and CD19 for B-Cells. (E) CD19 FMO control for B-Cells.

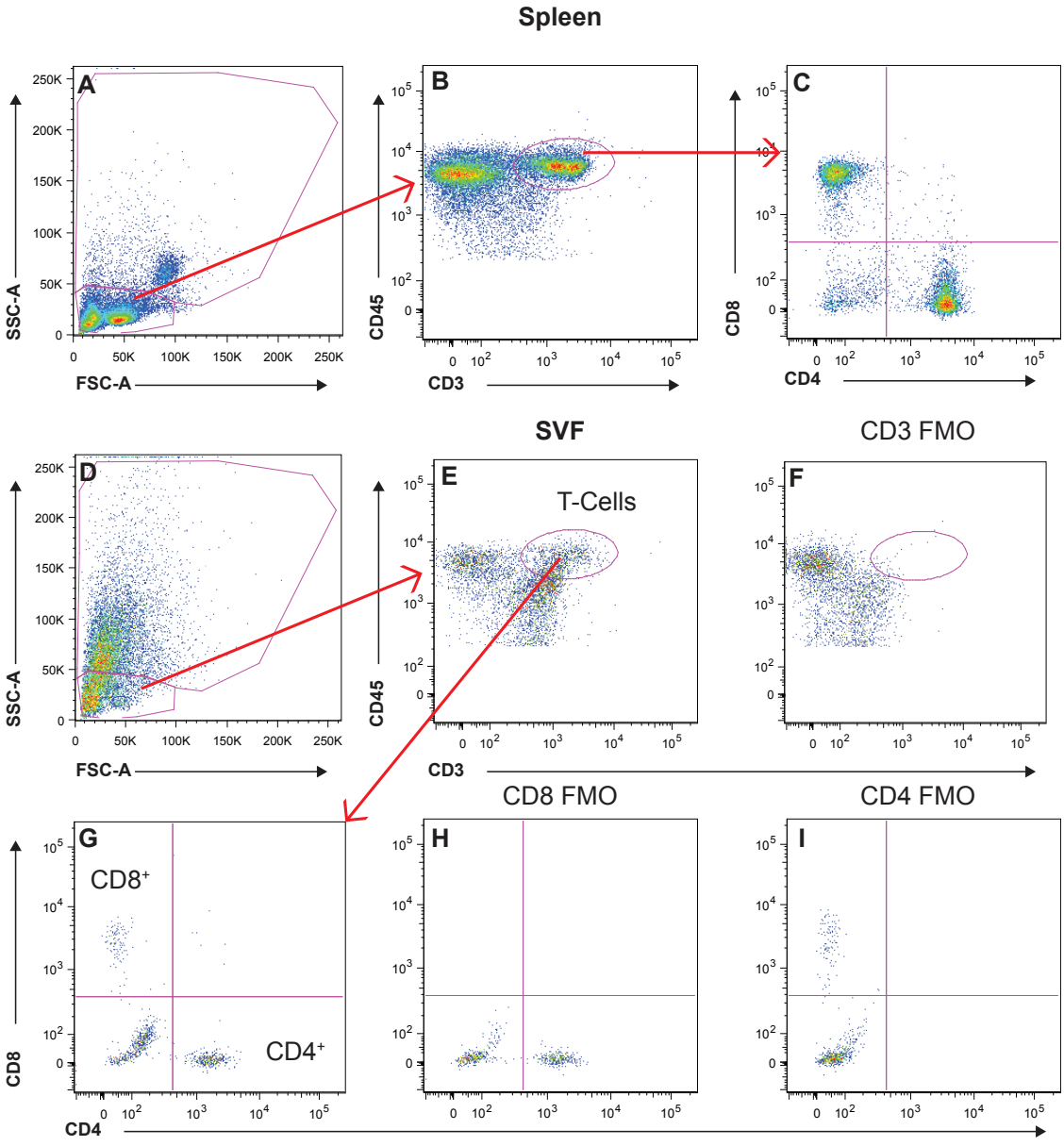

Figure A5: Gating scheme to identify SVF B-Cells. (A) Spleen lymphoid^{-} cells were gated on (B) CD45 and CD3 to for T-Cells (C) T-Cells were gated on CD4 and CD8. (D) SVF lymphoid cells were gated on (E) CD45 and CD3 for T-Cells. (F) CD3 FMO control for T-Cells. (G) T-Cells were gated on CD4 and CD8. (H) CD8 FMO control for T-Cells. (I) CD4 FMO control for T-Cells.

Peritoneal Macrophages Gating Strategy

The gating strategy for peritoneal macrophages was based on practical experience, gained from developing the above strategy. First, doublets were excluded by gating on singlets (Figure A6 A). Next, macrophages were identified as $CD11b^{+}F4/80^{+}$ cells (Figure A6 B), using FMO controls (Figure A6 C and D). Last, $TLR4^{+}$ macrophages ($F4/80^{+}TLR4^{+}$) can be identified (Figure A6 E) using an FMO control (Figure A6 F).

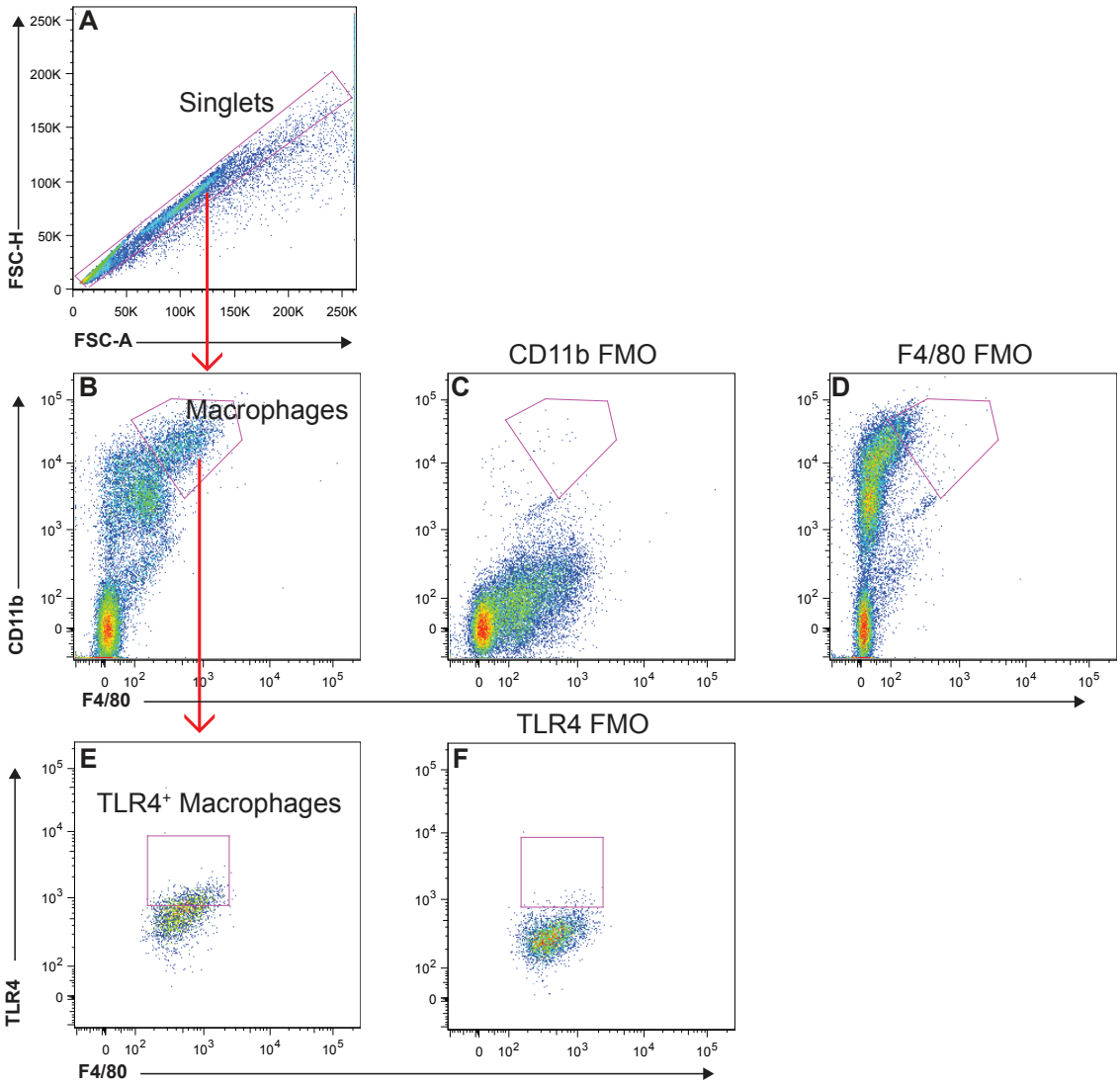

Figure A6: Gating scheme for peritoneal macrophages. (A) Singlets. (B) Macrophages are $CD11b^{+}F4/80^{+}$. (C) CD11b FMO control for macrophages. (D) F4/80 FMO control for macrophages. (E) $TLR4^{+}F4/80^{+}$ macrophages. (F) $TLR4^{+}$ FMO control for $TLR4^{+}$ macrophages.

Peritoneal Neutrophils Gating Strategy

The gating strategy for peritoneal neutrophils was based on practical experience, gained from developing the SVF gating strategy. First, doublets were excluded by gating on singlets (Figure A7 A). Next granulocytes were gated based on forward and side scatter (Figure A7 B). Neutrophils were identified as $CD11b^{+}Ly6G^{+}$ cells (Figure A7 C), with aid of FMO controls (Figure A7 D and E). TNFα expressing neutrophils were identified (Figure A7 F) using an FMO control (Figure A7 G). An additional TNFα FMO control was used, in which the isotype control for TNFα was added to the staining cocktail to account for intracellular background signal (Figure A7 H).

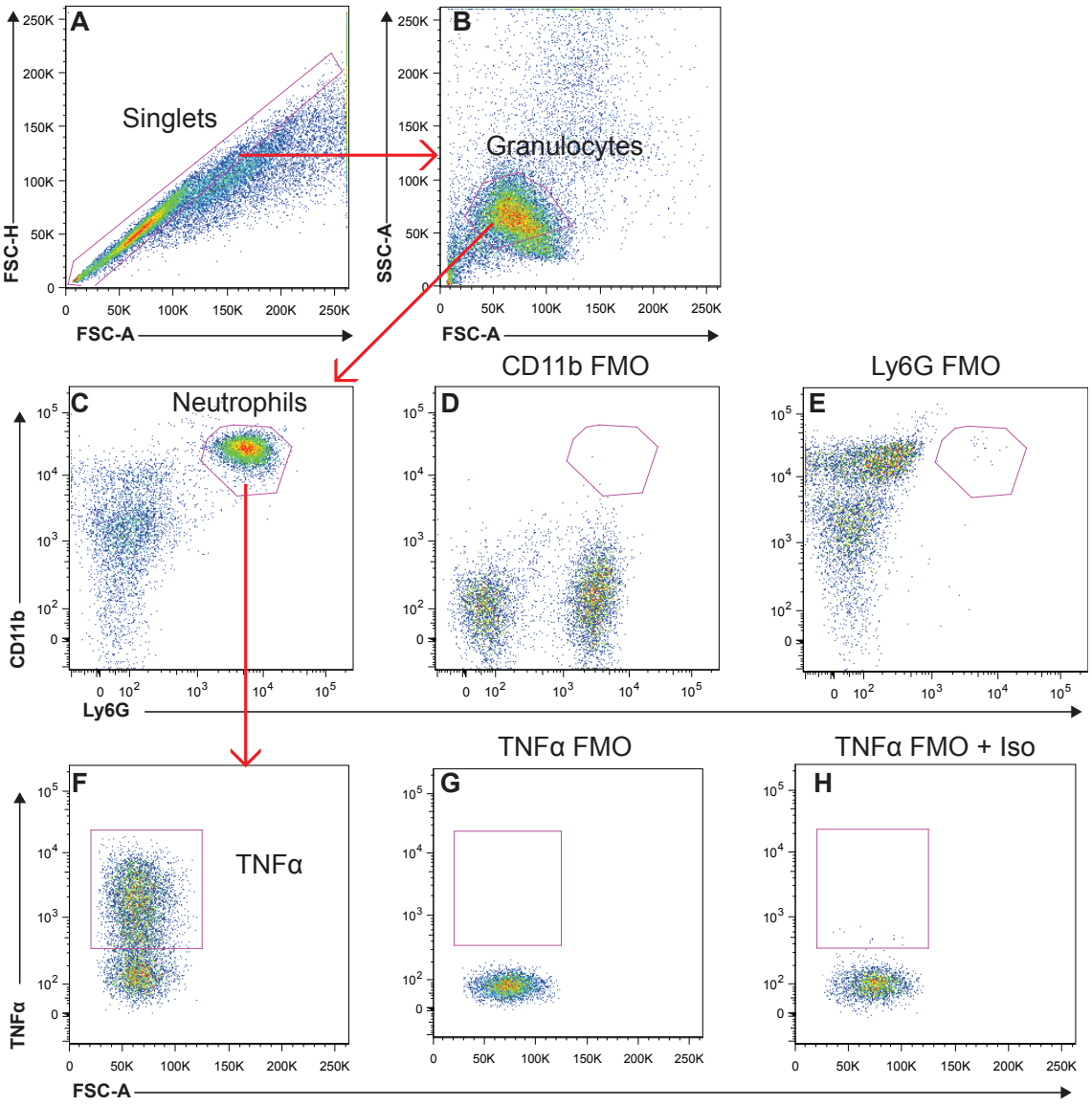

Figure A7: Gating scheme for peritoneal neutrophils. (A) Singlets. (B) Granulocytes (C) $CD11b^{+}Ly6G^{+}$ neutrophils. (D) CD11b FMO control for neutrophils. (E) Ly6G FMO control for neutrophils. (F) TNFα-expressing neutrophils. (G) TNFα FMO control for neutrophils. (H) TNFα FMO control with the control isotype for the TNFα antibody.

Appendix B

Myeloid-specific gp96 knockout mice are protected against alcohol-induced adipose tissue inflammation

Introduction

There has been a shortage of novel therapeutics to treat ALD in the past few decades, necessitating investigation into potential targets for future therapeutics. Our lab has demonstrated that targeting the cytoplasmic chaperone HSP90 with the drug 17-DMAG prevents both alcohol- and LPS-induced liver injury (225, 272). However, cytoplasmic HSP90 inhibitors also act upon its ER homolog, gp96 (273, 274). The extent to which 17-DMAG mediates the reversal of liver injury through gp96 remains unclear. HSP90 and gp96 share about 50% sequence homology and are structurally similar (275, 276). The nucleotide binding pocket, where 17-DMAG binds, is also highly conserved between HSP90 and gp96 (276). Structure-based drug design has produced several molecules that bind selectively to gp96, which will enable future detailed mechanistic studies (273, 277).

gp96, also referred to as GRP94, was initially discovered in response to glucose deprivation (276). Further work has demonstrated that it acts in the unfolded protein response (UPR) as a protein chaperone to help alleviate ER stress (274). Under homeostatic conditions, gp96 chaperones most members of the TLR family (excluding TLR3), as well as many integrin molecules (including CD11b and CD11c) and is required for their proper localization (278-281). Consequently, gp96-deficient macrophages are unable to respond to TLR stimulation, but still retain the ability to respond to the cytokines TNFα and IFNγ (279). These characteristics make this model a very valuable tool for studying

immune-related mechanisms. gp96 whole body knockout mice exhibit embryonic lethality, therefore conditional knockouts must be used in order to study this chaperone (274, 276).

Here, I use myeloid-specific gp96 knockout (gp96KO) mice to test the hypothesis that deleting gp96 from macrophages will decrease alcohol-induced adipose tissue inflammation, due to the absence of TLR4 on the surface of macrophages.

Results and Discussion

In order to determine whether gp96 expression in macrophages impacts adipose tissue inflammation, female myeloid-specific gp96 knockout mice (gp96KO) and their WT littermates were subjected to the NIAAA model (123). In these mice, gp96 expression is absent in macrophages, but retained in neutrophils (279). Perigonadal adipose tissue was collected and used for gene expression analysis. The NIAAA model resulted in a robust increase in the expression of both *Il6* and *Ccl2* in the adipose tissue of alcohol-fed, but not pair-fed, WT mice, similar to the results presented in Chapter II. Expression of *Tnf* remained unchanged in alcohol-fed mice. In contrast, the induction of both *Il6* and *Ccl2* was completely absent in the alcohol-fed gp96KO mice compared to pair-fed controls and was significantly decreased compared to alcohol-fed WT controls (Figure B1 A). Alcohol-induced adipose tissue cytokine production is inhibited in gp96KO mice.

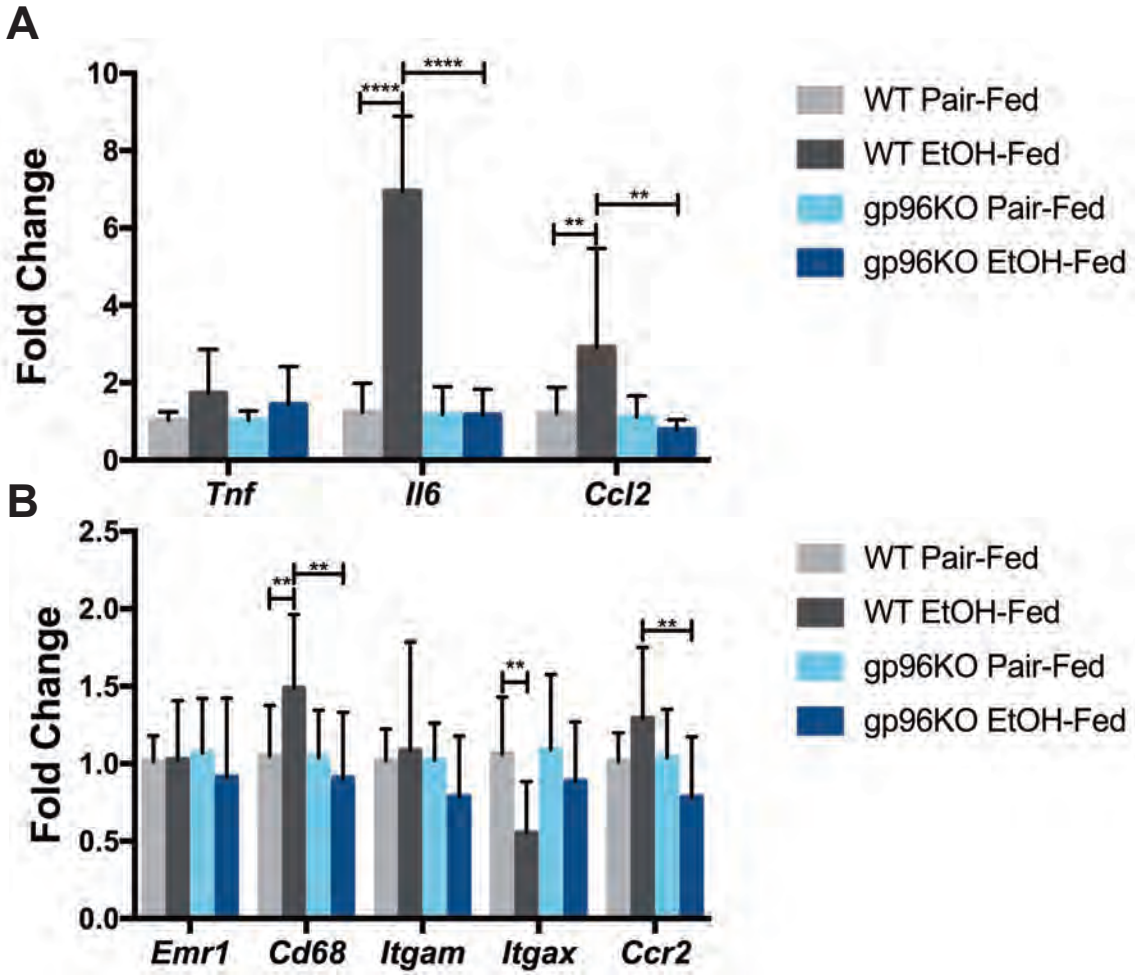

Figure B1: gp96KO mice are protected against alcohol-induced adipose tissue inflammation. Perigonadal adipose tissue mRNA levels of (A) *Tnf*, *Il6*, and *Ccl2* and (B) *Emr1*, *Cd68*, *Itgam*, *Itgax*, and *Ccr2* were analyzed by qPCR. * p<0.05, ** p<0.01, *** p<0.001, ****p<0.0001. Data are represented as mean ± SEM. n=6-9 from three independent experiments.

The expression of pro-inflammatory cell markers was also assessed in the adipose tissue of the gp96KO mice. The expression of *Cd68*, a marker of macrophage activation, is increased in alcohol-fed WT mice, but not alcohol-fed gp96KO mice. The expression of other cell markers, including *Emr1* (F4/80), *Itgam* (CD11b), and *Ccr2* all remained unchanged in alcohol-fed mice compared to pair-fed controls for both genotypes. The expression of *Itgax* (CD11c) was downregulated in alcohol-fed WT mice (Figure B1 B). This indicates that the resident adipose tissue macrophages are becoming activated and producing pro-inflammatory cytokines but new macrophages are not infiltrating into the tissue. Alcohol-fed gp96KO mice are protected against this adipose tissue macrophage activation.

Together, these data demonstrate that adipose tissue expresses pro-inflammatory cytokines in a model of early alcohol-induced liver injury. This effect is mediated by the expression of gp96 in macrophages, as the adipose tissue from alcohol-fed gp96KO mice does not express these pro-inflammatory cytokines. It remains to be determined through which client proteins gp96 is mediating adipose tissue inflammation. In Chapter III of this dissertation, I present evidence that TLR4, a client of gp96, mediates some aspects of alcohol-induced adipose tissue inflammation. Of the other known client proteins, both TLR2 and TLR9 have been implicated in alcohol-induced liver inflammation, but their role in adipose tissue inflammation is not known (67). CD11c, one of the integrins which gp96 chaperones, is required for diet-induced adipose tissue

Inflammation, and could also contribute to alcohol-induced adipose tissue inflammation (140). Exploring how each gp96 client protein, specifically the TLRs and integrins, impacts alcohol-induced adipose tissue inflammation will help to determine the mechanism through which gp96 promotes inflammation.

In order to deepen my understanding of the role of gp96 in alcohol-induced adipose tissue inflammation, I used the gp96KO mice and their WT littermates in the chronic, multiple-binge alcohol model described in Chapter III. This was done to compare the results to the NIAAA model to determine if gp96 is important for early adipose tissue inflammation, later adipose tissue inflammation, or both. Unfortunately, gp96KO mice experience a very high premature mortality rate when subjected to the chronic, multiple-binge experiment. I, as well as others in the laboratory, performed these experiments and demonstrated that the gp96KO mice have a premature mortality rate of approximately 60%-80%, compared to their WT littermates, which have a premature mortality rate of approximately 25%-50%. Therefore, despite multiple attempts, I was unable to use these mice in the multiple-binge model.

gp96 represents a novel, potential therapeutic target for ALD because its client proteins are highly important molecules for immune cell function. Deleting gp96 from macrophages blocks alcohol-induced adipose tissue inflammation. However, which gp96 client proteins mediate alcohol-induced adipose tissue inflammation remains to be fully determined.

Materials and Methods

Animals and experimental models

Mice were subjected to the NIAAA model, which recapitulates the chronic-binge drinking patterns of AH patients, as described earlier (123). The myeloid-specific gp96 knockout mice (*LysMCre*$^{+/-}$*Hsp90b1*$^{f/f}$) and their WT littermates (*LysMCre*$^{-}$*Hsp90b1*$^{f/f}$) were provided by Dr. Zihai Li at the Medical University of South Carolina (279). The mice were bred at our facility for our experiments. Briefly, female mice were divided into two groups. One group was fed a 5% ethanol (v/v) Lieber-DeCarli diet (Bio-Serv, #F1258SP) for 10 days, following a one-week ramp up period. On the eleventh day, mice received an ethanol gavage (5 g/kg body weight, 31.5% ethanol) and were sacrificed nine hours later. The other group was fed an isocaloric control diet (Bio-Serv, #F1258SP) during the feeding and a maltose dextrin (Bio-Serv, #3585) gavage was administered nine hours before sacrifice. Perigonadal adipose tissue was excised and snap frozen.

Ethics statement

All animals received proper care in accordance with the *Guide for the Care and Use of Laboratory Animals* from the National Institutes of Health. The protocol was approved by the Institutional Animal Care and Use Committee of the University of Massachusetts Medical School (protocol number A-2393). Animals were euthanized by carbon dioxide asphyxiation followed by cervical dislocation.

RNA extraction, cDNA synthesis, and qPCR analysis

Total RNA was extracted from flash frozen adipose tissue using the RNeasy Lipid Tissue Mini Kit (Qiagen, #74804), according to manufacturer's instructions. RNA concentration was measured with a NanoDrop 2000 (ThermoScientific). cDNA was synthesized using the Reverse Transcription System (Promega, #A3500). mRNA transcript levels were quantified using iTAQ Universal SYBR Green Supermix (Bio-Rad, #172-5121) and CFX Connect Real-Time PCR Detection System (Bio-Rad) and normalized to 18S ribosomal RNA. Primer sequences are listed in Table B1.

Statistical analysis

Data are represented as mean ± SEM. All statistical analysis was performed using Graphpad Prism 7.0. ANOVA was used to determine the difference between groups.

Table B1: List of Primer Sequences 5'-3'

Gene	Sequence
18s forward	GTAACCCGTTGAACCCCATT
18s reverse	CCATCCAATCGGTAGTAGCG
Ccl2 forward	CAGGTCCCTGTCATGCTTCT
Ccl2 reverse	TCTGGACCCATTCCTTCTTG
Ccr2 forward	GTGTACATAGCAACAAGCCTCAAAG
Ccr2 reverse	CCCCCACATAGGGATCATGA
Cd68 forward	CCCACAGGCAGCACAGTGGAC
Cd68 reverse	TCCACAGCAGAAGCTTTGGCCC
Emr1 forward	TGCATCTAGCAATGGACAGC
Emr1 reverse	GCCTTCTGGATCCATTTGAA
Il6 forward	ACAACCACGGCCTTCCCTACTT
Il6 reverse	CACGATTTCCCAGAGAACATGTG
Itgam forward	ATGGACGCTGATGGCAATACC
Itgam reverse	TCCCCATTCACGTCTCCCA
Itgax forward	CTGGATAGCCTTTCTTCTGCTG
Itgax reverse	GCACACTGTGTCCGAACTCA
Tnf forward	GAAGTTCCCAAATGGCCTCC
Tnf reverse	GTGAGGGTCTGGGCCATAGA

Appendix C

Chronic alcohol does not enhance adipose tissue lipolysis

Introduction

Lipolysis is the process through which triglycerides, such as those stored in adipocytes, are broken down into free fatty acids and glycerol (130, 131). Lipolysis is upregulated in times of energy need and can be stimulated through glucocorticoids and β-adrenergic signaling, but is down regulated in times of energy excess and is inhibited by insulin signaling (130, 131). ATGL catalyzes the first step, converting triglycerides to diglycerides with the release of one free fatty acid molecule. HSL functions next in this process, catalyzing the conversion of diglycerides into monoglycerides, again releasing a free fatty acid in the process. The last step catalyzed by MGL breaks down the monoglycerides into a free fatty acid and glycerol (131). The free fatty acids can then be used by other tissues, such as muscle and liver, as an energy source (130, 131).

Adipocyte lipolysis is dysregulated in obesity and is related to insulin resistance (130, 282). There are several proposed mechanisms through which this may occur, the most obvious being the ectopic lipid deposition in peripheral organs due to increased free fatty acids in circulation (282). More interestingly, the dysregulation of lipolysis could cause insulin resistance through adipose tissue inflammation (282). When mice on a high-fat diet are fasted, they exhibit an initial massive influx of macrophages to the adipose tissue, which wanes over time. This phenomenon is absent in mice that lack ATGL, one of the enzymes that catalyzes lipolysis (262). Further, adipose tissue macrophages can uptake excess lipid in the adipose tissue in order to prevent lipid uptake in peripheral

tissues (261, 262). There is a clear dynamic between lipolysis and adipose inflammation in obesity models, but whether a similar paradigm exists in ALD models remains to be determined.

Using both the Lieber-DeCarli and NIAAA models, it was demonstrated that chronic alcohol consumption increases adipocyte lipolysis. Adipocyte lipolysis is usually assessed by a decrease in adipocyte size, an increase in the activation of the enzymes that carry out triglyceride breakdown, and an increase circulating glycerol or free fatty acids, all of which have been demonstrated in these two models (193, 201, 202). In some instances, adipocyte diameter, and not adipocyte surface area, was used to determine adipocyte cell size (193, 202). Gene expression analysis was used to determine the activation of two enzymes that catalyze lipolysis, *Hsl* and *Atgl*. However, lipolysis is dictated at the protein level by the activity of these proteins, and HSL activation is dependent on its phosphorylation status (193, 283). In a follow up study, this same group established that chronic alcohol consumption increased the levels of phosphorylated HSL and total ATGL (protein) in the adipose tissue (202). Despite the caveats in the data, these authors were able to demonstrate that adipose tissue isolated from alcohol-fed animals released more free fatty acids *ex vivo* than pair-fed controls, indicating that alcohol consumption primes the adipose tissue for lipolysis (193, 202). Mice subjected to the NIAAA model also display elevated plasma glycerol levels along with increased phosphorylated HSL and total ATGL, which corroborates the above *ex vivo* data (201). Together, this

demonstrates that *in vivo* alcohol administration enhances adipocyte lipolysis. Future studies will need to employ the correct techniques in order to enable mechanistic studies into this phenomenon.

A direct link between alcohol-induced adipocyte lipolysis and hepatic steatosis has been proposed, but not yet fully evaluated. Supplementing alcohol-fed mice with “heavy water” (deuterium oxide) allows for the incorporation of deuterium into lipid species, which subsequently are analyzed by mass spectrometry. Over the course of the alcohol feeding, specific lipid species were depleted from the adipose tissue (presumably due to lipolysis). During the same time period, the authors identified a number of lipid species that accumulated in the liver (203). However, it is impossible to determine the exact source of the labeled lipids in the liver. While this data does support the idea that chronic alcohol enhances lipolysis, which then directly contributes to hepatic steatosis, a direct link between the two processes remains elusive.

A series of *in vitro* experiments determined that alcohol may in fact suppress lipolysis, contrary to the above *in vivo* data. Adipocytes isolated from alcohol-fed rats release less glycerol when stimulated with isoproterenol or CL316,243, two β-adrenergic agonists, when compared to adipocytes isolated from pair-fed animals (204, 205). However, *in vivo* analysis of triglyceride kinetics revealed that the rate of triglyceride breakdown in the adipose tissue of alcohol-fed rats was greater than in pair-fed rats (204). Insulin signaling in adipocytes suppresses lipolysis (130). Using hyperinsulinemic-euglyemic clamp studies,

Kang *et al*. established the ability of insulin to decrease circulating glycerol was inhibited in alcohol-fed rats, compared to pair-fed rats (204). Further work is needed in order to reconcile the differences between how alcohol impacts adipocyte lipolysis *in vivo* and *in vitro*.

Here I aimed to establish whether alcohol induces adipose tissue lipolysis, in order to determine if lipolysis is one of the drivers of alcohol-induced adipose tissue inflammation. I used mice subjected to both the NIAAA model and the chronic, multiple-binge model to determine if alcohol-induced lipolysis is related to the severity of liver injury. Last, I established an *in vitro* model of chronic alcohol exposure on the mouse adipocyte cell line, 3T3-L1, to enable further mechanistic studies of how alcohol exposure mediates lipolysis.

Results and Discussion

I wanted to determine whether chronic alcohol exposure, with one or several binges, induces active adipocyte lipolysis. Lipolysis is the process by which triglycerides are broken down into free fatty acids and glycerol molecules (130, 131). I quantified glycerol in the serum from female, C57BL/6 mice subjected to the NIAAA model. Circulating glycerol decreased 35% in alcohol-fed mice compared to pair-fed animals (Figure C1 A). The same trend occurred in female, C57BL/6J mice subjected to the chronic, multiple-binge model; there was a 37% decrease in circulating glycerol. This is opposite to what has been published so far. Mice fed alcohol exhibit an increase in circulating glycerol (201). One possible explanation for the different results is that the increase in glycerol is

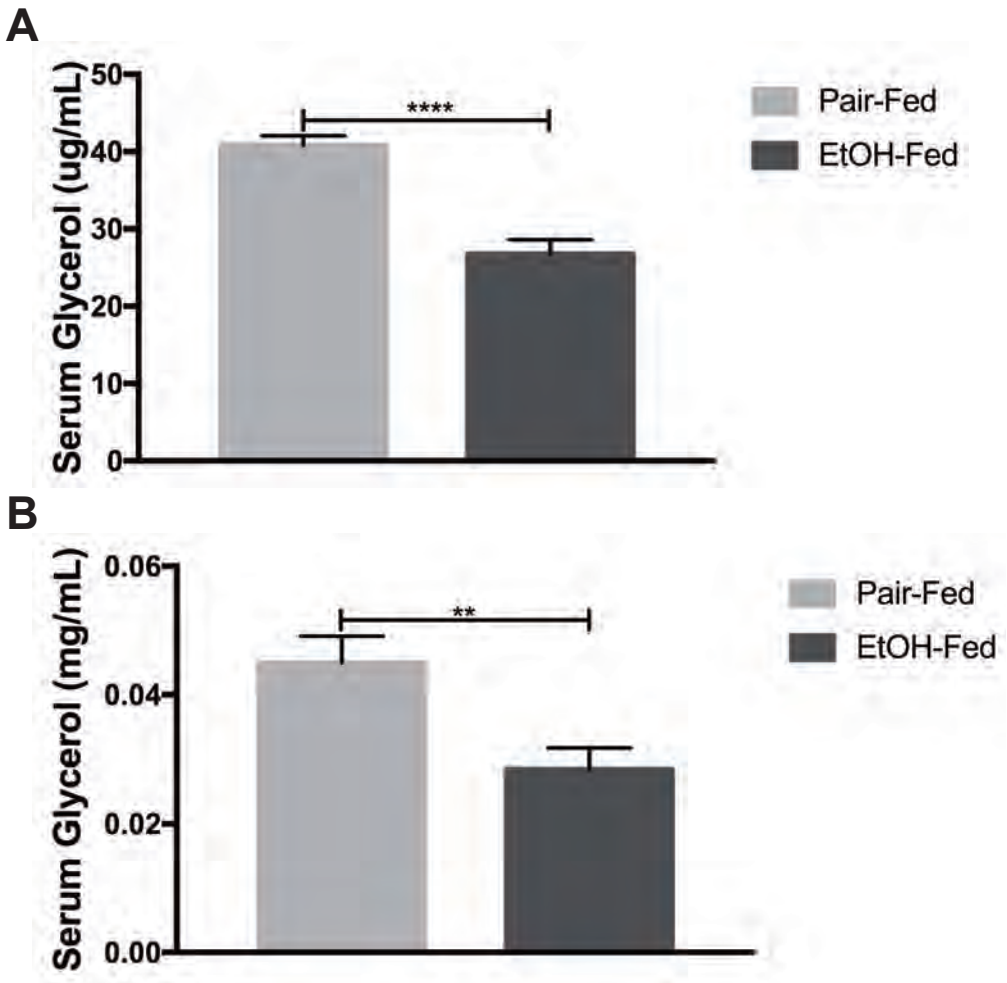

Figure C1: Chronic alcohol consumption decreases circulating glycerol. Serum glycerol quantified in mice subjected to (A) the NIAAA model (n=16-17 from two independent experiments) and (B) the chronic, multiple-binge model (n=9-12 from two independent experiments). * $p<0.05$, ** $p<0.01$, *** $p<0.001$, ****$p<0.0001$. Data are represented as mean ± SEM.

a transient phenomenon that I was not able to capture, as cell types such has hepatocytes, are able to uptake glycerol molecules (284). Therefore, I aimed to use alternative strategies in order to measure stable artifacts of lipolysis.

Adipocytes increase in size as they store lipids and decrease in size as they release their contents (285). I sought to determine whether chronic alcohol exposure, with one or several binges, changes adipocyte size. I quantified adipocyte size from perigonadal adipose tissue isolated from female, C57BL/6J mice subjected to the NIAAA model. The distribution of adipocyte size was the same between alcohol-fed mice and their pair-fed counterparts (Figure C2 A). This is in contrast with a previously published study, in which the authors also used the NIAAA model; however, they used male mice in their experiments and the impact of sex on alcohol-induced adipocyte lipolysis remains to be determined (201).

In order to determine if long-term alcohol consumption influences lipolysis differently that the NIAAA model, I performed the same cell size analysis in female, C57BL/6J mice subjected to the chronic, multiple-binge model. Other studies using a long-term Lieber-DeCarli diet, without binges, have demonstrated a decrease in adipocyte size in alcohol-fed animals (193, 202). Similar to my results in the NIAAA model, the chronic, multiple-binge model does not decrease adipocyte cell size (Figure C2 B). Moreover, the alcohol-fed mice have a lower frequency of small adipocytes and a higher frequency in mid-sized adipocytes.

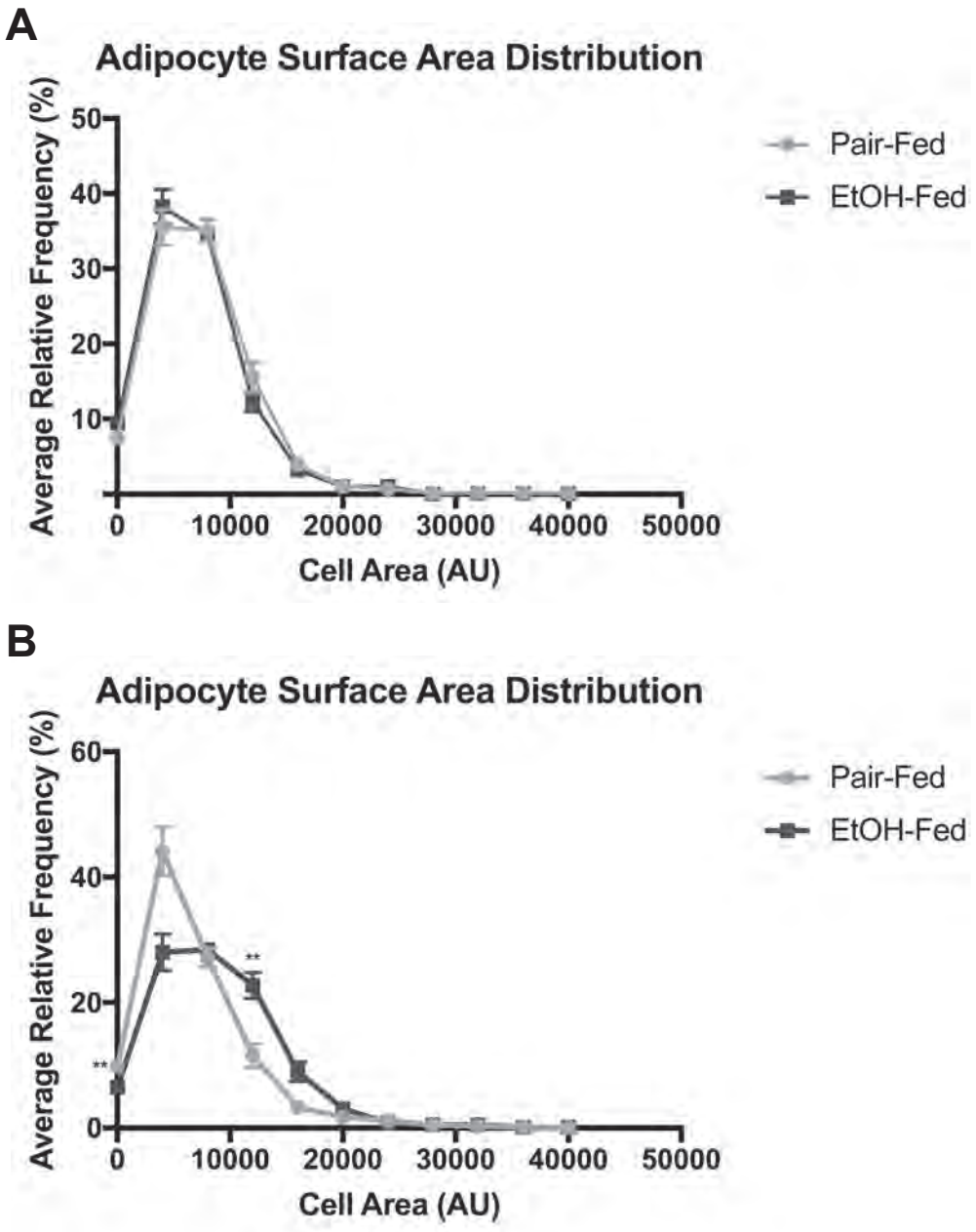

Figure C2: Chronic alcohol consumption does not decrease adipocyte size. Adipocyte surface area measured on H&E sections from perigonadal adipose tissue isolated from mice subjected to (A) the NIAAA model (n=6) and (B) the chronic, multiple-binge model (n=6-7). AU, arbitrary units. * $p<0.05$, ** $p<0.01$, *** $p<0.001$, ****$p<0.0001$. Data are represented as mean ± SEM.

This indicates that chronic, multiple-binge alcohol increases adipocyte size, which could be due to the inhibition of lipolysis.

Next, I wanted to determine if the absence of increased circulating glycerol and decreased cell size in the NIAAA model, presented in Figures C1 and C2 was due to the modulation of the lipolytic enzymes. The expression of ATGL, which catalyzes the first step of lipolysis, is upregulated in response to lipolytic stimuli and glucocorticoid signaling. The second step of lipolysis occurs when HSL is phosphorylated, which happens in response to β-adrenergic signaling (130, 131). I used western blotting to determine if the NIAAA model increases the phosphorylation of HSL and/or upregulates the expression of ATGL. As shown in Figure C3 A and quantified in Figure C3 B, chronic, single-binge alcohol consumption did not activate either HSL or ATGL. In fact, the NIAAA model slightly decreases the levels of phosphorylated HSL, but this is not significant. This trend supports the above data, in which serum glycerol is decreased (Figure C1 A) and adipocyte cell size does not change (Figure C2 A).

Interestingly, while the current *in vivo* literature supports active adipocyte lipolysis in alcohol-fed mice, there is *ex vivo* data that demonstrates alcohol suppresses lipolysis (204, 205). In order to determine if *in vitro* alcohol exposure inhibits lipolysis, I cultured differentiated 3T3-L1 cells in 50 mM ethanol, which mimics chronic alcohol consumption. I stimulated lipolysis with isoproterenol, a β-adrenergic agonist, for different time points and measured HSL and ATGL activation via western blotting and glycerol release into the cell supernatant.

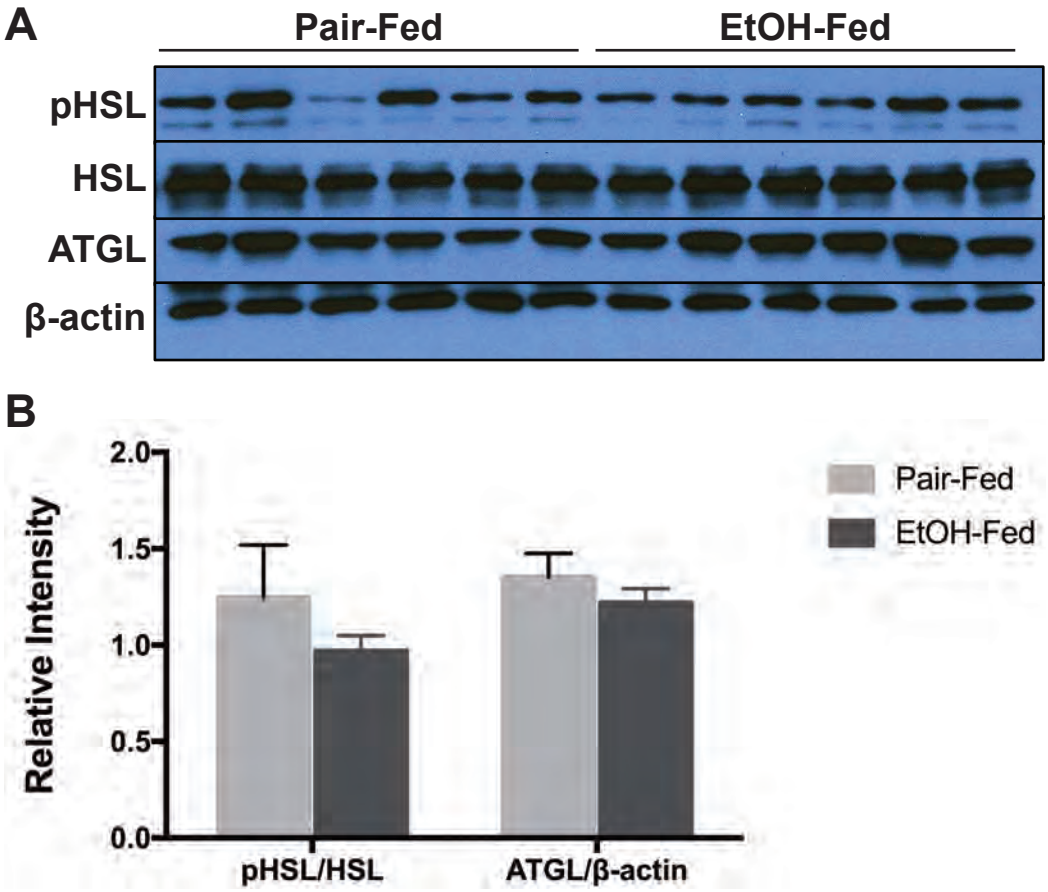

Figure C3: Chronic alcohol consumption does not enhance activation of lipolysis enzymes. (A) Western blot analysis of whole-cell lysates generated from perigonadal adipose tissue isolated from C57BL/6 mice subjected to the NIAAA model. (B) Quantification of bands from (A). pHSL is normalized to total HSL expression; ATGL is normalized to β-actin expression. n=6. * $p<0.05$, ** $p<0.01$, *** $p<0.001$, ****$p<0.0001$. Data are represented as mean ± SEM.

Isoproterenol greatly increased the phosphorylation of HSL, but had no impact on the expression of ATGL (Figure C4 A and B). When the 3T3-L1 cells were cultured in ethanol, the isoproterenol-mediated increase in HSL phosphorylation was completely blocked (Figure C4A and B). Culturing the cells in ethanol also inhibited glycerol release over time (Figure AC4 C). This effect was not specific to isoproterenol because ethanol also inhibited dexamethasone (a glucocorticoid agonist) stimulated glycerol release (Figure C4 D). This *in vitro* data complements the previously published *ex vivo* data, in which alcohol suppressed stimulated lipolysis (204, 205). These *in vitro* experiments also support the above data that suggests chronic alcohol consumption does not increase adipocyte lipolysis.

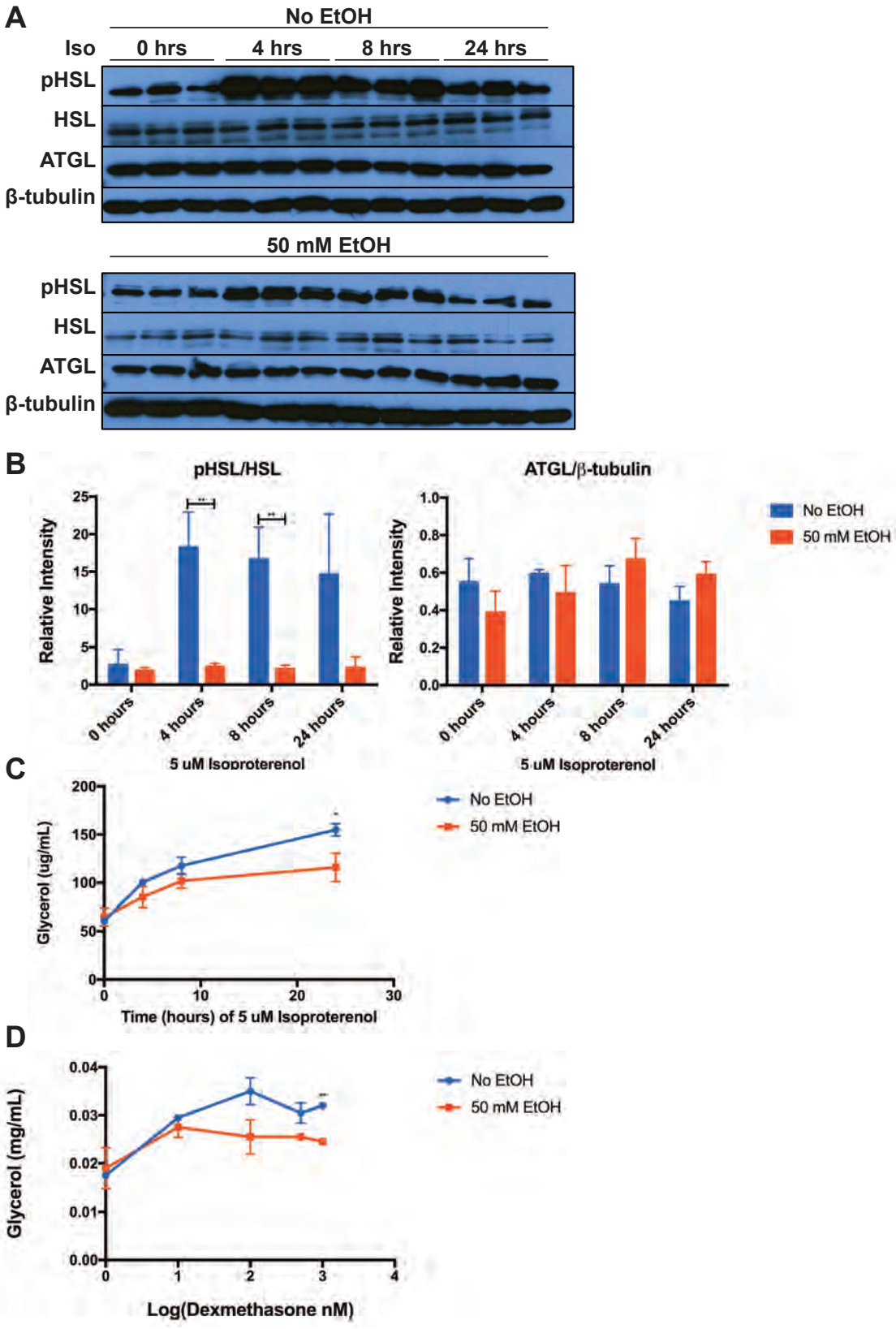
A
No EtOH
Iso
0 hrs
4 hrs
8 hrs
24 hrs
pHSL
HSL
ATGL
β-tubulin
50 mM EtOH
pHSL
HSL
ATGL
β-tubulin
B
pHSL/HSL
Relative Intensity
0 hours
4 hours
8 hours
24 hours
5 uM Isoproterenol
ATGL/β-tubulin
Relative Intensity
No EtOH
50 mM EtOH
C
Glycerol (ug/mL)
No EtOH
50 mM EtOH
Time (hours) of 5 uM Isoproterenol
D
Glycerol (mg/mL)
No EtOH
50 mM EtOH
Log(Dexmethasone nM)

Figure C4: Chronic alcohol exposure inhibits adipocyte lipolysis. Differentiated 3T3-L1 cells were cultured in 50 mM ethanol for 72 hours and then stimulated with either 5 μM isoproterenol for 0, 4, 8, and 24 hours (A-C) or 10 nM, 50 nM, 500 nM, and 1 μM dexamethasone for 24 hours (D). (A) Western blot analysis of whole-cell lysates. (B) Quantification of bands from (A). pHSL is normalized to total HSL expression; ATGL is normalized to β-tubulin expression. Glycerol release into the cell supernatant was quantified for (C) isoproterenol and (D) dexamethasone-stimulated cells. Iso, isoproterenol. * $p<0.05$, ** $p<0.01$, *** $p<0.001$, ****$p<0.0001$. Data are represented as mean ± SD.

Materials and Methods

Animals and experimental models

Eight- to ten-week old female C57BL/6J mice were purchased from Jackson Laboratories (strain 000664). Two experimental models of chronic alcohol consumption were used. In the first, mice were subjected to the NIAAA model (123). Briefly, mice were divided into two groups. One group had *ab libitum* access to a 5% ethanol (v/v) Lieber-DeCarli diet (Bio-Serv, #F1258SP) for 10 days, following a one-week ramp up period. On the eleventh day, mice received an ethanol gavage (5 g/kg body weight, 31.5% ethanol) and were sacrificed nine hours later. The other group was fed an isocaloric control diet (Bio-Serv, #F1259SP) during the feeding and a maltose dextrin (Bio-Serv, #3585) gavage was administered nine hours before sacrifice. For the second model, mice were subjected to a chronic, multiple-binge model of alcohol exposure modified from an early stage alcoholic steatohepatitis model (68). Mice were assigned to two groups. The first group had *ad libitum* access to a 5% ethanol (v/v) Lieber-DeCarli diet (Bio-Serv, #F1258SP) for five weeks, following a one-week period of ethanol acclimatization. After 10 days of 5% ethanol, mice received an ethanol gavage (5 g/kg body weight, 31.5% ethanol) once per week for the duration of the feeding for a total number of five gavages. The second group was under isocaloric control and was fed a control Lieber-DeCarli diet (Bio-Serv, #F1259SP) and received an isocaloric gavage of maltose dextrin (Bio-Serv, #3585). Mice were euthanized nine hours after the final gavage by CO_2

inhalation followed by cervical dislocation Blood was collected for serum isolation. Perigonadal adipose tissue was excised and fixed in 10% buffered formalin or snap frozen.

Ethics statement

All animals received proper care in accordance with the *Guide for the Care and Use of Laboratory Animals* from the National Institutes of Health. The protocol was approved by the Institutional Animal Care and Use Committee of the University of Massachusetts Medical School (protocol number A-2393).

Glycerol

Glycerol content in mouse serum and cell culture supernatants was quantified using the Free Glycerol Reagent (Sigma, #F6428) according to the manufacturer's instructions.

Adipocyte size analysis

Sections of formalin-fixed adipose tissue samples were embedded and stained with hematoxylin and eosin by the Morphology Core at the University of Massachusetts Medical School. Images were captured using an Olympus BX51 microscope (Olympus) and NIS-Elements Advance Research software (Nikon Instruments Inc.). The investigators capturing the images were blinded to the identity of the samples. Adipocyte size was measured by importing images into Image J (286, 287). An automated measuring technique was used to measure adipocyte surface area, which has been previously described (288). The

distribution of cell size was calculated using Graphpad Prism 7.0 and the bin size was set to 4000 arbitrary units.

Western blotting

Protein lysates from flash frozen adipose tissue and the 3T3-L1 cells were boiled in Laemmli SDS-Sample buffer (Boston BioProducts, #BP-110R) to denature proteins. Samples were resolved on 7.5% polyacrylamide-SDS PAGE gels and transferred to nitrocellulose membranes, which were blocked in 5% non-fat milk dissolved in Tris-buffered saline plus 0.1% Tween-20. Membranes were probed with the following primary antibodies: Phospho-HSL (Ser660) (Cell Signaling, #4126), HSL (Cell Signaling, #4107), ATGL (Cell Signaling, #2138), anti-beta tubulin antibody (Abcam, #ab6046), Monoclonal anti-β-Actin antibody (Sigma, #A2228) and with the following secondary antibodies: Goat Anti-Rabbit IgG H&L (Abcam, #ab7051), and Goat Anti-Mouse IgG-HRP (Santa Cruz Biotechnology, #sc-2005). HRP was detected using the Clarity Western ECL Substrate (Bio-Rad Laboratories, #170-5061) and the HyBlot CL Autoradiography Film (Denville Scientific, #E3012). Bands were quantified using the Quantity One software (Bio-Rad Laboratories).

3T3-L1 cell line

The 3T3-L1 cell line was provided by Dr. Michael Czech. Cells were seeded into 6-well plates in DMEM (Gibco, #11995) supplemented with 10% FBS (Gemini Bio-Products, #100-500) and 1% penicillin/streptomycin (Gibco, #15140) and grown to confluency for seven days. Cells were differentiated to adipocytes

using 4 μg/mL insulin (Sigma, #I-5500), 115 μg/mL IBMX (Sigma, #I-5879), and 97.5 ng/mL dexamethasone (Sigma, D-1756) for 3 days, and then were cultured in media for an additional seven days. To mimic chronic alcohol conditions, cells were cultured in 50 mM ethanol for 72 hours in a humidified chamber, as previously described (225). To stimulate lipolysis, cells were treated with either 5 μM isoproterenol (Sigma, #I5627) for the indicated times, or the indicated concentrations of dexamethasone (Sigma, #D4902) for 24 hours. Cell-free supernatant was collected and stored at -80°C for glycerol assay and the cells were lysed for western blotting analysis.

Statistical analysis

Data are represented as mean ± SEM or mean ± SD, as described. All statistical analysis was performed using Graphpad Prism 7.0. Student's t-test was used to determine the difference between groups.

Bibliography

1. World Health Organization. Global status report on alcohol and health 2014. Geneva, Switzerland: World Health Organization; 2014.
2. Gao B, Bataller R. Alcoholic liver disease: pathogenesis and new therapeutic targets. Gastroenterology 2011;141:1572-1585.
3. O'Shea RS, Dasarathy S, McCullough AJ. Alcoholic liver disease. Am J Gastroenterol 2010;105:14-32; quiz 33.
4. Jinjuvadia R, Liangpunsakul S, Translational R, Evolving Alcoholic Hepatitis Treatment C. Trends in Alcoholic Hepatitis-related Hospitalizations, Financial Burden, and Mortality in the United States. J Clin Gastroenterol 2015;49:506-511.
5. Kochanek KD, Murphy SL, Xu J, Tejada-Vera B. Deaths: Final Data for 2014. Natl Vital Stat Rep 2016;65:1-122.
6. Lucey MR, Mathurin P, Morgan TR. Alcoholic hepatitis. N Engl J Med 2009;360:2758-2769.
7. Yoon Y-H, Chen CM. Surveillance report #105: liver cirrhosis mortality in the United States: national, state, and regional trends, 2000-2013. Bethesda, MD: National Institute on Alcohol Abuse and Alcoholism; 2016.
8. Addolorato G, Bataller R, Burra P, DiMartini A, Graziadei I, Lucey MR, Mathurin P, et al. Liver Transplantation for Alcoholic Liver Disease. Transplantation 2016;100:981-987.
9. Lucey MR. Liver transplantation for alcoholic liver disease. Nat Rev Gastroenterol Hepatol 2014;11:300-307.
10. Kim WR, Smith JM, Skeans MA, Schladt DP, Schnitzler MA, Edwards EB, Harper AM, et al. OPTN/SRTR 2012 Annual Data Report: Liver. American Journal of Transplantation 2014;14:69-96.
11. Rehm J, Samokhvalov AV, Shield KD. Global burden of alcoholic liver diseases. J Hepatol 2013;59:160-168.
12. Davila JA, Morgan RO, Shaib Y, McGlynn KA, El-Serag HB. Hepatitis C infection and the increasing incidence of hepatocellular carcinoma: a population-based study. Gastroenterology 2004;127:1372-1380.
13. Naveau S, Giraud V, Borotto E, Aubert A, Capron F, Chaput JC. Excess weight risk factor for alcoholic liver disease. Hepatology (Baltimore, Md.) 1997;25:108-111.
14. Dugum M, McCullough A. Diagnosis and Management of Alcoholic Liver Disease. Journal of Clinical and Translational Hepatology 2015;3:109-116.
15. Mann RE, Smart RG, Govoni R. The epidemiology of alcoholic liver disease. Alcohol Research & Health: The Journal of the National Institute on Alcohol Abuse and Alcoholism 2003;27:209-219.
16. Becker U, Deis A, Sørensen TI, Grønbaek M, Borch-Johnsen K, Müller CF, Schnohr P, et al. Prediction of risk of liver disease by alcohol intake, sex, and age: a prospective population study. Hepatology (Baltimore, Md.) 1996;23:1025-1029.

17. Baraona E, Abittan CS, Dohmen K, Moretti M, Pozzato G, Chayes ZW, Schaefer C, et al. Gender differences in pharmacokinetics of alcohol. Alcoholism, Clinical and Experimental Research 2001;25:502-507.
18. Frezza M, di Padova C, Pozzato G, Terpin M, Baraona E, Lieber CS. High blood alcohol levels in women. The role of decreased gastric alcohol dehydrogenase activity and first-pass metabolism. The New England Journal of Medicine 1990;322:95-99.
19. Marshall AW, Kingstone D, Boss M, Morgan MY. Ethanol elimination in males and females: relationship to menstrual cycle and body composition. Hepatology (Baltimore, Md.) 1983;3:701-706.
20. Rao R. Endotoxemia and gut barrier dysfunction in alcoholic liver disease. Hepatology 2009;50:638-644.
21. Ikejima K, Enomoto N, Iimuro Y, Ikejima A, Fang D, Xu J, Forman DT, et al. Estrogen increases sensitivity of hepatic Kupffer cells to endotoxin. The American Journal of Physiology 1998;274:669.
22. Enomoto N, Yamashina S, Schemmer P, Rivera CA, Bradford BU, Enomoto A, Brenner DA, et al. Estriol sensitizes rat Kupffer cells via gut-derived endotoxin. The American Journal of Physiology 1999;277:671.
23. Iimuro Y, Frankenberg MV, Arteel GE, Bradford BU, Wall CA, Thurman RG. Female rats exhibit greater susceptibility to early alcohol-induced liver injury than males. The American Journal of Physiology 1997;272:1186.
24. Kono H, Wheeler MD, Rusyn I, Lin M, Seabra V, Rivera CA, Bradford BU, et al. Gender differences in early alcohol-induced liver injury: role of CD14, NF-kappaB, and TNF-alpha. American Journal of Physiology. Gastrointestinal and Liver Physiology 2000;278:652.
25. Yin M, Ikejima K, Wheeler MD, Bradford BU, Seabra V, Forman DT, Sato N, et al. Estrogen is involved in early alcohol-induced liver injury in a rat enteral feeding model. Hepatology (Baltimore, Md.) 2000;31:117-123.
26. Konstandi M, Cheng J, Gonzalez FJ. Sex steroid hormones regulate constitutive expression of Cyp2e1 in female mouse liver. Am J Physiol Endocrinol Metab 2013;304:E1118-1128.
27. Ki SH, Park O, Zheng M, Morales-Ibanez O, Kolls JK, Bataller R, Gao B. Interleukin-22 treatment ameliorates alcoholic liver injury in a murine model of chronic-binge ethanol feeding: role of signal transducer and activator of transcription 3. Hepatology (Baltimore, Md.) 2010;52:1291-1300.
28. Bataller R, Brenner DA. Liver fibrosis. J Clin Invest 2005;115:209-218.
29. Jaeschke H. Neutrophil-mediated tissue injury in alcoholic hepatitis. Alcohol 2002;27:23-27.
30. Parlesak A, Schäfer C, Schütz T, Bode JC, Bode C. Increased intestinal permeability to macromolecules and endotoxemia in patients with chronic alcohol abuse in different stages of alcohol-induced liver disease. Journal of Hepatology 2000;32:742-747.

31. Gustot T, Lemmers A, Moreno C, Nagy N, Quertinmont E, Nicaise C, Franchimont D, et al. Differential liver sensitization to toll-like receptor pathways in mice with alcoholic fatty liver. Hepatology 2006;43:989-1000.
32. Thakur V, Pritchard MT, McMullen MR, Nagy LE. Adiponectin normalizes LPS-stimulated TNF-alpha production by rat Kupffer cells after chronic ethanol feeding. American Journal of Physiology. Gastrointestinal and Liver Physiology 2006;290:998.
33. Pastorino JG, Hoek JB. Ethanol potentiates tumor necrosis factor-alpha cytotoxicity in hepatoma cells and primary rat hepatocytes by promoting induction of the mitochondrial permeability transition. Hepatology 2000;31:1141-1152.
34. Louvet A, Mathurin P. Alcoholic liver disease: mechanisms of injury and targeted treatment. Nature Reviews. Gastroenterology & Hepatology 2015;12:231-242.
35. Gao B, Seki E, Brenner DA, Friedman S, Cohen JI, Nagy L, Szabo G, et al. Innate immunity in alcoholic liver disease. Am J Physiol Gastrointest Liver Physiol 2011;300:G516-525.
36. Louvet A, Diaz E, Dharancy S, Coevoet H, Texier F, Thevenot T, Deltenre P, et al. Early switch to pentoxifylline in patients with severe alcoholic hepatitis is inefficient in non-responders to corticosteroids. J Hepatol 2008;48:465-470.
37. Naveau S, Chollet-Martin S, Dharancy S, Mathurin P, Jouet P, Piquet MA, Davion T, et al. A double-blind randomized controlled trial of infliximab associated with prednisolone in acute alcoholic hepatitis. Hepatology 2004;39:1390-1397.
38. Boetticher NC, Peine CJ, Kwo P, Abrams GA, Patel T, Aqel B, Boardman L, et al. A randomized, double-blinded, placebo-controlled multicenter trial of etanercept in the treatment of alcoholic hepatitis. Gastroenterology 2008;135:1953-1960.
39. Xu MJ, Zhou Z, Parker R, Gao B. Targeting inflammation for the treatment of alcoholic liver disease. Pharmacol Ther 2017.
40. Chiang DJ, McCullough AJ. The impact of obesity and metabolic syndrome on alcoholic liver disease. Clin Liver Dis 2014;18:157-163.
41. Setshedi M, Wands JR, Monte SM. Acetaldehyde adducts in alcoholic liver disease. Oxid Med Cell Longev 2010;3:178-185.
42. Zakhari S. Overview: how is alcohol metabolized by the body? Alcohol Res Health 2006;29:245-254.
43. Gao B, Tsukamoto H. Inflammation in Alcoholic and Nonalcoholic Fatty Liver Disease: Friend or Foe? Gastroenterology 2016;150:1704-1709.
44. Pasala S, Barr T, Messaoudi I. Impact of Alcohol Abuse on the Adaptive Immune System. Alcohol Res 2015;37:185-197.
45. Wu D, Cederbaum AI. Ethanol-induced apoptosis to stable HepG2 cell lines expressing human cytochrome P-4502E1. Alcohol Clin Exp Res 1999;23:67-76.
46. Thakur V, Pritchard MT, McMullen MR, Wang Q, Nagy LE. Chronic ethanol feeding increases activation of NADPH oxidase by lipopolysaccharide in

rat Kupffer cells: role of increased reactive oxygen in LPS-stimulated ERK1/2 activation and TNF-alpha production. J Leukoc Biol 2006;79:1348-1356.
47. Liaskou E, Klemsdal Henriksen EK, Holm K, Kaveh F, Hamm D, Fear J, Viken MK, et al. High-throughput T-cell receptor sequencing across chronic liver diseases reveals distinct disease-associated repertoires. Hepatology 2016;63:1608-1619.
48. You M, Fischer M, Deeg MA, Crabb DW. Ethanol induces fatty acid synthesis pathways by activation of sterol regulatory element-binding protein (SREBP). The Journal of Biological Chemistry 2002;277:29342-29347.
49. Wang Y, Viscarra J, Kim SJ, Sul HS. Transcriptional regulation of hepatic lipogenesis. Nat Rev Mol Cell Biol 2015;16:678-689.
50. Ji C, Chan C, Kaplowitz N. Predominant role of sterol response element binding proteins (SREBP) lipogenic pathways in hepatic steatosis in the murine intragastric ethanol feeding model. J Hepatol 2006;45:717-724.
51. Filhoulaud G, Guilmeau S, Dentin R, Girard J, Postic C. Novel insights into ChREBP regulation and function. Trends Endocrinol Metab 2013;24:257-268.
52. Marmier S, Dentin R, Daujat-Chavanieu M, Guillou H, Bertrand-Michel J, Gerbal-Chaloin S, Girard J, et al. Novel role for carbohydrate responsive element binding protein in the control of ethanol metabolism and susceptibility to binge drinking. Hepatology 2015;62:1086-1100.
53. Galli A, Pinaire J, Fischer M, Dorris R, Crabb DW. The transcriptional and DNA binding activity of peroxisome proliferator-activated receptor alpha is inhibited by ethanol metabolism. A novel mechanism for the development of ethanol-induced fatty liver. The Journal of Biological Chemistry 2001;276:68-75.
54. Burri L, Thoresen GH, Berge RK. The Role of PPARalpha Activation in Liver and Muscle. PPAR Res 2010;2010.
55. Nakajima T, Kamijo Y, Tanaka N, Sugiyama E, Tanaka E, Kiyosawa K, Fukushima Y, et al. Peroxisome proliferator-activated receptor alpha protects against alcohol-induced liver damage. Hepatology 2004;40:972-980.
56. Fischer M, You M, Matsumoto M, Crabb DW. Peroxisome proliferator-activated receptor alpha (PPARalpha) agonist treatment reverses PPARalpha dysfunction and abnormalities in hepatic lipid metabolism in ethanol-fed mice. J Biol Chem 2003;278:27997-28004.
57. Davies LC, Jenkins SJ, Allen JE, Taylor PR. Tissue-resident macrophages. Nat Immunol 2013;14:986-995.
58. Ju C, Tacke F. Hepatic macrophages in homeostasis and liver diseases: from pathogenesis to novel therapeutic strategies. Cell Mol Immunol 2016;13:316-327.
59. Karakucuk I, Dilly SA, Maxwell JD. Portal tract macrophages are increased in alcoholic liver disease. Histopathology 1989;14:245-253.
60. Wang M, You Q, Lor K, Chen F, Gao B, Ju C. Chronic alcohol ingestion modulates hepatic macrophage populations and functions in mice. Journal of Leukocyte Biology 2014;96:657-665.

61. Cui K, Yan G, Xu C, Chen Y, Wang J, Zhou R, Bai L, et al. Invariant NKT cells promote alcohol-induced steatohepatitis through interleukin-1beta in mice. J Hepatol 2015;62:1311-1318.
62. Adachi Y, Bradford BU, Gao W, Bojes HK, Thurman RG. Inactivation of Kupffer cells prevents early alcohol-induced liver injury. Hepatology (Baltimore, Md.) 1994;20:453-460.
63. Adachi Y, Moore LE, Bradford BU, Gao W, Thurman RG. Antibiotics prevent liver injury in rats following long-term exposure to ethanol. Gastroenterology 1995;108:218-224.
64. Hritz I, Mandrekar P, Velayudham A, Catalano D, Dolganiuc A, Kodys K, Kurt-Jones E, et al. The critical role of toll-like receptor (TLR) 4 in alcoholic liver disease is independent of the common TLR adapter MyD88. Hepatology (Baltimore, Md.) 2008;48:1224-1231.
65. Bala S, Petrasek J, Mundkur S, Catalano D, Levin I, Ward J, Alao H, et al. Circulating microRNAs in exosomes indicate hepatocyte injury and inflammation in alcoholic, drug-induced, and inflammatory liver diseases. Hepatology (Baltimore, Md.) 2012;56:1946-1957.
66. Zhou H, Yu M, Roychowdhury S, Sanz-Garcia C, Pollard KA, McMullen MR, Liu X, et al. Myeloid-MyD88 Contributes to Ethanol-Induced Liver Injury in Mice Linking Hepatocellular Death to Inflammation. Alcohol Clin Exp Res 2017;41:719-726.
67. Roh YS, Zhang B, Loomba R, Seki E. TLR2 and TLR9 contribute to alcohol-mediated liver injury through induction of CXCL1 and neutrophil infiltration. American Journal of Physiology. Gastrointestinal and Liver Physiology 2015;309:30.
68. Xu M-J, Cai Y, Wang H, Altamirano J, Chang B, Bertola A, Odena G, et al. Fat-Specific Protein 27/CIDEC Promotes Development of Alcoholic Steatohepatitis in Mice and Humans. Gastroenterology 2015;149:1041.e1046.
69. Kolaczkowska E, Kubes P. Neutrophil recruitment and function in health and inflammation. Nat Rev Immunol 2013;13:159-175.
70. Bertola A, Park O, Gao B. Chronic plus binge ethanol feeding synergistically induces neutrophil infiltration and liver injury in mice: a critical role for E-selectin. Hepatology (Baltimore, Md.) 2013;58:1814-1823.
71. Altamirano J, Miquel R, Katoonizadeh A, Abraldes JG, Duarte-Rojo A, Louvet A, Augustin S, et al. A histologic scoring system for prognosis of patients with alcoholic hepatitis. Gastroenterology 2014;146:1231-1239 e1231-1236.
72. Matos LC, Batista P, Monteiro N, Ribeiro J, Cipriano MA, Henriques P, Girao F, et al. Lymphocyte subsets in alcoholic liver disease. World J Hepatol 2013;5:46-55.
73. Haydon G, Lalor PF, Hubscher SG, Adams DH. Lymphocyte recruitment to the liver in alcoholic liver disease. Alcohol 2002;27:29-36.
74. Chedid A, Mendenhall CL, Moritz TE, French SW, Chen TS, Morgan TR, Roselle GA, et al. Cell-mediated hepatic injury in alcoholic liver disease.

Veterans Affairs Cooperative Study Group 275. Gastroenterology 1993;105:254-266.
75. Lemmers A, Moreno C, Gustot T, Marechal R, Degre D, Demetter P, de Nadai P, et al. The interleukin-17 pathway is involved in human alcoholic liver disease. Hepatology 2009;49:646-657.
76. Vivier E, Tomasello E, Baratin M, Walzer T, Ugolini S. Functions of natural killer cells. Nat Immunol 2008;9:503-510.
77. Pan HN, Sun R, Jaruga B, Hong F, Kim WH, Gao B. Chronic ethanol consumption inhibits hepatic natural killer cell activity and accelerates murine cytomegalovirus-induced hepatitis. Alcohol Clin Exp Res 2006;30:1615-1623.
78. Zhang F, Little A, Zhang H. Chronic alcohol consumption inhibits peripheral NK cell development and maturation by decreasing the availability of IL-15. J Leukoc Biol 2017;101:1015-1027.
79. Perney P, Portales P, Corbeau P, Roques V, Blanc F, Clot J. Specific alteration of peripheral cytotoxic cell perforin expression in alcoholic patients: a possible role in alcohol-related diseases. Alcohol Clin Exp Res 2003;27:1825-1830.
80. Bandyopadhyay K, Marrero I, Kumar V. NKT cell subsets as key participants in liver physiology and pathology. Cell Mol Immunol 2016;13:337-346.
81. Maricic I, Sheng H, Marrero I, Seki E, Kisseleva T, Chaturvedi S, Molle N, et al. Inhibition of type I natural killer T cells by retinoids or following sulfatide-mediated activation of type II natural killer T cells attenuates alcoholic liver disease in mice. Hepatology 2015;61:1357-1369.
82. Mathews S, Feng D, Maricic I, Ju C, Kumar V, Gao B. Invariant natural killer T cells contribute to chronic-plus-binge ethanol-mediated liver injury by promoting hepatic neutrophil infiltration. Cell Mol Immunol 2016;13:206-216.
83. Cook RT, Waldschmidt TJ, Cook BL, Labrecque DR, McLatchie K. Loss of the CD5+ and CD45RAhi B cell subsets in alcoholics. Clin Exp Immunol 1996;103:304-310.
84. Bird GL, Sheron N, Goka AK, Alexander GJ, Williams RS. Increased plasma tumor necrosis factor in severe alcoholic hepatitis. Ann Intern Med 1990;112:917-920.
85. Lawler JF, Jr., Yin M, Diehl AM, Roberts E, Chatterjee S. Tumor necrosis factor-alpha stimulates the maturation of sterol regulatory element binding protein-1 in human hepatocytes through the action of neutral sphingomyelinase. J Biol Chem 1998;273:5053-5059.
86. Endo M, Masaki T, Seike M, Yoshimatsu H. TNF-alpha induces hepatic steatosis in mice by enhancing gene expression of sterol regulatory element binding protein-1c (SREBP-1c). Exp Biol Med (Maywood) 2007;232:614-621.
87. Iimuro Y, Gallucci RM, Luster MI, Kono H, Thurman RG. Antibodies to tumor necrosis factor alfa attenuate hepatic necrosis and inflammation caused by chronic exposure to ethanol in the rat. Hepatology 1997;26:1530-1537.

88. Yin M, Wheeler MD, Kono H, Bradford BU, Gallucci RM, Luster MI, Thurman RG. Essential role of tumor necrosis factor alpha in alcohol-induced liver injury in mice. Gastroenterology 1999;117:942-952.
89. Fisher NC, Neil DA, Williams A, Adams DH. Serum concentrations and peripheral secretion of the beta chemokines monocyte chemoattractant protein 1 and macrophage inflammatory protein 1alpha in alcoholic liver disease. Gut 1999;45:416-420.
90. Mandrekar P, Ambade A, Lim A, Szabo G, Catalano D. An essential role for monocyte chemoattractant protein-1 in alcoholic liver injury: regulation of proinflammatory cytokines and hepatic steatosis in mice. Hepatology 2011;54:2185-2197.
91. Bonini JA, Martin SK, Dralyuk F, Roe MW, Philipson LH, Steiner DF. Cloning, expression, and chromosomal mapping of a novel human CC-chemokine receptor (CCR10) that displays high-affinity binding for MCP-1 and MCP-3. DNA Cell Biol 1997;16:1249-1256.
92. Shi W, Zhu Q, Gu J, Liu X, Lu L, Qian X, Shen J, et al. Anti-IL-17 antibody improves hepatic steatosis by suppressing interleukin-17-related fatty acid synthesis and metabolism. Clin Dev Immunol 2013;2013:253046.
93. Tilg H, Wilmer A, Vogel W, Herold M, Nolchen B, Judmaier G, Huber C. Serum levels of cytokines in chronic liver diseases. Gastroenterology 1992;103:264-274.
94. Petrasek J, Bala S, Csak T, Lippai D, Kodys K, Menashy V, Barrieau M, et al. IL-1 receptor antagonist ameliorates inflammasome-dependent alcoholic steatohepatitis in mice. J Clin Invest 2012;122:3476-3489.
95. de Oliveira S, Rosowski EE, Huttenlocher A. Neutrophil migration in infection and wound repair: going forward in reverse. Nat Rev Immunol 2016;16:378-391.
96. Hill DB, Marsano LS, McClain CJ. Increased plasma interleukin-8 concentrations in alcoholic hepatitis. Hepatology 1993;18:576-580.
97. Gonzalez-Reimers E, Sanchez-Perez MJ, Santolaria-Fernandez F, Abreu-Gonzalez P, De la Vega-Prieto MJ, Vina-Rodriguez J, Aleman-Valls MR, et al. Changes in cytokine levels during admission and mortality in acute alcoholic hepatitis. Alcohol 2012;46:433-440.
98. Wieser V, Adolph TE, Enrich B, Kuliopulos A, Kaser A, Tilg H, Kaneider NC. Reversal of murine alcoholic steatohepatitis by pepducin-based functional blockade of interleukin-8 receptors. Gut 2017;66:930-938.
99. Chang B, Xu MJ, Zhou Z, Cai Y, Li M, Wang W, Feng D, et al. Short- or long-term high-fat diet feeding plus acute ethanol binge synergistically induce acute liver injury in mice: an important role for CXCL1. Hepatology 2015;62:1070-1085.
100. Horiguchi N, Wang L, Mukhopadhyay P, Park O, Jeong WI, Lafdil F, Osei–Hyiaman D, et al. Cell Type–Dependent Pro- and Anti-Inflammatory Role of Signal Transducer and Activator of Transcription 3 in Alcoholic Liver Injury. Gastroenterology 2008;134:1148-1158.

101. Chen J, Bao H, Sawyer S, Kunos G, Gao B. Effects of short and long term ethanol on the activation of signal transducer and activator transcription factor 3 in normal and regenerating liver. Biochem Biophys Res Commun 1997;239:666-669.
102. Chen J, Kunos G, Gao B. Ethanol rapidly inhibits IL-6-activated STAT3 and C/EBP mRNA expression in freshly isolated rat hepatocytes. FEBS Lett 1999;457:162-168.
103. Miller AM, Wang H, Bertola A, Park O, Horiguchi N, Ki SH, Yin S, et al. Inflammation-associated interleukin-6/signal transducer and activator of transcription 3 activation ameliorates alcoholic and nonalcoholic fatty liver diseases in interleukin-10-deficient mice. Hepatology 2011;54:846-856.
104. Hong F, Kim WH, Tian Z, Jaruga B, Ishac E, Shen X, Gao B. Elevated interleukin-6 during ethanol consumption acts as a potential endogenous protective cytokine against ethanol-induced apoptosis in the liver: involvement of induction of Bcl-2 and Bcl-x(L) proteins. Oncogene 2002;21:32-43.
105. El-Assal O, Hong F, Kim WH, Radaeva S, Gao B. IL-6-deficient mice are susceptible to ethanol-induced hepatic steatosis: IL-6 protects against ethanol-induced oxidative stress and mitochondrial permeability transition in the liver. Cell Mol Immunol 2004;1:205-211.
106. Zhang X, Tachibana S, Wang H, Hisada M, Williams GM, Gao B, Sun Z. Interleukin-6 is an important mediator for mitochondrial DNA repair after alcoholic liver injury in mice. Hepatology 2010;52:2137-2147.
107. Hong F, Radaeva S, Pan HN, Tian Z, Veech R, Gao B. Interleukin 6 alleviates hepatic steatosis and ischemia/reperfusion injury in mice with fatty liver disease. Hepatology 2004;40:933-941.
108. Gao B. Hepatoprotective and anti-inflammatory cytokines in alcoholic liver disease. Journal of Gastroenterology and Hepatology 2012;27:89-93.
109. Byun JS, Suh YG, Yi HS, Lee YS, Jeong WI. Activation of toll-like receptor 3 attenuates alcoholic liver injury by stimulating Kupffer cells and stellate cells to produce interleukin-10 in mice. J Hepatol 2013;58:342-349.
110. Petrasek J, Dolganiuc A, Csak T, Nath B, Hritz I, Kodys K, Catalano D, et al. Interferon regulatory factor 3 and type I interferons are protective in alcoholic liver injury in mice by way of crosstalk of parenchymal and myeloid cells. Hepatology 2011;53:649-660.
111. Kong X, Feng D, Mathews S, Gao B. Hepatoprotective and anti-fibrotic functions of interleukin-22: therapeutic potential for the treatment of alcoholic liver disease. J Gastroenterol Hepatol 2013;28 Suppl 1:56-60.
112. Xing WW, Zou MJ, Liu S, Xu T, Wang JX, Xu DG. Interleukin-22 protects against acute alcohol-induced hepatotoxicity in mice. Biosci Biotechnol Biochem 2011;75:1290-1294.
113. Kawai T, Akira S. The role of pattern-recognition receptors in innate immunity: update on Toll-like receptors. Nature Immunology 2010;11:373-384.
114. Miyake K. Endotoxin recognition molecules, Toll-like receptor 4-MD-2. Semin Immunol 2004;16:11-16.

115. Uesugi T, Froh M, Arteel GE, Bradford BU, Thurman RG. Toll-like receptor 4 is involved in the mechanism of early alcohol-induced liver injury in mice. Hepatology (Baltimore, Md.) 2001;34:101-108.
116. Yin M, Bradford BU, Wheeler MD, Uesugi T, Froh M, Goyert SM, Thurman RG. Reduced early alcohol-induced liver injury in CD14-deficient mice. J Immunol 2001;166:4737-4742.
117. Uesugi T, Froh M, Arteel GE, Bradford BU, Wheeler MD, Gabele E, Isayama F, et al. Role of lipopolysaccharide-binding protein in early alcohol-induced liver injury in mice. J Immunol 2002;168:2963-2969.
118. Zmijewski E, Lu S, Harrison-Findik DD. TLR4 signaling and the inhibition of liver hepcidin expression by alcohol. World Journal of Gastroenterology 2014;20:12161-12170.
119. Inokuchi S, Tsukamoto H, Park E, Liu Z-X, Brenner DA, Seki E. Toll-like receptor 4 mediates alcohol-induced steatohepatitis through bone marrow-derived and endogenous liver cells in mice. Alcoholism, Clinical and Experimental Research 2011;35:1509-1518.
120. Roychowdhury S, McMullen MR, Pritchard MT, Hise AG, van Rooijen N, Medof ME, Stavitsky AB, et al. An early complement-dependent and TLR-4-independent phase in the pathogenesis of ethanol-induced liver injury in mice. Hepatology (Baltimore, Md.) 2009;49:1326-1334.
121. DeCarli LM, Lieber CS. Fatty liver in the rat after prolonged intake of ethanol with a nutritionally adequate new liquid diet. J Nutr 1967;91:331-336.
122. Lieber CS, DeCarli LM, Sorrell MF. Experimental methods of ethanol administration. Hepatology 1989;10:501-510.
123. Bertola A, Mathews S, Ki SH, Wang H, Gao B. Mouse model of chronic and binge ethanol feeding (the NIAAA model). Nature Protocols 2013;8:627-637.
124. Choi G, Runyon BA. Alcoholic hepatitis: a clinician's guide. Clin Liver Dis 2012;16:371-385.
125. Tsukamoto H, French SW, Reidelberger RD, Largman C. Cyclical pattern of blood alcohol levels during continuous intragastric ethanol infusion in rats. Alcohol Clin Exp Res 1985;9:31-37.
126. Tsukamoto H, Reidelberger RD, French SW, Largman C. Long-term cannulation model for blood sampling and intragastric infusion in the rat. Am J Physiol 1984;247:R595-599.
127. Ueno A, Lazaro R, Wang PY, Higashiyama R, Machida K, Tsukamoto H. Mouse intragastric infusion (iG) model. Nat Protoc 2012;7:771-781.
128. Tsukamoto H, French SW, Benson N, Delgado G, Rao GA, Larkin EC, Largman C. Severe and progressive steatosis and focal necrosis in rat liver induced by continuous intragastric infusion of ethanol and low fat diet. Hepatology 1985;5:224-232.
129. Lazaro R, Wu R, Lee S, Zhu NL, Chen CL, French SW, Xu J, et al. Osteopontin deficiency does not prevent but promotes alcoholic neutrophilic hepatitis in mice. Hepatology 2015;61:129-140.

130. Ahmadian M, Duncan RE, Sul HS. The skinny on fat: lipolysis and fatty acid utilization in adipocytes. Trends Endocrinol Metab 2009;20:424-428.
131. Zechner R, Zimmermann R, Eichmann TO, Kohlwein SD, Haemmerle G, Lass A, Madeo F. FAT SIGNALS--lipases and lipolysis in lipid metabolism and signaling. Cell Metab 2012;15:279-291.
132. Ouchi N, Parker JL, Lugus JJ, Walsh K. Adipokines in inflammation and metabolic disease. Nature Reviews. Immunology 2011;11:85-97.
133. Castoldi A, Naffah de Souza C, Câmara NOS, Moraes-Vieira PM. The Macrophage Switch in Obesity Development. Frontiers in Immunology 2015;6:637.
134. Weisberg SP, McCann D, Desai M, Rosenbaum M, Leibel RL, Ferrante AW. Obesity is associated with macrophage accumulation in adipose tissue. The Journal of Clinical Investigation 2003;112:1796-1808.
135. Xu H, Barnes GT, Yang Q, Tan G, Yang D, Chou CJ, Sole J, et al. Chronic inflammation in fat plays a crucial role in the development of obesity-related insulin resistance. The Journal of Clinical Investigation 2003;112:1821-1830.
136. Lumeng CN, Bodzin JL, Saltiel AR. Obesity induces a phenotypic switch in adipose tissue macrophage polarization. The Journal of Clinical Investigation 2007;117:175-184.
137. Lumeng CN, DeYoung SM, Bodzin JL, Saltiel AR. Increased Inflammatory Properties of Adipose Tissue Macrophages Recruited During Diet-Induced Obesity. Diabetes 2007;56:16-23.
138. Oh DY, Morinaga H, Talukdar S, Bae EJ, Olefsky JM. Increased macrophage migration into adipose tissue in obese mice. Diabetes 2012;61:346-354.
139. Lumeng CN, DelProposto JB, Westcott DJ, Saltiel AR. Phenotypic switching of adipose tissue macrophages with obesity is generated by spatiotemporal differences in macrophage subtypes. Diabetes 2008;57:3239-3246.
140. Patsouris D, Li P-P, Thapar D, Chapman J, Olefsky JM, Neels JG. Ablation of CD11c-positive cells normalizes insulin sensitivity in obese insulin resistant animals. Cell Metabolism 2008;8:301-309.
141. Gensel JC, Zhang B. Macrophage activation and its role in repair and pathology after spinal cord injury. Brain Res 2015;1619:1-11.
142. Weisberg SP, Hunter D, Huber R, Lemieux J, Slaymaker S, Vaddi K, Charo I, et al. CCR2 modulates inflammatory and metabolic effects of high-fat feeding. J Clin Invest 2006;116:115-124.
143. Amano SU, Cohen JL, Vangala P, Tencerova M, Nicoloro SM, Yawe JC, Shen Y, et al. Local proliferation of macrophages contributes to obesity-associated adipose tissue inflammation. Cell Metab 2014;19:162-171.
144. Haase J, Weyer U, Immig K, Kloting N, Bluher M, Eilers J, Bechmann I, et al. Local proliferation of macrophages in adipose tissue during obesity-induced inflammation. Diabetologia 2014;57:562-571.

145. Braune J, Weyer U, Hobusch C, Mauer J, Bruning JC, Bechmann I, Gericke M. IL-6 Regulates M2 Polarization and Local Proliferation of Adipose Tissue Macrophages in Obesity. J Immunol 2017;198:2927-2934.
146. Cho KW, Morris DL, DelProposto JL, Geletka L, Zamarron B, Martinez-Santibanez G, Meyer KA, et al. An MHC II-dependent activation loop between adipose tissue macrophages and CD4+ T cells controls obesity-induced inflammation. Cell Reports 2014;9:605-617.
147. Morris DL, Cho KW, Delproposto JL, Oatmen KE, Geletka LM, Martinez-Santibanez G, Singer K, et al. Adipose tissue macrophages function as antigen-presenting cells and regulate adipose tissue CD4+ T cells in mice. Diabetes 2013;62:2762-2772.
148. Cho KW, Zamarron BF, Muir LA, Singer K, Porsche CE, DelProposto JB, Geletka L, et al. Adipose Tissue Dendritic Cells Are Independent Contributors to Obesity-Induced Inflammation and Insulin Resistance. Journal of Immunology (Baltimore, Md.: 1950) 2016;197:3650-3661.
149. Bertola A, Ciucci T, Rousseau D, Bourlier V, Duffaut C, Bonnafous S, Blin-Wakkach C, et al. Identification of adipose tissue dendritic cells correlated with obesity-associated insulin-resistance and inducing Th17 responses in mice and patients. Diabetes 2012;61:2238-2247.
150. Stefanovic-Racic M, Yang X, Turner MS, Mantell BS, Stolz DB, Sumpter TL, Sipula IJ, et al. Dendritic cells promote macrophage infiltration and comprise a substantial proportion of obesity-associated increases in CD11c+ cells in adipose tissue and liver. Diabetes 2012;61:2330-2339.
151. Elgazar-Carmon V, Rudich A, Hadad N, Levy R. Neutrophils transiently infiltrate intra-abdominal fat early in the course of high-fat feeding. Journal of Lipid Research 2008;49:1894-1903.
152. Talukdar S, Oh DY, Bandyopadhyay G, Li D, Xu J, McNelis J, Lu M, et al. Neutrophils mediate insulin resistance in mice fed a high-fat diet through secreted elastase. Nature Medicine 2012;18:1407-1412.
153. Winer DA, Winer S, Shen L, Wadia PP, Yantha J, Paltser G, Tsui H, et al. B cells promote insulin resistance through modulation of T cells and production of pathogenic IgG antibodies. Nature Medicine 2011;17:610-617.
154. Nishimura S, Manabe I, Takaki S, Nagasaki M, Otsu M, Yamashita H, Sugita J, et al. Adipose Natural Regulatory B Cells Negatively Control Adipose Tissue Inflammation. Cell Metabolism 2013;18:759-766.
155. Winer S, Chan Y, Paltser G, Truong D, Tsui H, Bahrami J, Dorfman R, et al. Normalization of obesity-associated insulin resistance through immunotherapy. Nature Medicine 2009;15:921-929.
156. Nishimura S, Manabe I, Nagasaki M, Eto K, Yamashita H, Ohsugi M, Otsu M, et al. CD8+ effector T cells contribute to macrophage recruitment and adipose tissue inflammation in obesity. Nature Medicine 2009;15:914-920.
157. Feuerer M, Herrero L, Cipolletta D, Naaz A, Wong J, Nayer A, Lee J, et al. Lean, but not obese, fat is enriched for a unique population of regulatory T cells that affect metabolic parameters. Nature Medicine 2009;15:930-939.

158. Wensveen FM, Jelencic V, Valentic S, Sestan M, Wensveen TT, Theurich S, Glasner A, et al. NK cells link obesity-induced adipose stress to inflammation and insulin resistance. Nat Immunol 2015;16:376-385.
159. Cildir G, Akıncılar SC, Tergaonkar V. Chronic adipose tissue inflammation: all immune cells on the stage. Trends in Molecular Medicine 2013;19:487-500.
160. Reilly SM, Ahmadian M, Zamarron BF, Chang L, Uhm M, Poirier B, Peng X, et al. A subcutaneous adipose tissue-liver signalling axis controls hepatic gluconeogenesis. Nature Communications 2015;6:6047.
161. Vielma SA, Klein RL, Levingston CA, Young MRI. Skewing of immune cell cytokine production by mediators from adipocytes and endothelial cells. Adipocyte 2014;3:126-131.
162. Hotamisligil GS, Shargill NS, Spiegelman BM. Adipose expression of tumor necrosis factor-alpha: direct role in obesity-linked insulin resistance. Science 1993;259:87-91.
163. Sabio G, Das M, Mora A, Zhang Z, Jun JY, Ko HJ, Barrett T, et al. A stress signaling pathway in adipose tissue regulates hepatic insulin resistance. Science 2008;322:1539-1543.
164. Matthews VB, Allen TL, Risis S, Chan MH, Henstridge DC, Watson N, Zaffino LA, et al. Interleukin-6-deficient mice develop hepatic inflammation and systemic insulin resistance. Diabetologia 2010;53:2431-2441.
165. Kraakman MJ, Kammoun HL, Allen TL, Deswaerte V, Henstridge DC, Estevez E, Matthews VB, et al. Blocking IL-6 trans-signaling prevents high-fat diet-induced adipose tissue macrophage recruitment but does not improve insulin resistance. Cell Metab 2015;21:403-416.
166. Kanda H, Tateya S, Tamori Y, Kotani K, Hiasa K, Kitazawa R, Kitazawa S, et al. MCP-1 contributes to macrophage infiltration into adipose tissue, insulin resistance, and hepatic steatosis in obesity. J Clin Invest 2006;116:1494-1505.
167. Tamura Y, Sugimoto M, Murayama T, Ueda Y, Kanamori H, Ono K, Ariyasu H, et al. Inhibition of CCR2 ameliorates insulin resistance and hepatic steatosis in db/db mice. Arterioscler Thromb Vasc Biol 2008;28:2195-2201.
168. Kirk EA, Sagawa ZK, McDonald TO, O'Brien KD, Heinecke JW. Monocyte chemoattractant protein deficiency fails to restrain macrophage infiltration into adipose tissue [corrected]. Diabetes 2008;57:1254-1261.
169. Scherer PE, Williams S, Fogliano M, Baldini G, Lodish HF. A novel serum protein similar to C1q, produced exclusively in adipocytes. J Biol Chem 1995;270:26746-26749.
170. Hu E, Liang P, Spiegelman BM. AdipoQ is a novel adipose-specific gene dysregulated in obesity. J Biol Chem 1996;271:10697-10703.
171. Maeda N, Shimomura I, Kishida K, Nishizawa H, Matsuda M, Nagaretani H, Furuyama N, et al. Diet-induced insulin resistance in mice lacking adiponectin/ACRP30. Nat Med 2002;8:731-737.
172. Kim JY, van de Wall E, Laplante M, Azzara A, Trujillo ME, Hofmann SM, Schraw T, et al. Obesity-associated improvements in metabolic profile through expansion of adipose tissue. J Clin Invest 2007;117:2621-2637.

173. Ohashi K, Parker JL, Ouchi N, Higuchi A, Vita JA, Gokce N, Pedersen AA, et al. Adiponectin promotes macrophage polarization toward an anti-inflammatory phenotype. J Biol Chem 2010;285:6153-6160.
174. Yokota T, Oritani K, Takahashi I, Ishikawa J, Matsuyama A, Ouchi N, Kihara S, et al. Adiponectin, a new member of the family of soluble defense collagens, negatively regulates the growth of myelomonocytic progenitors and the functions of macrophages. Blood 2000;96:1723-1732.
175. Yamaguchi N, Argueta JG, Masuhiro Y, Kagishita M, Nonaka K, Saito T, Hanazawa S, et al. Adiponectin inhibits Toll-like receptor family-induced signaling. FEBS Lett 2005;579:6821-6826.
176. Xu A, Wang Y, Keshaw H, Xu LY, Lam KSL, Cooper GJS. The fat-derived hormone adiponectin alleviates alcoholic and nonalcoholic fatty liver diseases in mice. The Journal of Clinical Investigation 2003;112:91-100.
177. Meyer MR, Haas E, Barton M. Gender differences of cardiovascular disease: new perspectives for estrogen receptor signaling. Hypertension 2006;47:1019-1026.
178. Karastergiou K, Smith SR, Greenberg AS, Fried SK. Sex differences in human adipose tissues - the biology of pear shape. Biol Sex Differ 2012;3:13.
179. Brown LM, Gent L, Davis K, Clegg DJ. Metabolic impact of sex hormones on obesity. Brain Res 2010;1350:77-85.
180. Estrany ME, Proenza AM, Gianotti M, Llado I. High-fat diet feeding induces sex-dependent changes in inflammatory and insulin sensitivity profiles of rat adipose tissue. Cell Biochem Funct 2013;31:504-510.
181. Singer K, Maley N, Mergian T, DelProposto J, Cho KW, Zamarron BF, Martinez-Santibanez G, et al. Differences in Hematopoietic Stem Cells Contribute to Sexually Dimorphic Inflammatory Responses to High Fat Diet-induced Obesity. The Journal of biological chemistry 2015;290:13250-13262.
182. Dakin RS, Walker BR, Seckl JR, Hadoke PW, Drake AJ. Estrogens protect male mice from obesity complications and influence glucocorticoid metabolism. Int J Obes (Lond) 2015;39:1539-1547.
183. Giles DA, Moreno-Fernandez ME, Stankiewicz TE, Graspeuntner S, Cappelletti M, Wu D, Mukherjee R, et al. Thermoneutral housing exacerbates nonalcoholic fatty liver disease in mice and allows for sex-independent disease modeling. Nature Medicine 2017;23:829-838.
184. Kasztelan-Szczerbinska B, Surdacka A, Slomka M, Rolinski J, Celinski K, Smolen A, Szczerbinski M. Association of serum adiponectin, leptin, and resistin concentrations with the severity of liver dysfunction and the disease complications in alcoholic liver disease. Mediators of inflammation 2013;2013:148526.
185. Kalafateli M, Triantos C, Tsochatzis E, Michalaki M, Koutroumpakis E, Thomopoulos K, Kyriazopoulou V, et al. Adipokines levels are associated with the severity of liver disease in patients with alcoholic cirrhosis. World journal of gastroenterology 2015;21:3020-3029.

186. Buechler C, Schaeffler A, Johann M, Neumeier M, Koehl P, Weiss T, Wodarz N, et al. Elevated adiponectin serum levels in patients with chronic alcohol abuse rapidly decline during alcohol withdrawal. Journal of gastroenterology and hepatology 2009;24:558-563.
187. Naveau S, Cassard-Doulcier A-M, Njiké-Nakseu M, Bouchet-Delbos L, Barri-Ova N, Boujedidi H, Dauvois B, et al. Harmful effect of adipose tissue on liver lesions in patients with alcoholic liver disease. Journal of Hepatology 2010;52:895-902.
188. Voican CS, Njiké-Nakseu M, Boujedidi H, Barri-Ova N, Bouchet-Delbos L, Agostini H, Maitre S, et al. Alcohol withdrawal alleviates adipose tissue inflammation in patients with alcoholic liver disease. Liver International: Official Journal of the International Association for the Study of the Liver 2015;35:967-978.
189. Kang L, Sebastian BM, Pritchard MT, Pratt BT, Previs SF, Nagy LE. Chronic ethanol-induced insulin resistance is associated with macrophage infiltration into adipose tissue and altered expression of adipocytokines. Alcoholism, Clinical and Experimental Research 2007;31:1581-1588.
190. Chen X, Sebastian BM, Nagy LE. Chronic ethanol feeding to rats decreases adiponectin secretion by subcutaneous adipocytes. American Journal of Physiology. Endocrinology and Metabolism 2007;292:621.
191. Chen X, Sebastian BM, Tang H, McMullen MM, Axhemi A, Jacobsen DW, Nagy LE. Taurine supplementation prevents ethanol-induced decrease in serum adiponectin and reduces hepatic steatosis in rats. Hepatology (Baltimore, Md.) 2009;49:1554-1562.
192. Lin HZ, Yang SQ, Zeldin G, Diehl AM. Chronic ethanol consumption induces the production of tumor necrosis factor-alpha and related cytokines in liver and adipose tissue. Alcoholism, Clinical and Experimental Research 1998;22:237S.
193. Sun X, Tang Y, Tan X, Li Q, Zhong W, Sun X, Jia W, et al. Activation of peroxisome proliferator-activated receptor-γ by rosiglitazone improves lipid homeostasis at the adipose tissue-liver axis in ethanol-fed mice. American Journal of Physiology. Gastrointestinal and Liver Physiology 2012;302:548.
194. Sebastian BM, Roychowdhury S, Tang H, Hillian AD, Feldstein AE, Stahl GL, Takahashi K, et al. Identification of a cytochrome P4502E1/Bid/C1q-dependent axis mediating inflammation in adipose tissue after chronic ethanol feeding to mice. The Journal of Biological Chemistry 2011;286:35989-35997.
195. Shen Z, Liang X, Rogers CQ, Rideout D, You M. Involvement of adiponectin-SIRT1-AMPK signaling in the protective action of rosiglitazone against alcoholic fatty liver in mice. American Journal of Physiology. Gastrointestinal and Liver Physiology 2010;298:364.
196. Song Z, Zhou Z, Deaciuc I, Chen T, McClain CJ. Inhibition of adiponectin production by homocysteine: a potential mechanism for alcoholic liver disease. Hepatology 2008;47:867-879.

197. Tang H, Sebastian BM, Axhemi A, Chen X, Hillian AD, Jacobsen DW, Nagy LE. Ethanol-induced oxidative stress via the CYP2E1 pathway disrupts adiponectin secretion from adipocytes. Alcohol Clin Exp Res 2012;36:214-222.
198. Mandal P, Park PH, McMullen MR, Pratt BT, Nagy LE. The anti-inflammatory effects of adiponectin are mediated via a heme oxygenase-1-dependent pathway in rat Kupffer cells. Hepatology 2010;51:1420-1429.
199. Mandal P, Pratt BT, Barnes M, McMullen MR, Nagy LE. Molecular mechanism for adiponectin-dependent M2 macrophage polarization: link between the metabolic and innate immune activity of full-length adiponectin. J Biol Chem 2011;286:13460-13469.
200. You M, Considine RV, Leone TC, Kelly DP, Crabb DW. Role of adiponectin in the protective action of dietary saturated fat against alcoholic fatty liver in mice. Hepatology 2005;42:568-577.
201. Zhao C, Liu Y, Xiao J, Liu L, Chen S, Mohammadi M, McClain CJ, et al. FGF21 mediates alcohol-induced adipose tissue lipolysis by activation of systemic release of catecholamine in mice. Journal of Lipid Research 2015;56:1481-1491.
202. Zhong W, Zhao Y, Tang Y, Wei X, Shi X, Sun W, Sun X, et al. Chronic alcohol exposure stimulates adipose tissue lipolysis in mice: role of reverse triglyceride transport in the pathogenesis of alcoholic steatosis. The American Journal of Pathology 2012;180:998-1007.
203. Wei X, Shi X, Zhong W, Zhao Y, Tang Y, Sun W, Yin X, et al. Chronic alcohol exposure disturbs lipid homeostasis at the adipose tissue-liver axis in mice: analysis of triacylglycerols using high-resolution mass spectrometry in combination with in vivo metabolite deuterium labeling. PLoS One 2013;8:e55382.
204. Kang L, Chen X, Sebastian BM, Pratt BT, Bederman IR, Alexander JC, Previs SF, et al. Chronic ethanol and triglyceride turnover in white adipose tissue in rats: inhibition of the anti-lipolytic action of insulin after chronic ethanol contributes to increased triglyceride degradation. J Biol Chem 2007;282:28465-28473.
205. Kang L, Nagy LE. Chronic ethanol feeding suppresses beta-adrenergic receptor-stimulated lipolysis in adipocytes isolated from epididymal fat. Endocrinology 2006;147:4330-4338.
206. Ambade A, Mandrekar P. Oxidative stress and inflammation: essential partners in alcoholic liver disease. International Journal of Hepatology 2012;2012:853175.
207. You M, Rogers CQ. Adiponectin: a key adipokine in alcoholic fatty liver. Experimental Biology and Medicine (Maywood, N.J.) 2009;234:850-859.
208. Rogers CQ, Ajmo JM, You M. Adiponectin and alcoholic fatty liver disease. IUBMB life 2008;60:790-797.
209. Schäffler A, Schölmerich J. Innate immunity and adipose tissue biology. Trends in Immunology 2010;31:228-235.

210. Baker RG, Hayden MS, Ghosh S. NF-κB, inflammation, and metabolic disease. Cell Metabolism 2011;13:11-22.
211. Rosen ED, Spiegelman BM. What we talk about when we talk about fat. Cell 2014;156:20-44.
212. Mandrekar P, Bala S, Catalano D, Kodys K, Szabo G. The Opposite Effects of Acute and Chronic Alcohol on Lipopolysaccharide-Induced Inflammation Are Linked to IRAK-M in Human Monocytes. The Journal of Immunology 2009;183:1320-1327.
213. Fulham MA, Mandrekar P. Sexual Dimorphism in Alcohol Induced Adipose Inflammation Relates to Liver Injury. PloS One 2016;11:e0164225.
214. Mathis D. Immunological goings-on in visceral adipose tissue. Cell Metabolism 2013;17:851-859.
215. Kim JI, Huh JY, Sohn JH, Choe SS, Lee YS, Lim CY, Jo A, et al. Lipid-overloaded enlarged adipocytes provoke insulin resistance independent of inflammation. Molecular and Cellular Biology 2015;35:1686-1699.
216. Saberi M, Woods N-B, de Luca C, Schenk S, Lu JC, Bandyopadhyay G, Verma IM, et al. Hematopoietic cell-specific deletion of toll-like receptor 4 ameliorates hepatic and adipose tissue insulin resistance in high-fat-fed mice. Cell Metabolism 2009;10:419-429.
217. Shi H, Kokoeva MV, Inouye K, Tzameli I, Yin H, Flier JS. TLR4 links innate immunity and fatty acid-induced insulin resistance. The Journal of Clinical Investigation 2006;116:3015-3025.
218. Clausen BE, Burkhardt C, Reith W, Renkawitz R, Förster I. Conditional gene targeting in macrophages and granulocytes using LysMcre mice. Transgenic Research 1999;8:265-277.
219. McAlees JW, Whitehead GS, Harley ITW, Cappelletti M, Rewerts CL, Holdcroft AM, Divanovic S, et al. Distinct Tlr4-expressing cell compartments control neutrophilic and eosinophilic airway inflammation. Mucosal Immunology 2015;8:863-873.
220. Hoshino K, Takeuchi O, Kawai T, Sanjo H, Ogawa T, Takeda Y, Takeda K, et al. Cutting edge: Toll-like receptor 4 (TLR4)-deficient mice are hyporesponsive to lipopolysaccharide: evidence for TLR4 as the Lps gene product. J Immunol 1999;162:3749-3752.
221. Murawski MR, Bowen GN, Cerny AM, Anderson LJ, Haynes LM, Tripp RA, Kurt-Jones EA, et al. Respiratory syncytial virus activates innate immunity through Toll-like receptor 2. J Virol 2009;83:1492-1500.
222. Zhang X, Goncalves R, Mosser DM. The isolation and characterization of murine macrophages. Current Protocols in Immunology 2008;Chapter 14:Unit 14.11.
223. Vladimer GI, Weng D, Paquette SWM, Vanaja SK, Rathinam VAK, Aune MH, Conlon JE, et al. The NLRP12 inflammasome recognizes Yersinia pestis. Immunity 2012;37:96-107.

224. Wang JP, Bowen GN, Zhou S, Cerny A, Zacharia A, Knipe DM, Finberg RW, et al. Role of specific innate immune responses in herpes simplex virus infection of the central nervous system. Journal of Virology 2012;86:2273-2281.
225. Ambade A, Catalano D, Lim A, Kopoyan A, Shaffer SA, Mandrekar P. Inhibition of heat shock protein 90 alleviates steatosis and macrophage activation in murine alcoholic liver injury. Journal of Hepatology 2014;61:903-911.
226. Kwon H-J, Won Y-S, Park O, Chang B, Duryee MJ, Thiele GE, Matsumoto A, et al. Aldehyde dehydrogenase 2 deficiency ameliorates alcoholic fatty liver but worsens liver inflammation and fibrosis in mice. Hepatology (Baltimore, Md.) 2014;60:146-157.
227. Yin H, Hu M, Liang X, Ajmo JM, Li X, Bataller R, Odena G, et al. Deletion of SIRT1 from hepatocytes in mice disrupts lipin-1 signaling and aggravates alcoholic fatty liver. Gastroenterology 2014;146:801-811.
228. Cohen JI, Roychowdhury S, McMullen MR, Stavitsky AB, Nagy LE. Complement and alcoholic liver disease: role of C1q in the pathogenesis of ethanol-induced liver injury in mice. Gastroenterology 2010;139:674, 674.e671.
229. Mauer J, Chaurasia B, Goldau J, Vogt MC, Ruud J, Nguyen KD, Theurich S, et al. Signaling by IL-6 promotes alternative activation of macrophages to limit endotoxemia and obesity-associated resistance to insulin. Nature Immunology 2014;15:423-430.
230. Girasole G, Jilka RL, Passeri G, Boswell S, Boder G, Williams DC, Manolagas SC. 17 beta-estradiol inhibits interleukin-6 production by bone marrow-derived stromal cells and osteoblasts in vitro: a potential mechanism for the antiosteoporotic effect of estrogens. J Clin Invest 1992;89:883-891.
231. Messingham KA, Heinrich SA, Kovacs EJ. Estrogen restores cellular immunity in injured male mice via suppression of interleukin-6 production. J Leukoc Biol 2001;70:887-895.
232. Org E, Mehrabian M, Parks BW, Shipkova P, Liu X, Drake TA, Lusis AJ. Sex differences and hormonal effects on gut microbiota composition in mice. Gut Microbes 2016;7:313-322.
233. Haro C, Rangel-Zuniga OA, Alcala-Diaz JF, Gomez-Delgado F, Perez-Martinez P, Delgado-Lista J, Quintana-Navarro GM, et al. Intestinal Microbiota Is Influenced by Gender and Body Mass Index. PLoS One 2016;11:e0154090.
234. Hartmann P, Seebauer CT, Schnabl B. Alcoholic liver disease: the gut microbiome and liver cross talk. Alcohol Clin Exp Res 2015;39:763-775.
235. Szabo G. Gut-liver axis in alcoholic liver disease. Gastroenterology 2015;148:30-36.
236. Betrapally NS, Gillevet PM, Bajaj JS. Changes in the Intestinal Microbiome and Alcoholic and Nonalcoholic Liver Diseases: Causes or Effects? Gastroenterology 2016;150:1745-1755 e1743.
237. Lackner C, Spindelboeck W, Haybaeck J, Douschan P, Rainer F, Terracciano L, Haas J, et al. Histological parameters and alcohol abstinence determine long-term prognosis in patients with alcoholic liver disease. J Hepatol 2017;66:610-618.

238. Mandrekar P, Catalano D, Dolganiuc A, Kodys K, Szabo G. Inhibition of myeloid dendritic cell accessory cell function and induction of T cell anergy by alcohol correlates with decreased IL-12 production. J Immunol 2004;173:3398-3407.
239. Schäffler A, Schölmerich J, Salzberger B. Adipose tissue as an immunological organ: Toll-like receptors, C1q/TNFs and CTRPs. Trends in Immunology 2007;28:393-399.
240. Song MJ, Kim KH, Yoon JM, Kim JB. Activation of Toll-like receptor 4 is associated with insulin resistance in adipocytes. Biochem Biophys Res Commun 2006;346:739-745.
241. Wang W, Deng M, Liu X, Ai W, Tang Q, Hu J. TLR4 activation induces nontolerant inflammatory response in endothelial cells. Inflammation 2011;34:509-518.
242. Tiemessen MM, Jagger AL, Evans HG, van Herwijnen MJ, John S, Taams LS. CD4+CD25+Foxp3+ regulatory T cells induce alternative activation of human monocytes/macrophages. Proc Natl Acad Sci U S A 2007;104:19446-19451.
243. Mosser DM, Edwards JP. Exploring the full spectrum of macrophage activation. Nat Rev Immunol 2008;8:958-969.
244. Grivennikov SI, Tumanov AV, Liepinsh DJ, Kruglov AA, Marakusha BI, Shakhov AN, Murakami T, et al. Distinct and nonredundant in vivo functions of TNF produced by t cells and macrophages/neutrophils: protective and deleterious effects. Immunity 2005;22:93-104.
245. Eguchi J, Wang X, Yu S, Kershaw EE, Chiu PC, Dushay J, Estall JL, et al. Transcriptional control of adipose lipid handling by IRF4. Cell Metab 2011;13:249-259.
246. Sorensen I, Adams RH, Gossler A. DLL1-mediated Notch activation regulates endothelial identity in mouse fetal arteries. Blood 2009;113:5680-5688.
247. Suganami T, Mieda T, Itoh M, Shimoda Y, Kamei Y, Ogawa Y. Attenuation of obesity-induced adipose tissue inflammation in C3H/HeJ mice carrying a Toll-like receptor 4 mutation. Biochemical and Biophysical Research Communications 2007;354:45-49.
248. Davis JE, Gabler NK, Walker-Daniels J, Spurlock ME. Tlr-4 deficiency selectively protects against obesity induced by diets high in saturated fat. Obesity (Silver Spring, Md.) 2008;16:1248-1255.
249. Orr JS, Puglisi MJ, Ellacott KLJ, Lumeng CN, Wasserman DH, Hasty AH. Toll-like receptor 4 deficiency promotes the alternative activation of adipose tissue macrophages. Diabetes 2012;61:2718-2727.
250. Poggi M, Bastelica D, Gual P, Iglesias MA, Gremeaux T, Knauf C, Peiretti F, et al. C3H/HeJ mice carrying a toll-like receptor 4 mutation are protected against the development of insulin resistance in white adipose tissue in response to a high-fat diet. Diabetologia 2007;50:1267-1276.
251. Jia L, Vianna CR, Fukuda M, Berglund ED, Liu C, Tao C, Sun K, et al. Hepatocyte Toll-like receptor 4 regulates obesity-induced inflammation and insulin resistance. Nature Communications 2014;5:3878.

252. Guerville M, Boudry G. Gastrointestinal and hepatic mechanisms limiting entry and dissemination of lipopolysaccharide into the systemic circulation. Am J Physiol Gastrointest Liver Physiol 2016;311:G1-G15.
253. Hersoug LG, Moller P, Loft S. Gut microbiota-derived lipopolysaccharide uptake and trafficking to adipose tissue: implications for inflammation and obesity. Obes Rev 2016;17:297-312.
254. Mimura Y, Sakisaka S, Harada M, Sata M, Tanikawa K. Role of hepatocytes in direct clearance of lipopolysaccharide in rats. Gastroenterology 1995;109:1969-1976.
255. Hunter CA, Jones SA. IL-6 as a keystone cytokine in health and disease. Nat Immunol 2015;16:448-457.
256. Beulens JW, de Zoete EC, Kok FJ, Schaafsma G, Hendriks HF. Effect of moderate alcohol consumption on adipokines and insulin sensitivity in lean and overweight men: a diet intervention study. Eur J Clin Nutr 2008;62:1098-1105.
257. Beulens JW, van Beers RM, Stolk RP, Schaafsma G, Hendriks HF. The effect of moderate alcohol consumption on fat distribution and adipocytokines. Obesity (Silver Spring) 2006;14:60-66.
258. Mandal P, Roychowdhury S, Park PH, Pratt BT, Roger T, Nagy LE. Adiponectin and heme oxygenase-1 suppress TLR4/MyD88-independent signaling in rat Kupffer cells and in mice after chronic ethanol exposure. J Immunol 2010;185:4928-4937.
259. Shklyaev S, Aslanidi G, Tennant M, Prima V, Kohlbrenner E, Kroutov V, Campbell-Thompson M, et al. Sustained peripheral expression of transgene adiponectin offsets the development of diet-induced obesity in rats. Proc Natl Acad Sci U S A 2003;100:14217-14222.
260. Leroux A, Ferrere G, Godie V, Cailleux F, Renoud ML, Gaudin F, Naveau S, et al. Toxic lipids stored by Kupffer cells correlates with their pro-inflammatory phenotype at an early stage of steatohepatitis. J Hepatol 2012;57:141-149.
261. Aouadi M, Vangala P, Yawe JC, Tencerova M, Nicoloro SM, Cohen JL, Shen Y, et al. Lipid storage by adipose tissue macrophages regulates systemic glucose tolerance. Am J Physiol Endocrinol Metab 2014;307:E374-383.
262. Kosteli A, Sugaru E, Haemmerle G, Martin JF, Lei J, Zechner R, Ferrante AW, Jr. Weight loss and lipolysis promote a dynamic immune response in murine adipose tissue. J Clin Invest 2010;120:3466-3479.
263. Fisher FM, Maratos-Flier E. Understanding the Physiology of FGF21. Annu Rev Physiol 2016;78:223-241.
264. Lin Z, Tian H, Lam KS, Lin S, Hoo RC, Konishi M, Itoh N, et al. Adiponectin mediates the metabolic effects of FGF21 on glucose homeostasis and insulin sensitivity in mice. Cell Metab 2013;17:779-789.
265. Talukdar S, Owen BM, Song P, Hernandez G, Zhang Y, Zhou Y, Scott WT, et al. FGF21 Regulates Sweet and Alcohol Preference. Cell Metab 2016;23:344-349.
266. Talukdar S, Zhou Y, Li D, Rossulek M, Dong J, Somayaji V, Weng Y, et al. A Long-Acting FGF21 Molecule, PF-05231023, Decreases Body Weight and

Improves Lipid Profile in Non-human Primates and Type 2 Diabetic Subjects. Cell Metab 2016;23:427-440.
267. O'Neill LA, Golenbock D, Bowie AG. The history of Toll-like receptors - redefining innate immunity. Nat Rev Immunol 2013;13:453-460.
268. Zhao XJ, Dong Q, Bindas J, Piganelli JD, Magill A, Reiser J, Kolls JK. TRIF and IRF-3 binding to the TNF promoter results in macrophage TNF dysregulation and steatosis induced by chronic ethanol. J Immunol 2008;181:3049-3056.
269. Grant R, Youm YH, Ravussin A, Dixit VD. Quantification of adipose tissue leukocytosis in obesity. Methods Mol Biol 2013;1040:195-209.
270. Cho KW, Morris DL, Lumeng CN. Flow cytometry analyses of adipose tissue macrophages. Methods Enzymol 2014;537:297-314.
271. Vandanmagsar B, Youm YH, Ravussin A, Galgani JE, Stadler K, Mynatt RL, Ravussin E, et al. The NLRP3 inflammasome instigates obesity-induced inflammation and insulin resistance. Nat Med 2011;17:179-188.
272. Ambade A, Catalano D, Lim A, Mandrekar P. Inhibition of heat shock protein (molecular weight 90 kDa) attenuates proinflammatory cytokines and prevents lipopolysaccharide-induced liver injury in mice. Hepatology 2012;55:1585-1595.
273. Duerfeldt AS, Peterson LB, Maynard JC, Ng CL, Eletto D, Ostrovsky O, Shinogle HE, et al. Development of a Grp94 inhibitor. J Am Chem Soc 2012;134:9796-9804.
274. Eletto D, Dersh D, Argon Y. GRP94 in ER quality control and stress responses. Semin Cell Dev Biol 2010;21:479-485.
275. Maki RG, Old LJ, Srivastava PK. Human homologue of murine tumor rejection antigen gp96: 5'-regulatory and coding regions and relationship to stress-induced proteins. Proc Natl Acad Sci U S A 1990;87:5658-5662.
276. Marzec M, Eletto D, Argon Y. GRP94: An HSP90-like protein specialized for protein folding and quality control in the endoplasmic reticulum. Biochim Biophys Acta 2012;1823:774-787.
277. Patel PD, Yan P, Seidler PM, Patel HJ, Sun W, Yang C, Que NS, et al. Paralog-selective Hsp90 inhibitors define tumor-specific regulation of HER2. Nat Chem Biol 2013;9:677-684.
278. Randow F, Seed B. Endoplasmic reticulum chaperone gp96 is required for innate immunity but not cell viability. Nat Cell Biol 2001;3:891-896.
279. Yang Y, Liu B, Dai J, Srivastava PK, Zammit DJ, Lefrancois L, Li Z. Heat shock protein gp96 is a master chaperone for toll-like receptors and is important in the innate function of macrophages. Immunity 2007;26:215-226.
280. Liu B, Yang Y, Qiu Z, Staron M, Hong F, Li Y, Wu S, et al. Folding of Toll-like receptors by the HSP90 paralogue gp96 requires a substrate-specific cochaperone. Nat Commun 2010;1:79.
281. Staron M, Yang Y, Liu B, Li J, Shen Y, Zuniga-Pflucker JC, Aguila HL, et al. gp96, an endoplasmic reticulum master chaperone for integrins and Toll-like

receptors, selectively regulates early T and B lymphopoiesis. Blood 2010;115:2380-2390.
282. Morigny P, Houssier M, Mouisel E, Langin D. Adipocyte lipolysis and insulin resistance. Biochimie 2016;125:259-266.
283. Zimmermann R, Lass A, Haemmerle G, Zechner R. Fate of fat: the role of adipose triglyceride lipase in lipolysis. Biochim Biophys Acta 2009;1791:494-500.
284. Maeda N, Funahashi T, Shimomura I. Metabolic impact of adipose and hepatic glycerol channels aquaporin 7 and aquaporin 9. Nat Clin Pract Endocrinol Metab 2008;4:627-634.
285. Duncan RE, Ahmadian M, Jaworski K, Sarkadi-Nagy E, Sul HS. Regulation of lipolysis in adipocytes. Annu Rev Nutr 2007;27:79-101.
286. Schneider CA, Rasband WS, Eliceiri KW. NIH Image to ImageJ: 25 years of image analysis. Nature Methods 2012;9:671-675.
287. Schindelin J, Arganda-Carreras I, Frise E, Kaynig V, Longair M, Pietzsch T, Preibisch S, et al. Fiji: an open-source platform for biological-image analysis. Nature Methods 2012;9:676-682.
288. Rojas-Rodriguez R, Lifshitz LM, Bellve KD, Min SY, Pires J, Leung K, Boeras C, et al. Human adipose tissue expansion in pregnancy is impaired in gestational diabetes mellitus. Diabetologia 2015;58:2106-2114.